



Altered Histone 4 K12 Acetylation is Associated with Age Dependent Memory Impairment in Mice

PhD Thesis

in partial fulfilment of the requirements
for the degree “Dr. rer. nat.”
in the Neuroscience Program
at the Georg August University Göttingen,
Faculty of Biology

Submitted by

Shahaf Peleg

born in

Beer Sheva

2010

Declaration

I hereby declare that the PhD thesis entitled, “Altered Histone 4 K12 Acetylation is Associated with Age Dependent Memory Impairment in Mice”, was written independently and with no other sources and aids than quoted. I would like to gratefully acknowledge Dr. Athanasios Zovoilis for the bioinformatics analysis of the Chip-seq and the microarray. In addition I would like to acknowledge Dr. Salinas-Riester and Lennart Opitz for the generation of the microarray data.

Göttingen, 20th September 2010

Shahaf Peleg

Table of contents

TABLE OF CONTENTS	3
ACKNOWLEDGEMENTS	7
ABBREVIATION LIST	9
I INTRODUCTION	10
1.1 Eukaryotic Aging	10
1.2 Gene expression alteration in brain aging	11
1.3 Epigenetics	12
1.4 Acygenetics	14
1.4.1 Histone acetylation	14
1.4.2 HATs and HDACs	15
1.4.3 HDAC inhibitors	17
1.4.4 The link between mitochondria and Histone acetylation	17
1.5 Learning and memory	18
1.6 Decline of cognitive function during aging	19
1.7 The role of epigenetic mechanism on memory formation and possible therapy for AAMI	21
1.8 Aim of the study	23
II METHODS AND METIRIALS	24
2.1 Animals and behavior testing	24
2.1.1 Fear conditioning	24

2.1.2 Water Maze	25
2.1.3 Cannulation and injection	26
2.2 Protein lyses, sub-celluar fractionation and Immunobloting	27
2.3 Perfusion and Immunohistochemistry	29
2.4 Microscope	30
2.5 Antibodies	30
2.6 Chromatin-immunoprecipitation (ChIP)	30
2.7 Quantitative Real time PCR (qPCR)	31
2.8 HAT/ HDAC assay	34
2.9 Citrate Assay	35
2.10 Microarray study	35
2.11 Data mining for microarray	36
2.12 ChIP-sequencing	37
2.12.1 Solexa pipeline analysis and mapping to mouse genome	37
2.12.2 Identification of H4K12 and H3K9 acetylation enriched regions	37
2.12.3 Profiles of H4K12 and H3K9 enrichment around TSS and across gene bodies regions	39
2.12.4 Definition of gene coordinates and visualization of ChIP-seq data along the genome	39
2.12.5 Analysis of base coverage of chromatin modifications	39
2.13 Statistical analysis	40
III RESULTS	41
3.1 16-month old mice display impaired learning and memory	41

3.2 Molecular analysis of naïve 3-month old mice versus 16-month old mice.	43
3.2.1 Markers for neuronal plasticity and integrity are similar	43
3.2.2 Levels of hippocampal bulk histone-acetylation are similar among the naïve groups	44
3.2.3 Similar HAT and HDAC levels and nuclear activity between the naïve groups	45
3.3 Impaired learning and memory in 16-month-old mice after fear conditioning correlates with H4K12 acetylation.	47
3.4 Dysregulated H4K12 acetylation in 16-month-old mice after fear conditioning is observed in all hippocampal sub regions.	49
3.5 Impaired transcriptome plasticity during memory consolidation in 16-month-old mice	51
3.6 16-month-old mice display reduced H4K12 acetylation levels along the coding regions of learning induced up regulated genes	57
3.7 Intrahippocampal injection of HDAC inhibitors, which increase H4K12 acetylation, restore gene expression and learning behaviour in 16-month-old mice	63
3.7.1 SAHA	64
3.7.2 Sodium-Butyrate	68
3.7.3 MS-275	70
3.8 Mechanisms underlying H4K12 acetylation deficits in 16 month-old mice	72
3.8.1 HAT and HDAC activity	73

3.8.2 16 month-old mice display a deficit in citrate up-regulation	
in response to fear conditioning	74
IV DISCUSSION	76
4.1 Histone acetylation and gene expression up-regulation are	
important for the formation of associative memory	76
4.2 The uniqueness of H4K12 acetylation	80
4.2.1 H4K12 acetylation in coding regions has a unique effect on level	
of gene expression	80
4.2.2 Age-associated H4K12 acetylation deregulation in various models	83
4.3 The involvement of acygenetics in aging	85
4.4 HDAC inhibitors as therapeutic avenue for AAMI	88
V SUMMARY	92
VI REFERENCES	94
CURRICULUM VITAE	106
LIST OF PUBLICATIONS	107
APPENDIX	108
Shearing, one day ChIP protocol and SYBR Green RT-PCR	108

Acknowledgements

First and above all, I would like to thank Dr. Andre Fischer for giving me the opportunity and accepting me to his lab to undertake one of the most unique and challenging project, for his constant support, guidance and extreme patience, for keeping his door opened for any type of discussions, for putting lots of trust in me when I first came and for the devoted help during my three years in his lab.

I am very grateful to our post doc Thanasis who put an incredible effort in the bioinformatics analysis of the crucial Chip-seq and microarray data. Without him, this project would have never been as complete as it is.

I am grateful to Professor Matthias Baehr and Wolfgang Fischle, my committee members, for their advices and support and helping me guide my project.

I would like to thank my other lab members for their constant support. Especially, I would like to thank Susi, who helped me in every day aspect in the lab and for amazing devotion to her work (Including carrying PCR a day before her own major brain operation!). To Govind, who was my lab rotation supervisor, and not only taught me the basic methods but also was always keen to give me advices in my experiment, written reports, oral presentation and posters. To Roberto, for the good time in the lab and also for presenting the most important journal club in my entire career. To Jess, who helped me developing the ChIP protocol and for assisting with the editing of the thesis. For Dario, Roman, Torsten and all the other lab members of the Fischer Lab for all their help during my PhD.

I would like to thank the Minerva Siftung for the financial support during my PhD.

I am grateful for the contribution of our co-workers in my project. For Gabriella and Lennart for their amazing work on the microarrays studies. Especially I would like to thank Larent Farinelli for taking his time to help a young PhD student to carry out the most important experiment in my work. Without his willingness to help, this project will miss its key finding.

Many thanks to my fellow students in Beer Sehva, Hadas and Amir, for sharing with me the wonderful three years during the Bachelor in Biology and for standing by me. I would also like to thank Dr Ofer Ovadia for his constant enthusiasm and showing us how a teacher can do more that what he is required.

I would like to thank Mara, Nikhil and Mandy for all the good laughs we had together

on the second floor and the mensa.

I would like to thank Frank Herbert, for opening the eyes of a child and making him see a whole new world. Without his inspiration this child would have remained medium and ignorant till this very day.

Especially, I am extremely grateful to Michael, Sandre, Steffen and Ivana from our coordination offices that work so hard to make it so easy for us foreign student to call Goettingen our home. I'd like to thank the Neuroscience Program for the wonderful opportunity to carry my higher education in such a prestigious place.

Finally, I am thankful for the city of Goettingen, its wonderful people, crazy weather and pastoral atmosphere in making me so happy for the last four years. *Ein Teil meiner Seele wird immer hier bleiben.*

Abbreviation list

AAMI - Age-Associated Memory Impairment

ACL/ACLY - ATP-citrate lyase

ACSF - Artificial Cerebrospinal Fluid

AD – Alzheimer disease

ChIP – Chromatin Immuno Precipitation

ChIP-seq – ChIP sequencing

DG - Dentate gyrus

ES – Electric Shock

FMN2 – Formin 2

FC - Fear Conditioning

H3/4 – Histone 3 or 4

HAT - Histone Acetyl Transferase

HDAC - Histone Deacetylase

HDACi - HDAC inhibitor

K5/8/9/12/14/16 – Lysine 5/8/9/12/14/16

KEGG - Kyoto Encyclopedia of Genes and Genomes

NaB - Sodium Butyrate

PCR - Polymerase chain reaction

RT-PCR – Real time PCR

SAHA - Suberoylanilide Hydroxamic Acid

S.E.M - Standard Error of the Mean

SICER - Statistical model for Identification of chip-Enriched Regions

TSA - Trichostatin A

TSS - Transcription Start Site

Veh – Vehicle (Control)

I Introduction

1.1 Eukaryotic aging

During the last one hundred years, with the advancement of technology and the improvement of medicine, the human population has dramatically increased. As a result, life span and the elderly population have increased as well. Whereas smaller number of people reached old age before the 1900s, the average life span in the last 160 years has increased at a steady rate in the developed countries (Oeppen, 2002), reaching today at 75 and 82 for European men and women respectively (According to the World Factbook, 2008). Therefore, we were recently able to start researching human aging in greater detail.

With our industrial improvement, we were also able to start investigating aging in different organisms, from simple worms to mice and primates. The wildlife normally does not reach old age as with time, the animal's fitness gradually declines with aging. Nowadays, however, animals are kept in the safety of research labs in order to reach old age, allowing us to investigate aging in various models.

Aging itself is the number one risk for a wide spectrum of diseases in various tissues, ranging from Alzheimer and Parkinson disease in the brain to cardiovascular disease, cancer, osteoporosis and many more. Ultimately, given enough time without even a distinctive disease, aging is the underlying cause for death resulting from irreversible systemic molecular disorder (Hayflick, 2000). Inevitably, the underlying cause of the death of the elderly is the loss of physiological capacity in vital organs. Aging is a special phenomena due to the fact that it is a gradual and accumulative process and that the vast decisive majority of all Eukaryotes, and possibly to some extent also Prokaryotes, display aging. The fact that such variety of organisms age suggest that the onset of aging is not likely to rise from a specific protein, complex of proteins or possibly single pathways. If

that was the case, evolution might have found a way around it in the long course of time of Eukaryotes' development. It is more likely that the mechanisms that are related to aging are highly conserved processes, which are essential to the maintenance of life and most importantly, gradually prone to error with time.

1.2 Gene expression alteration in brain aging

A pivotal study showed that during brain aging (Lu, 2004), a gradual shift in gene expression is observed in the human cortex. Certain genes were up regulated with aging, whereas others were down regulated. However, subsequent studies (Loerch, 2008; Berchtold, 2008) showed that the actual identity of the genes up- and down-regulated genes with brain aging was quite different between different brain tissues within an organism or between different organisms. Even closely related organisms display different age- dysregulated genes in similar tissue. Moreover, the genes' identity differs even between the two sexes of the same organism (Berchtold, 2008). Hence, it is difficult to associate or unify brain aging under specific pathways, based on the gene expression dysregulation alone. As the process of aging remains poorly understood, current therapies for the age-related maladies help the symptoms but cannot prevent nor delay the ultimate progression and accumulation of age related damage. Even caloric restriction (Weindruch, 1986; Kenyon, 1993; Colman, 2009), perhaps the most studied and proven treatment to extend life, can only delay the various effects of aging.

Even though the genes, which are dysregulated during brain aging, are not similar across different organisms and tissues, gene expression alteration nonetheless is observed with aging in each of them. It is possible that another and more basic mechanism could be more uniformly dysregulated in aging in similar way in various organisms/tissue. One such candidate is a mechanism, which allows the eukaryotic cells to orchestrate their gene expression in response to different demands and enable them to efficiently adapt to changes: Epigenetics.

1.3 Epigenetics

The term epigenetic (first coined by Waddington in 1942) is commonly defined today as heritable changes in gene expression that cannot be explained by the DNA sequence. The two most studied epigenetic phenomena are DNA-methylation and histone-tail modifications (Fig 1).

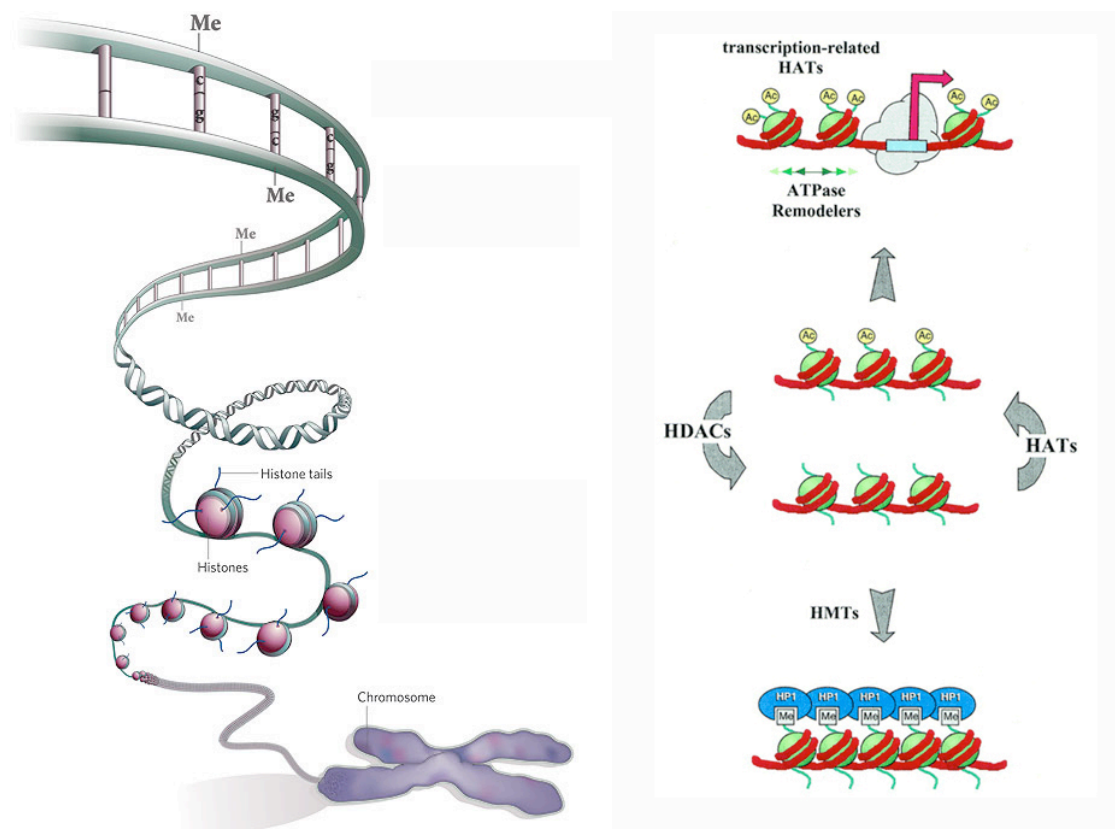


Figure 1. Epigenetic modifications that effect the transcription of genes.

Left panel: DNA can be directly modified by methylation on cytosines within CpG islands. Histones are proteins attached to the DNA to provide secondary structure and help condense it. Each histone has a tail, which is subjected to various modifications. Right panel: When HATs acetylate the histone tail, the DNA-Histone interaction weakens. This in turn promotes the binding of transcription factors and the activation of gene expression. When HDACs deacetylate the histone tail, the DNA-Histone interaction strengthens, thereby promoting further histone tail methylation and repression of gene expression. (Adapted from Qiu, 2006 *Nature* and Eberharter and Becker, 2002 *EMBO reports*.)

DNA methylation is restricted to cytosine nucleotides and this modification normally occurs in specific regions called CpG islands. DNA methylation is mostly located at the promoter regions of genes and serves for gene silencing. This epigenetic mechanism plays a crucial role in various processes such as cell differentiation during the development of an organism. DNA methylation is a rather stable process (Cedar, 2009). In bees, the DNA methylation pattern form in the early larval stage can determine whether the larva will become a worker bee or a queen. This leads to differences in brain morphology, size, the ability to produce offspring and even life span (Kucharski, 2008). The life span of the queen bee is fifty times greater than that of the worker bee. The extraordinary fact is that DNA sequence itself is identical in both the queen and the working bee.

Unlike the rather stable DNA methylation modification, histone modifications are more dynamic, although DNA methylation has a profound effect on histone modification (Lande-Diner, 2007; Cedar, 2009). Eukaryotic DNA is wrapped around a complex of eight histones (dimers of H2A, H2B, H3, H4) to form the basic unit/level of chromatin structure, which is surrounded by 147 base pairs of DNA. The basic amino-terminal tails of histones carry diverse post-translational modifications, such as acetylation, methylation and ubiquitination, which build up discrete patterns of chemical marks recognized and bound by other proteins (Strahl, 2000).

Histone methylation occurs on the H3 and H4 tails, and it can leads to either activation or suppression of gene expression. The methylation is mediated by methyltransferases, which utilize methionine (SAM - S-adenosyl-L-methionine) as a precursor and histone demethylases. Recently, transient increase of histone methylation was implicated with the formation of new memories (Gupta, 2010).

Perhaps out of all the histone modifications, histone acetylation is ideal for the study of aging. As mentioned, the histone acetylation is more dynamic process unlike DNA methylation (Cedar, 2009). Moreover, histone acetylation is mainly

linked with activation of genes' expression (Rice, 2001). In contrast, histone methylation is linked with the opposing biological processes of transcriptional up-regulation and heterochromatin assembly leading to epigenetic silencing, depending on the amino acid residue, which is methylated (Rice, 2001). Since histone acetylation has only single property (activation of expression) rather the dual and opposite properties histone in methylation (activation and inhibition of expression), it is simpler to try and link it with age related dysregulation.

Acetylation is not restricted to histones (Lin, 2009). Various proteins in different cellular compartments can be acetylated, and thus have their activity modified. The precursor for the acetylation process is highly dependant on the availability mitochondria derived metabolic molecules (Miller, 1973; Wellen, 2009). Therefore, as mitochondria dysfunction had been implicated in the process of aging (Bishop, 2010), acetylation of histones, and possibly other proteins, could be altered with aging as well. We therefore focused the attention on the epigenetic process of histone acetylation, the proteins that modulate it, drugs that can alter this process and its possible link to metabolism, hereafter in sum termed as *Acygenetics*.

1.4 Acygenetics

1.4.1 Histone acetylation

Lysine acetylation of H3 and most H4 sites leads to the relaxation of chromatin, thereby making the DNA accessible to DNA binding proteins such as transcription factors (Fig 1). As a result, RNA synthesis is enhanced (Allfrey, 1964; Clayton, 2006). It is believed that the acetylation causes the histones to lose negative charge (Norton, 1989), thus decreasing the ionic interaction between the histone and the DNA strand. This leads to the formation of a relaxed chromatin structure (Görisch, 2005). This in turn, leads to easier access of transcription factors to bind to the DNA. Histone acetylation is therefore traditionally considered to promote gene

expression. A more precise definition suggests that histone acetylation can in fact initiate transcription on one hand and can modulate the level and rate of transcription on the other hand, depending on the acetylated tail residue. The various histone acetylation sites on the tail can act sequentially or in combination to form a 'histone code'. This code, or distinctive DNA structure, is read by other proteins and allow a specificity of proteins' binding on the DNA. Therefore the histone code leads to regulation of downstream events such as transcription activation (Strahl, 2000).

Numerous studies have shown the different functions of histone acetylation in various organisms. For example, hyper-acetylation of histone 3 lysine 9 around the promoter site was shown to be associated with highly expressed genes (Nishida, 2006). When the promoter lacked H3K9 acetylation, the expression of the corresponding genes was very low. Histone 3 lysine 56 acetylation was implicated in mediating a DNA repair mechanism (Chen, 2008). Histone 4 lysine 16 acetylation (H4K16ac) has recently been shown to have an effect on telomeres and impact the life span in yeast (Dang, 2009). Interestingly, K16 was shown to normally be the first residue to be acetylated in histone 4 (Munks, 1991; Zhang, 2002, discussed in Taipale, 2005). In other words, in order to acetylate the other lysine residues, H4K16ac site must be already acetylated. Histone 4 acetylation was linked to spermatogenesis in *Drosophila* (Awe, 2010). Taken together, histone acetylation plays vital roles in great variety of processes.

1.4.2 HATs and HDACs

The acetylation of histones is regulated by histone-acetyl transferases (HAT) and histone-deacetylases (HDAC), which transfer or remove acetyl-groups on specific lysine residues of histone-tails, respectively (Strahl, 2000).

The HATs use acetyl-CoA to acetylate a conserved lysine group. The activity of the HATs is intimately associated with the activation of gene transcription. The specificity of each HAT in terms of which residues it can acetylate in a specific tissue remains to be elucidated. As with histone acetylation sites, various HATs play various roles in different pathways.

For example, CBP was shown to be critically involved in memory consolidation in mice (Korzus, 2004; Alarcón, 2004). GCN5, another HAT, is a highly conserved component of large complexes from yeast to higher eukaryotes. It is involved in transcription activation. Moreover, cells lacking GCN5 are more sensitive to DNA damage and exhibit accelerated senescence (Burgess, 2010).

HDACs are divided into four classes based on their cellular localization and homology (De Ruijter, 2003; Gregoretti, 2004). All the eleven mammalian HDACs require zinc ion as a co-factor, while the SIRT require NAD⁺ as a co-factor. The HDACs themselves are subjected to modifications as such acetylation and phosphorylation, which effect their function and sub cellular localization. (Brandtl, 2009). Class I consists of HDAC 1,2,3 and 8. They are homologous to Rpd3 in yeast, and they contain a nuclear localization sequence while lacking the nuclear export sequence. Therefore they are mainly located therefore in the nucleus (De Rooter, 2003). Class II includes the subclass IIa, HDAC 4, 5, 7 and IIb, HDAC 6 and 10. These HDACs are mainly located in the cytoplasm although they can shuttle into the nucleus. For instance, HDAC 4 and 5 are shuttled into the nucleus when dephosphorylated (Grozingler, 2000). Class III of histone deacetylases are named Sirtuins and includes SIRT 1-7 (Michan, 2007). The sirtuins were described as potential mediators of caloric restriction and as pharmacological targets to treat metabolic disorders (Guarente, 2006). Recently Sir1 was shown to regulate memory and plasticity (Gao, 2010). Class IV only representative is HDAC11 (Gregoretti, 2004) that has been shown to interact with HDAC6 (Gao, 2002).

1.4.3 HDAC inhibitors

As HDAC activity leads to the repression of gene expression, it has been hypothesized that using HDAC inhibitors (HDACi) will increase the expression of genes that are regulated by the HDACs.

HDACi contain a zinc binding group. The HDACi binds to the corresponding catalytic site of the HDAC (Drummond, 2005) and thus inhibits the HDAC from deacetylating histones, and possibly other protein targets. Trichostatin A (TSA), sodium butyrate (NaB) and suberoylanilide hydroxamic acid (SAHA) inhibit class I and II HDACs but not the SIRT proteins (Carew, 2008). TSA belong to the most potent drug group, hydroxamic acids. While SAHA and NaB are able to inhibit both HDAC classes I and II, it remains controversial which class they preferentially inhibit (Carew, 2008). Very recently it was shown *in vitro* (Kligore, 2010) that both SAHA and NaB, mainly inhibit class I but are much less potent for the other HDACs (SAHA could also efficiently inhibit HDAC6). MS275 has been shown to have greater inhibition on HDAC1, having 100 times more affinity to HDAC1 than HDAC2 (Khan, 2008).

1.4.4 The link between mitochondria and histone acetylation

Eukaryotes display many key differences from their Prokaryotic ancestors, ranging from the formation of nucleus, different ribosomal subunits, cellular compartmentalization and more. Perhaps two of the most striking differences are the presence of the mitochondria and the ability for an elaborate gene expression regulation, which is partly mediated by acygenetics. Mitochondria enabled the eukaryotes to produce far more energy than the prokaryotes both by more efficient production of ATP and other metabolic molecules such as citrate, which is further synthesized into acetyl-CoA. Acygenetics created new opportunities for an elaborate gene expression regulation, which led a higher level of organisms'

sophistication. Interestingly, acygenetics has a crucial dependence on metabolites from the mitochondria (Wellen, 2009). The acetylation process requires specific acetyl-CoA from a mitochondria derived citrate. It could be hypothesized that without mitochondria, acygenetics could not have evolved in the first place. Importantly, during aging, a marked decline in the mitochondria function is observed (Bishop, 2010).

There are considerable numbers of studies on histone acetylation/HAT or HDAC/HDACi in great variety of fields, which illustrate the importance of histone acetylation for gene regulation. Also, as histone acetylation is so important for various cell functions, dysregulation of histone acetylation was associated with various maladies. Hence, it is not surprising that targeting histone acetylation mechanisms was proposed as a suitable therapy for various maladies such as cancer, addiction, neurodegeneration, Huntington disease and many more (Ashktorab, 2009; Renthal, 2007; Fischer, 2007; Steffan, 2001). We therefore speculated that histone acetylation dysregulation might occur with the normal course of aging and play a role in age-associated memory impairment.

1.5 Learning and memory

The remarkable capability of the nervous system of animals to adapt their behavioural responses to ever-changing environmental conditions is thought to rely on the plasticity of neuronal circuits and synaptic connections. This capability reaches its highest form in the human brain.

Our brain is able to acquire knowledge, skills, better understanding and be innovative in a process called learning. The expression of our learning is imprinted in brain areas or in our words and memories. Defining the concepts of learning and memory in molecular parameters is rather difficult and perhaps quite impossible (John R. Searle discussing consciousness). We know for instance that by blocking

protein translation in *Aplysia*, the *Aplysia* cannot form new long-term memories (Schacher, 1988). Another interesting finding pointed out the importance of cytoskeleton dynamics in the formation of new memories (Fischer, 2004). Inhibiting the cytoskeleton dynamics in mice weakens the ability of to display freezing in the fear-conditioning test (The fear conditioning test is described in fig 2 in the materials and methods section under 2.1.1).

A major breakthrough in our understanding of learning and memory in humans came following the discovery of the importance of the hippocampus, a sub-region of the brain found to be crucial for the formation of new memories. In 1953, the patient HM suffered from seizures, and his doctors decided to treat his epilepsy by removing his hippocampus. As a result, his entire entorhinal cortex, which forms the major sensory input to the hippocampus, was destroyed. As a consequence of this operation, HM lost his ability to form new memories for the rest his life, while still retaining to high degree his ability to recall pre-operation events (Scoville, 1957). Although he still retained working memory and procedural memory, he could not create new long-term memories. Thus, in this unfortunate way, the importance of the hippocampal function in creating new memories was discovered. Since then, the hippocampus sub-region has gained “celebrity” status as countless research groups put considerable effort into elucidating its functions. At 1971, the hippocampus was shown to be intimately involved in spatial navigation as was demonstrated in the performance of rodents in Morris water maze (O’Keefe, 1971). (The water maze test is described in section 2.1.2 in materials and methods). Since then countless studies have been published since, which focus on the hippocampus and its role in cognition. (Best, 1999).

1.6 Decline of cognitive function during aging

The hippocampus is a prime target of diverse forms of neurodegeneration associated with cognitive impairments and memory loss. Hippocampal function,

such as the capacity to form and retrieve declarative memories, declines with age (Rosenzweig, 2003), a process that has been euphemistically termed ‘benign senescent forgetfulness’ (Kral, 1962) or age-associated memory impairment (AAMI) (Crook, 1986). Dementia is a more severe loss of one’s ability to form and retrieve new memories. Alzheimer disease is perhaps the most well known form of dementia, and extensive research has been carried out in the last decades in order to elucidate its causes (Haass, 2007).

However, even with normal and healthy aging, a mild and gradual decline in cognitive function can be observed. This can eventually lead in the long run to dementia. Therefore, it is extremely beneficial to investigate the onset of the decline, when few factors come into play, rather than in later stages, when dementia occurs and many factors can attribute the underlying causes. The mechanisms responsible for this gradual decline are poorly understood. Neuronal loss or neurodegeneration, protein aggregates or synapse dysfunction seem adequate be attributed as candidate underlying mechanisms (Crews, 2010). However, as the decline of cognition is already observed in middle-aged people, and neuron loss and synaptic dysfunction are not as prominent at this point in life, it is possible that the onset of AAMI can be caused by another underlying mechanism.

Several lines of evidence have indicated that age- associated memory impairment is accompanied by the selective and gradual down-regulation of genes involved with synaptic function (Lu, 2004). As discussed earlier, age dependant gene expression dysregulation is not a uniform phenomenon, based on the genes’ list (Loerch, 2008; Berchtold, 2008). However, recent studies suggest that epigenetic changes in the chromatin structure could be a key mechanism during memory formation and also contribute to the pathogenesis of neurodegenerative diseases.

1.7 The role of epigenetic mechanism on memory formation and possible therapy for AAMI

A number of recent studies showed that epigenetic mechanisms, such as chromatin remodelling via histone acetylation, are intimately involved in synaptic plasticity, learning and memory

In 2004, David Sweatt group (Levanson, 2004) observed a transient increase in global hippocampal histone acetylation one hour after fear conditioning (fear conditioning described in fig 2 materials and methods section under 2.1.1). This suggested that during the formation of new memories, the structure of the chromatin alters. The increase in the histone acetylation hints that gene expression is elevated and protein translation is thereby increased, a process, which as discussed previously, is crucial for memory formation. The Sweatt group used pan-histone acetylation antibodies for H3ac and H4ac but did not pursue in detail for individual acetylation sites.

By using a mouse model that allows for temporal induction of neuronal loss, (Fischer, 2007) it was shown that environmental enrichment reversed memory loss. Interestingly, the enrichment was associated with an increase of histone acetylation. Using HDAC inhibitors in this mouse model, the group of Tsai demonstrated that the HDACi increased histone acetylation, resulting in increase in dendrites, synapses and enhanced the learning abilities.

In line with these studies, the same group demonstrated that HDAC2 negatively regulates memory (Guan, 2009). Mice lacking HDAC2 display increased fear learning. HDAC2 knockout mice also exhibit higher histone acetylation level. Taken together, the studies suggest that HDACi, might serve as a suitable therapeutic avenue for treating dementia, and perhaps even Alzheimer and other advanced neurodegenerative diseases. In fact, several studies identified the activity of HDAC as potential target for therapy in Alzheimer (AD) and Huntington

diseases and other diseases and disorders. (Steffan, 2001; Ferrante, 2003; Hockly, 2003; Fischer, 2007; reviewed in Abel, 2008). Recently, a new study demonstrated (Kligore, 2010) that administrating various HDACi to young AD model mice (APP-Pre1) enhances memory consolidation. These mice display memory impairment in young age already in young age.

To summarise, recent studies suggested that histone acetylation is involved with the formation of memory, and that HDACi treatment enhances memory consolidation. Therefore, we were intrigued whether there are any epigenetic markers dysregulated in the brain during the normal course of aging. Furthermore, we wished to test if such epigenetic dysregulation might be involved with age-associated memory impairment. We wanted to test the hypothesis that epigenetic mechanism might underlie age-associated gene expression dysregulation in the aged brain. Finally we hypothesized that if our basic assumptions were correct, HDACi treatment might be also able to enhance the learning capabilities in aged mice.

1.8 Aim of the study

The main aim of the study was to identify a hippocampal histone acetylation signature in the onset of age related memory impairment. In order to elucidate the mechanism, we planned to combine behavioural and molecular approaches. We first aimed to detect the age in which Age Associated Memory Impairment (AAMI) is manifested by testing different mice age groups in behavior experiments. Once suitable groups were selected, we wished to detect acygenetic markers for AAMI and to test whether they had an effect on gene expression dysregulation.

Another aim of the study was to find if HDAC inhibitors might enhance memory consolidation in aged wild type mice and if so, which acygenetic targets are affected by the HDACi.

II Materials and Methods

2.1 Animals and behavior testing:

2.1.1 Fear conditioning

Mice (C57Bl6/J, Janvier) were housed under standard conditions with free access to food and water. All experiments were carried out in accordance with the animal protection law and were approved by the District Government of Germany. Behavior testing was performed as described previously (Fischer, 2007) using TSE Systems apparatuses and software as well as Freeze Scan software (Clever Systems).

In brief mice were single housed and habituated to the testing room at least 3 days before behavior experiments. To measure associative learning we employed the contextual fear-conditioning paradigm. The training consisted of a single exposure to the conditioning context (3 minutes) followed by a single electric foot shock (1mA, constant current for 2 seconds) and the memory test was performed 24 hours later (Figure 2). During the 3 minutes memory test, the freezing behavior was determined every 10 seconds. For each mouse, a total of 18 measurements were taken. The freezing behavior was quantified by calculating the number of measurements when the mouse showed a freezing behavior divided by the total number of measurements. (% Freezing = Freezing counts/18 *100). The testing cage was carefully cleaned with 70% ethanol and then dried before placing new mice in the cage.

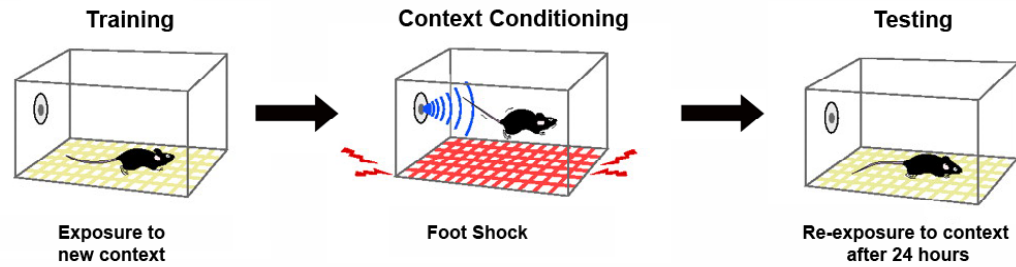


Figure 2. Contextual Fear Conditioning paradigm.

Mice were introduced to a new cage (novel context) and were allowed to explore it. After 3 minutes, the mice received a mild foot shock for 2 seconds. After the shock the mice return to their home cage. When the mice were reintroduced to the fear conditioning cage 24 hours later, the mice exhibit a freezing behavior, as they learn to associate the cage with the shock. (Adapted from Kandel, 2001 *Science*.)

2.1.2 Water Maze

The water maze (Morris, 1981) training was performed in a circular tank (diameter 1.2 m) filled with opaque water (1.5 Liters SAKRET Tiefengrund). A platform (11 x 11 cm) was submerged 1 cm below the water's surface in the center of the target quadrant. The swimming path of the mice was recorded by a video camera and analyzed by the Videomot 2 software (TSE). For each training session, the mouse was placed into the maze subsequently from four random points of the tank and was allowed to search for the platform for 60 seconds. If the mice did not find the platform within 60 seconds, they were gently guided to it. Mice were allowed to remain on the platform for 15 seconds. During the memory test (probe test) the platform was removed from the tank and the mice were allowed to swim in the maze for 60 seconds. At the end of the experiment the ability of mice to find a visible platform was performed to control for locomotor or sight deficits.

2.1.3 Cannulation and injection

16 month-old mice were anesthetized with 0.5 ml of filtered Avertin to avoid unnecessary infection (Fischer, 2002). The Avertin was prepared by dissolving 1 gram of 2,2,2-tribromoethanol to 1 mL of isoamylalcohol. Next, 1 mL of sterile water was gradually added until volume of 10 mL was reached. Further sterile water was added in increments of 5 mL until a total volume of 72 mL was reached. Between each water addition, the flask was thoroughly vortexed. The Avertin was then filtered and was stored in -20 degrees until use. During experiment, the avertin was wrapped in aluminum foil in order to avoid light, which cause the toxicity.

The anesthetized mice head were fixed in a Benchmark stereotaxic Instrument. The skin above the skull was carefully removed and the connective tissue beneath it was carefully cut. The exposed skull was cleaned with ethanol 70%. Using a cleaned 0.5 driller, two holes were bilaterally drilled in the mice skull (anterior/posterior -1.70 mm relative to bregma; medial/lateral +1 mm and -0.9 mm; dorsoventral -2mm). 2mm microcannulae was carefully mounted on the skull. The microcannulae was fixed with dental cement. During the first 5 minutes, the mice head was kept fixed until the cement hardened and the microcannulae was adequately fixed. Mice were carefully placed back in their cage, their body covered by tissue-tech and their head clear above the bedding. The cage was placed above a heating plate until the mice woke up from the anesthesia to increase the survival rate of the old mice.

During the administration of HDACi, mice were anesthetized with Isoforan. 0.5 mL of Isoforan was pipetted on a small tissue paper, which was placed in 0.5L beacon. The mice were place in the beacon until they were anesthetized. The drugs were bilaterally injected for one minute into the hippocampus by using a 3mm injector with 1mm adaptor. After one minute, the injector remained in the microcannulae for additional 10 second. After the injection, the dummy was placed in the microcannulae and the mice were carefully placed in their home cages.

A stock solution of SAHA (Tocris) was prepared in DMSO. Before the experiment SAHA (40 $\mu\text{g}/\mu\text{l}$) was dissolved in artificial cerebrospinal fluid (aCSF, D-glucose 10mM, MgSO_4 2.4mM, CaCl_2 2.5mM, NaCl 124mM, KCl 3.3mM, KH_2PO_4 1.2mM and NaHCO_3 26.4mM) and injected bilaterally into the hippocampus (0.25 μl , 0.25 $\mu\text{l}/\text{min}$). As such, the total amount of SAHA injected into the hippocampus was 10 μg . MS-275 was dissolved in DMSO and diluted in aCSF (3 $\mu\text{g}/\mu\text{l}$) and injected bilaterally into the hippocampus (0.25 μl , 0.25 $\mu\text{l}/\text{min}$). As such, the total amount of MS-275 injected into the hippocampus was 750ng. Sodiumbutyrate (NaB) was dissolved in aCSF and 50 μg were injected bilaterally into the hippocampus (0.25 μl , 0.25 $\mu\text{l}/\text{min}$).

2.2 Protein lyses, sub-cellular fractionation and Immunoblotting

The hippocampus tissue was isolated and prepared as previously described (Fischer, 2007) and was immediately kept in liquid nitrogen. The frozen tissue was kept at -80 at all times until usage. Brain tissue was homogenized in TX-buffer (50 mM Tris HCl, 150 mM NaCl, 2mM EDTA, 1% Triton-100, 1% NP-40, 0,1% SDS), subjected to the Bioruptor (Diagenode) for 15 minuets (High; 30 seconds ON, 30 seconds OFF). Next, the lysate was centrifuged at 12000 rpm for 10 minuets. The supernatant was used for immunoblotting.

Another method for protein isolation was Subcellular fractionation of hippocampus, which was made by using the Proteo Extract. Subcellular Proteome Extraction Kit (Calbiochem) to isolate cytosolic, membrane and nucleus protein fractions from Hippocampus tissue. 500 μL of ice cold Extraction buffer I with 2,5 μL Protease Inhibitor Cocktail were added to the tissue, which was homogenized with a sterile stroke and incubated for 10 minuets at 4 $^\circ\text{C}$ with gentle agitation on an end-over-end shaker. Lysate was pellet by centrifugation at 4 $^\circ\text{C}$ at 750 rcf for 10 minuets. Supernatant, containing the cytosolic fraction (Fraction I) was removed and stored on ice. Pellet was re-suspended with 500 μl ice cold Extraction Buffer II and 2,5 μL

Protease Inhibitor Cocktail. After incubation at 4°C for 30 minutes by gentle agitation, insoluble material was pelleted at 5500 rcf for 10 minutes. Supernatant containing the membrane fraction (Fraction II) were removed and stored on ice. Pellet were re-suspended by gentle flicking the tube with 250 µL Extraction Buffer III and 2,5 µL Benzonase Nuclease and incubated for 10 minutes at 4 °C by gentle agitation. Next the sample was centrifuged at 8500 rcf for 10 minutes. The supernatant containing the nuclear fraction (Fraction III) was removed and stored on ice.

The protein concentration was determined using Bradford protein assay (Bradford, 1976). In brief 3µL of sample was mix with 1ml of 1x Bradford dye (Bradford stock solution 5x. The dilution was made with PBS 7.0 pH). The mixed sample was incubated for 5 minutes. Next, the concentration was measured in a spectrometer.

The desired sample fraction was then mixed with 5x loading dye and was heated for 5 minutes in 95 degrees. Samples (40µg of the total lysate or 10-20µg of nuclear fraction lysate) were loaded on 12% acrylamide gel (Laemmli, 1970; performed as in Fischer, 2007) for total of 2.5 hours (45 minutes 60V followed by 105 minutes 100V). The gel was transferred 12 minutes on iBlot machine. (PVDF membranes for histone acetylation, Nitrocellulose membranes for HAT/HDAC). The membranes were blocked with 3% milk powder in PBS 7.4 Ph, 0.1% tween for one hour. Next, the membranes were incubated with first antibody for 1-2 days (Longer incubation normally of H4Kx antibodies). Membranes were incubated for 45 minutes with fluorescent secondary antibodies (1:15,000 in 0.5% milk in PBS-Tween), and then washed with PBS-Tween 3x 10 minutes. Before quantification using an Odyssey Imager (Licor), the membranes were washed with PBS briefly. It was made sure that responses were within the linear range.

2.3 Perfusion and Immunohistochemistry

Mice were anesthetized with an intraperitoneal injection of 0.75 ml of Avertin. The mice abdominal skin was cut by a longitudinal incision. The thoracic diaphragm was carefully cut laterally on both sides across the ribs with a sharp scissor. The heart was exposed and a perfusion needle was inserted into left ventricle of the heart. Shortly after inserting the needle, a small cut in the right auricle allowed the outflow of return circulation of the heart. Filtered PBS was pumped through the needle for 5 minutes (rate '9') until the liver was with no blood coloring. Next the fixation itself was done with ice-cold filtered 4% paraformaldehyde (PFA). After the fixation, the brain was carefully removed and was post fixed in 4% by gentle agitation for over night at 4 degrees. The next day, the tissue was placed in 30% sucrose for 3 days in 4 degrees. Later, the brain was carefully wiped from any liquid, were frozen in tin foil above liquid nitrogen until frozen and was placed in -80. Frozen brains were than embed with Tissue Tech and cut with a cryotome into 40 μ m thick coronal sections and stored in 1x PBS with Penicillin/ Streptomycin at 4°C.

For Immunohistochemistry (Coons, 1942; performed as in Fischer, 2007), brain sections were washed three times in TBS (PBS 7.4 pH containing 0.2% TX-100) for 10 minuets and blocked in Blocking Serum (5% goat serum, TBS 0.3%) for 2 hours. Next, free-floating immunostaining was performed with primary antibody (1:500/1000 diluted in Blocking serum) over night at 4°C, with small agitation. Sections were washed three times for 10-15 minuets with washing buffer (1% Goat serum in TBS 0.2%) before incubating 2 hours with secondary anti-rabbit Cy3-labeled or anti-mouse Alexa488-labeled antibody (1:500/1000 cy3 in TBS 0.3%). Finally, the sections were treated with 4',6-diamidino-2-phenylindole (DAPI) for 30 minutes and then mounted, dehydrated, and cover slipped with Mowiol.

2.4 Microscope

Fluorescence pictures were acquired and later quantified using Leica SP2 AOBS confocal microscope with Leica confocal Software (LCS). Gain and background settings were identical to all groups compared per experiments. In addition, all pictures per experiment containing all the groups compared were taken in the same microscope session without switching off the laser or changing any settings. Prior to the beginning of the pictures acquisition, the laser was allowed to heat up and proximally 30 blank picture slices were taken to achieve optimal laser power.

2.5 Antibodies

Antibodies for histone-acetylation and Psd95 were from Upstate (1:1000 for immunoblot and immunostaining). The H4K12 antibody employed for ChIP was from Abcam and H3k9 ChIP antibody was from Millipore. Synaptoporin, GLuR1 and Map2 antibodies were from Synaptic Systems (1:250 for immunostaining/immunoblot). Histone 4 was from abcam (1:500). Formin 2 antibody was a gift from Philip Leder.

2.6 Chromatin-immunoprecipitation (ChIP)

For ChIP (Jackson, 1978; Solomon, 1988; modified for whole tissue experiments by Diagenode company and our lab) the DNA-shearing Kit and One-Day ChIP Kit protocol from Diagenode (Diagenode, Belgium) was used according to the manufactures protocol (Detailed preparation and efficient work-flow including modified RT-PCR protocol in the Appendix A).

The following modifications were made to optimize the procedure for hippocampal tissue. Tissue was homogenized with twice the amount of the different buffers indicated during pre-shearing. DNA shearing was performed the Bioruptor (Diagenode) with the following settings (25 minutes in total, High, 30 seconds ON, 30 seconds OFF). Sheared chromatin samples were incubated for 60 minutes with 4 μ l of antibody in ultra sonic bath. Subsequently, the antibody-antigen complex was further incubated with pre-blocked beads and an extra of 500 μ l of ChIP buffer for 60 minutes. Afterwards, the beads were washed twice instead of a single wash step stated in the protocol. The antibody-beads complex was incubated for 45 minutes in the presence of Proteinase K. Purified DNA was analyzed on a Bioanalyzer (Agilent) using pico-RNA chip.

2.7 Quantitative Real Time PCR (qPCR)

qPCR was performed using a Roche 480 light cycler. cDNA was generated using the Transcriptor High Fidelity cDNA Synthesis Kit (Roche) and qPCR for individual genes were performed using the Roche Universal probe library (UPL) (Table 1A). Data was normalized to the housekeeping gene hypoxanthine phosphoribosyltransferase (Hprt) or the corresponding input in case of ChIP experiments (Detailed and modified ChIP-RT-PCR in Appendix A).

For the ChIP experiments, qPCR for specific genomic DNA was performed using SYBR Green I Master Kit (Roche). Primers for promoter regions were selected to be specific for the first 300bp upstream of the TSS. Primers for coding regions were selected on the basis of ChIP-Seq results (Table 1B).

Table 1a: Primer-Sequences used for qPCR analysis

Gene	Sequence (5' – 3')	UPL Probe
<i>Acly F</i>	GCCCTGGAAGTGGAGAAGAT	#10
<i>Acly R</i>	CCGTCCACATTCAGGATAAGA	#10
<i>Fmn2 F</i>	AACAGCAGAAGCCTTTTGTCA	#89
<i>Fmn2 R</i>	TTCTGCCAGTGGGAAGACA	#89
<i>Gsk3a F</i>	GAGCCACAGATTACACCTCGT	#76
<i>Gsk3a R</i>	CTGGCCGAGAAGTAGCTCAG	#76
<i>Hprt1 F</i>	TCCTCCTCAGACCGCTTTT	#95
<i>Hprt1 R</i>	CCTGGTTCATCATCGCTAATC	#95
<i>Marcks11 F</i>	GGCAGCCAGAGCTCTAAGG	#19
<i>Marcks11 R</i>	TCACGTGGCCATTCTCCT	#19
<i>Myst4 F</i>	GCAACAAAGGGCAGCAAG	#19
<i>Myst4 R</i>	AGACATCTTTAGGAAACCAAGACC	#19
<i>Ncdn F</i>	GCTCCTTAGCACCTCTCCAG	#75
<i>Ncdn R</i>	GCAGCTGCGAAGAAACCT	#75
<i>Prkca F</i>	ACAGACTTCAACTTCTCATGGT	#60
<i>Prkca R</i>	CTGTCAGCAAGCATCACCTT	#60
<i>Shanks3 F</i>	AGGACGTCCGCAATTACAAC	#97
<i>Shanks3 R</i>	AAGCTCAAAGTTCCTGCAA	#97
<i>Hdac1 F</i>	TGCTGGACTTACGAAACAGC	#81
<i>Hdac1 R</i>	GTCGTTGTAGGGCAGCTCAT	#81
<i>Hdac2 F</i>	CTCCACGGGTGGTTCCT	#45
<i>Hdac2 R</i>	CCCAATTGACAGCCATATCA	#45
<i>Hdac3 F</i>	TTCAACGTGGGTGATGACTG	#32
<i>Hdac3 R</i>	TTAGCTGTGTTGCTCCTTGC	#32
<i>Hdac4 F</i>	CACACCTCTTGAGGGTACAA	#53
<i>Hdac4 R</i>	AGCCCATCAGCTGTTTTGTC	#53
<i>Hdac8 F</i>	GCAGCTGGCAACTCTGATT	#63
<i>Hdac8 R</i>	GTCAAGTATGTCCAGCAACGAG	#63
<i>Hat1 F</i>	CCGGGAAAGATTACTGCAAG	#9
<i>Hat1 R</i>	CATAAACCCCTTCTAGCATGTTGC	#9

<i>Gcn5 F</i>	GAAGAGGACCCCTCATCCTCA	#60
<i>Gcn5 R</i>	GGAGAATTTGCCCGTAGAT	#60
<i>Pcaf F</i>	GGAGAAACTCGGCGTGTACT	#13
<i>Pcaf R</i>	CAGCCATTGCATTTACAGGA	#13
<i>Taf6l F</i>	GATGACCCACAGCTGATGAA	#51
<i>Taf6l R</i>	CCCCTGACCACATAAACAAAGT	#51
<i>Myst2 F</i>	AACTTCCAGGGCAAGGAGAT	#72
<i>Myst2 R</i>	AATGTCCACGGGATTCACA	#72
<i>Myst3 F</i>	CTCGTGTTTACCTCCCGTGT	#38
<i>Myst3 R</i>	AGATGGGGATTGGTTCAGC	#38
<i>P300 F</i>	ACATGATGCCTCGGATGACT	#64
<i>P300 R</i>	TAGGGGGCTGTGGCATATT	#64
<i>Cbp F</i>	CAGGCAGGTGTTTCACAGG	#1
<i>Cbp R</i>	GCATGTTTCAGAGGGTTAGGG	#1

Table 1B: Primer-Sequences used for ChIP-qPCR analysis

Gene	Sequence 5'-3'
<i>Fmn2</i> promoter R	TGTGTGTGTGTGTTCCCTGATGT
<i>Fmn2</i> promoter L	TGACAGGTTATCTCTGGGACCT
<i>Fmn2</i> coding region R	TTGGGGATGCTTTACTGATTCT
<i>Fmn2</i> coding region L	TAGGGGTGGACTTTGAAACACT
<i>Myst4</i> promoter R	ATCAGGGTAGAGACAGCTCCTG
<i>Myst4</i> promoter L	ACTGAGGTGCGGTCTTCTTAAA
<i>Myst4</i> coding region R	AAGAGCAGAAGGAGCTTTCAGA
<i>Myst4</i> coding region L	CCTGGTGATTTATGTGGACTCA
<i>Prkca</i> promoter R	GGAGAGCTAGCGTGTGTATGTG
<i>Prkca</i> promoter L	AGTCTGCGTGTCCAGCTCTGT
<i>Prkca</i> coding region R	AATTATCTGGACCCATGCTGAC
<i>Prkca</i> coding region L	TTTGCTGCTAGTTGTTGATGCT
<i>Shanks3</i> promoter R	AAAGGGGAGCTGGAAATAAAAG

<i>Shanks3</i> promoter L	GAGAGGAAACTCTGCTTCCTGA
<i>Shanks3</i> coding region R	CTGATAGTCCCTATGCCAACCT
<i>Shanks3</i> coding region L	GAGAGGGTTCTCGTGCAAAG
<i>Marcks11</i> promoter R	GCCTCTCCACTGTGAAGTATGA
<i>Marcks11</i> promoter L	GTGTGGAAATGAGAGAGGTTCC
<i>Marcks11</i> coding region R	CGTCCCAGCCGAACTATC
<i>Marcks11</i> coding region L	GAGCGCACTCACCTGTCC
<i>Gks3a</i> promoter R	CGGAATGGAGACAGAAGGTACT
<i>Gsk3a</i> promoter L	GGGCTTGACTTCACTTTTCAAC
<i>Gsk3a</i> coding region R	CCAAGCTACCTTGAACCTTTTG
<i>Gsk3a</i> coding region L	GGTAATGGCTCATTCGGAGTAG
<i>Acly</i> promoter R	CGGCTCTAGGAGGAGAACCTA
<i>Acly</i> promoter L	GGGATAAGAACGTCAGTTGCTC
<i>Acly</i> coding region R	ATAAAGCTTAGACCCGCACAAA
<i>Acly</i> coding region L	GGCTTTCTCGAAGAGGTGAGTA
<i>Ncdn</i> promoter R	CACTCCGCACTCTGACCAAT
<i>Ncdn</i> promoter L	TTCTCCTTAGCTCGAGCACT
<i>Ncdn</i> coding region R	CTGTCAGGCACTGGTAGGTGT
<i>Ncdn</i> coding region L	TGAACAAGATCCCCATCCTTAG

2.8 HAT/ HDAC assay

Nuclear lysates were prepared from hippocampal tissue using the ProteoExtract® Subcellular Proteome Extraction (Calbiochem 539790-1KIT). HAT assay was performed using the HAT Assay Kit (BioVision, K332-100) according to the manufactures protocol. HDAC assay was performed using the Fluorometric HDAC assay kit (BioVision, k330-100) according to the manufactures protocol. In brief, 120 µg of nuclear extract were incubated for 4 hours with the assay mix in Greiner 96 U Bottom Transparent Polystyrol plate. Analysis was performed using a

TECAN Infinite 200 Elisa reader.

2.9 Citrate Assay

Citrate was measured using the Fluorometric Citrate Assay Kit (BioVision, k655-100) according to the manufacturer's protocol. The following modifications were made to manufacturer's protocol. The tissue was homogenized with 300 μ l of the assay buffer. Following centrifugation, 25 μ L of the supernatant was diluted with 25 μ L of assay buffer. The samples were incubated for 30 minutes in 50 Greiner 96 Flat Bottom Black Polystyrol plates. Following incubation, samples were measured using a TECAN Infinite 200 Elisa reader.

2.10 Microarray study

The microarray study was carried out as mono-color experiment. Total RNA was Cy3 labeled according to Agilent's Low RNA Input Fluorescent Linear Amplification Kit and hybridized to Agilent Whole Mouse Genome 4x44K G4122F microarrays according to the manufacturer's protocol. Quantity and Cy-dye incorporation rates of the generated target material were assessed using a NanoDrop ND-100. Post processing washes were done according to the Agilent Technologies SSPE protocol (v2.1), replacing wash solution 3 by acetonitril, followed by immediate scanning using an Agilent G2505B scanner. Intensity data were extracted using Agilent's Feature Extraction (FE) software, version 9.5.3.1 and analyzed using the Limma (Smyth, 2004) package of Bioconductor (Gentelman, 2004). The microarray data analysis consists of the following steps:

1. Between-array normalization, 2. Fitting the data to a linear model and 3. Detection of differential gene expression. VSN normalization (Huber, 2002) was

applied to the intensity values as a method for between-array normalization, to assure that the intensities had similar distributions across arrays. To estimate the average group values for each gene and assess differential gene expression, a simple linear model was fit to the data, and group-value averages and standard deviations for each gene were obtained. To find genes with significant expression changes between groups, empirical Bayes statistics were applied to the data by moderating the standard errors of the estimated values (Smyth, 2004) P-values were obtained from the moderated t-statistic and corrected for multiple testing with the Benjamini-Hochberg method (Benjamini, 1995). For each gene, the null hypothesis, that there is no differential expression between degradation levels, was rejected when its adjusted p-value was lower than 0.05. The microarray data discussed in this paper are generated conforming to the MIAME guidelines and have been deposited in NCBI's Gene Expression Omnibus. Data are accessible through GEO Series accession number GSE20270:

(<http://www.ncbi.nlm.nih.gov/geo/query/acc.cgi?acc=GSE20270>).

2.11 Data mining for microarray

GO association analysis was carried out using the topGO package of Bioconductor (Alexa, 2006). KEGG pathway enrichment analysis was performed using the functional annotation tool of the Database for Annotation, Visualization, and Integrated Discovery (Shimohata, 2000; Huang 2009; Dennis, 2003) with an EASE score threshold (a modified Fisher Exact p-value) of 0.05. For visualization of the associations between pathway genes and differentially expressed genes, array data were mapped to KEGG resources (Kanehisa, 2000) using the KegArray software package (Kanehisa Laboratories: <http://www.genome.jp>).

2.12 ChIP-sequencing

Sequencing was performed in an Illumina “GAII” Genome Analyzer at FASTERIS SA (Plan-les-Ouates, Switzerland) using the Chrysalis 36 cycles v3.0 sequencing kit. Protocols for Illumina Solexa Sequencing and quality evaluation are provided by Illumina (Illumina, San - Diego, Ca) at http://www.illumina.com/applications.ilmn#dna_sequencing

Each biological replicate of 3 and 16 month-old mice was run separately.

2.12.1 Solexa pipeline analysis and mapping to mouse genome

Sequence reads were obtained and mapped using the GAPipeline1.5 analysis pipeline and ELAND algorithm. In brief, ELAND finds all matches with a maximum of 2 errors in the first 32 bases on the reference sequence, the *Mus Musculus* Full Genome (NCBI Assembly M37). Up to the 10 position best match position on the genome are recorded.

The output of the uniquely mapped reads was converted to browser extensible data (Bednarik, 1991) files detailing the genome coordinates of each read. For all samples, between 78.2% and 94.5% of the reads were mapped on the genome producing in case of H4K12ac a total number of 5.5 and 6.1 millions uniquely mapped reads for young and old, respectively and in case of H3K9ac a total of 5.3 and 4.9 million reads for young and old, respectively. Ratios between numbers of reads/replicate were comparable for samples with the same histone modification (H4K12: young (2:2.2:1.3), old (2.2:2:1.8); H3K9: young (1.6:3.7), old (1.6:3.3)).

2.12.2 Identification of H4K12 and H3K9 acetylation enriched regions

Chromatin modification profiles are frequently noisy and diffuse (Zang, 2009). To

extract signal from background noise, we identified H4K12 and H3K9 enriched domains in the genome using the Statistical model for Identification of chip-Enriched Regions (SICER) described by (Zang, 2009). In that work, this algorithm has proved to be superior in identifying statistically significant chromatin modifications against algorithms until now commonly used in ChIP-*seq* peak finding, which are more suitable for transcriptional factor binding site identification. Moreover filtering with islands applied with SICER has previously been shown to be a reliable method for data normalization in quantitative comparison of histone-modification profiles. SICER produces clusters of enriched windows (islands) unlikely to appear by chance based on a random background model. To increase depth of sequencing SICER was run for pooled replicate reads of each group (young/old).

Running parameters for SICER were as follows: i) Window size: 200. ii) Gap size. As noted by the developers of SICER, gap size is an important parameter to be adjusted to the characteristics of the modification tested (usually smaller for localized signals similar to transcriptional factor binding patterns, bigger for more diffuse). We performed, as described in the above mentioned work of Zang et al, plotting of total island scores calculated by SICER against different gap values $g=0$, $g=200$, $g=400$ and $g=600$ and defined $g=400$ to be near the saturation point of the resulting aggregate scores for H4K12 and H3K9. This is in agreement with the relative diffuse profiles of these two modifications described previously in T cells. Thus, a gap value of 400 was used. iii) E-value.

To control the genome wide error rate of identified islands under the random background we used an E-value of 1000 and 500 for H4K12 and H3K9, respectively, which correspond, as previously described by Wang et al (Wang, 2009), to an FDR of 3% in young H4K12, 5% in old H4K12, 5% in young H3K9 and 4% in old H3K9.

2.12.3 Profiles of H4K12 and H3K9 enrichment around TSS and across gene bodies regions

For each gene, uniquely mapped reads were filtered to take into account only those mapped within identified islands as previously described (Wang, 2009). For profiling around TSS, for each modification, using custom python scripts, number of reads was calculated in each point 1bp to 1kb or 5kb in both directions relative to the aligned TSS of selected groups of genes. For normalization, all reads counts have been weighted according to the number of counts in each group (young/old). For profiling within gene bodies, reads were summed in windows equal to 1% of the gene length (or 5% in case of figure 17) and divided to the total length of each section to produce a Tag density value along the aligned gene bodies of a specific group of genes. Normalized Tag density was obtained based on the ratio of number of reads between young and old for the specific modification.

2.12.4 Definition of gene coordinates and visualization of ChIP-seq data along the genome

The analyzed TSS and gene bodies coordinates were based on transcription start and end sites inferred from mouse RefSeqs (downloaded from the UCSC Genome Browser, Sep.2009). Visualization of reads along the mouse genome was performed using the UCSC Genome Browser. The respective wiggle files were constructed based on the filtered by SICER reads binned into non-overlapping windows of 100bp along the genome and normalized to the total number of reads.

2.12.5 Analysis of base coverage of chromatin modifications

To identify the percentage of coverage for a chromatin modification we did the following: Gene intervals were downloaded by UCSC as described previously, including 1kb upstream of TSS of the genes. Genome wide intervals complements

to the above gene intervals were calculated to represent non-coding regions. Enriched islands identified by SICER were intersected with these intervals to identify overlapping pieces of intervals.

Then the respective base coverage of these pieces was calculated and divided with either the total base coverage of gene and non-coding intervals (to define what percentage of each feature is enriched with the modification) or with the total base coverage of enriched regions (to define which percentage of this region belongs to coding or non coding regions). BED files of ELAND uniquely mapped reads for each sample as well as BED files with SICER outputs of enriched regions for each modification are available as galaxy datasets through the Galaxy data-sharing platform (Taylor, 2007; Blankenberg, 2007) (<http://main.g2.bx.psu.edu/u/fischerlab/h/sm1186088>; published history sm1186088).

2.13 Statistical analysis

The data was analyzed by unpaired student's t-test and one-way ANOVA (Analysis Of Variance). Errors are displayed as Standard Error of the Mean (S.E.M.)

III Results

3.1 16-month old mice display impaired learning and memory

In order to detect an age at which cognitive impairment first manifests, we subjected 3-, 8- and 16 month-old mice to contextual fear conditioning. Fear conditioning is a commonly used test for hippocampus-dependant associative memory (Fig 2). All the groups were able to learn the task, which was shown by an increase in freezing behaviour 24 hours after re-exposure to context (The cage). However, 16 month-old mice displayed significantly less freezing behaviour than the younger mice (Fig 3A). Importantly all the groups showed similar activity during training (Fig 3B) as well as similar responses to the electric stimulus (Fig 3C). Thus the difference in the freezing behaviour cannot be attributed to different explorative behaviour.

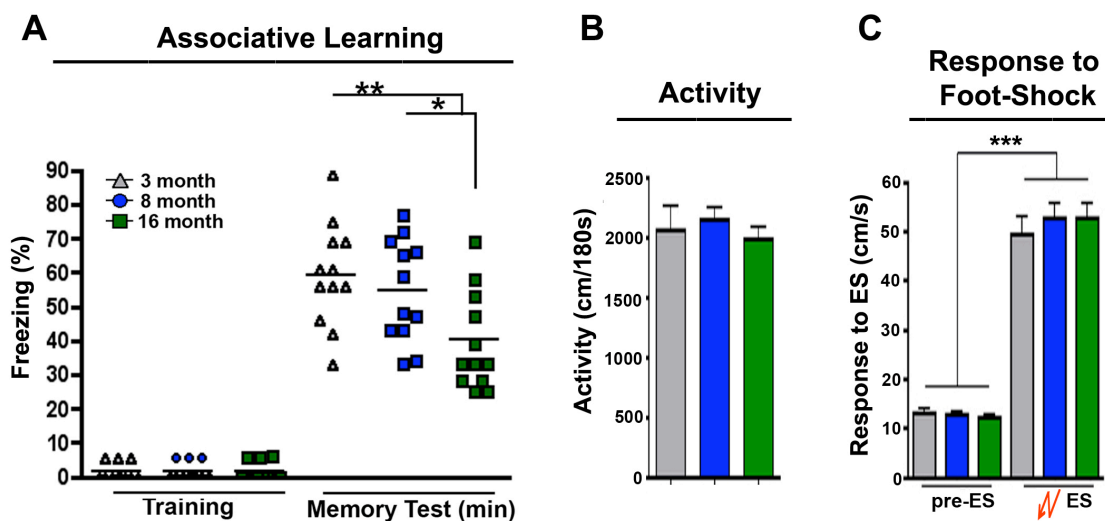


Figure 3. Impaired associative learning and memory in 16 month-old mice.

(A) 3 month, 8 month and 16 month-old mice (n=12 per each group) were subjected to fear conditioning. While all groups were able to learn the task ($P < 0.0001$ freezing “test” vs. “training”), 16 month-old mice displayed impaired learning ($*P < 0.05$; $**P < 0.01$). (B) Distance travelled during the 3 minutes test did not differ between the groups. (C) The response to an electric foot shock (0.7mA, 2 seconds constant) was similar among the groups ($***P < 0.001$ pre-ES vs. ES). Error bars indicate S.E.M.

Additional groups of mice were trained in Morris water-maze, an established test for hippocampus-dependant spatial memory. All groups improved in their ability to find the hidden platform throughout the training. However, the escape latency was significantly impaired in 16 month-old mice compared to the younger groups (Fig 4A). Importantly, all mice were able to reach the visible platform and their swim speed was similar among the groups. Therefore, the impairment of 16 month-old mice in the water-maze cannot be explained by poor vision. In addition, 16 month-old mice consistently spent less time in the target quadrant during a subsequent probe test (Fig 4B). The findings from both fear conditioning and water maze suggest that impairments in hippocampus-dependent memory formation have already manifested in 16 month-old mice.

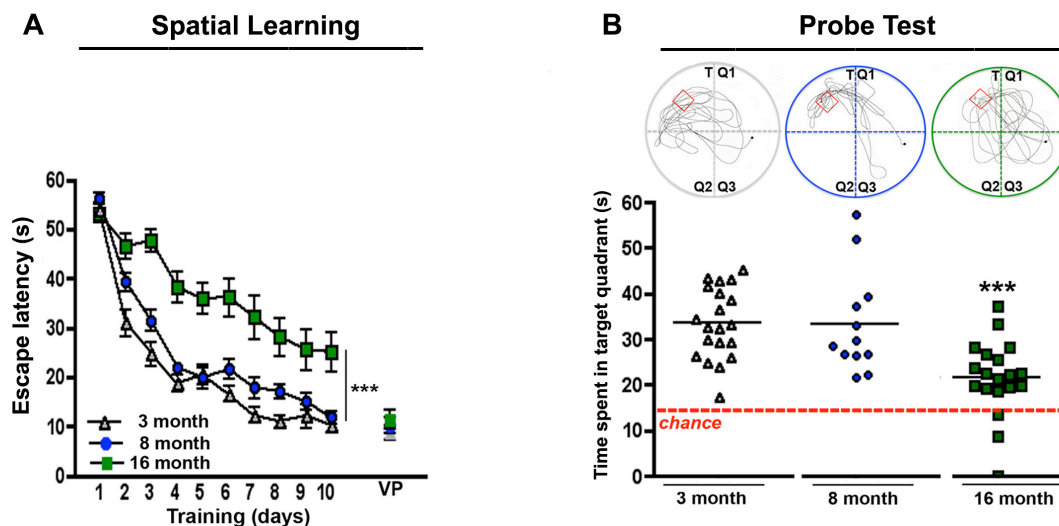


Figure 4. Impaired spatial learning and memory in 16 month-old mice.

(A) 3 month (n=20), 8 month (n=12) and 16 month-old mice (n=20) were trained in the water maze paradigm. All groups improved in their ability to find the hidden platform. ($P < 0.001$ day 1 vs. day 10). However, 16 month-old mice displayed reduced escape latency throughout the training. ($***P < 0.001$). Error bars indicate S.E.M. (B) Upper panel: representative swim paths of mice during the probe tests. Lower panel: During a probe test, 16 month-old mice showed reduced preference for the target quadrant (T). Q, quadrant. T, Target. VP, visible platform.

3.2 Molecular analysis of naïve 3-month old mice versus 16-month old mice

As the performance of 3 month-old mice was similar to 8 month-old mice, we chose to focus only on the 3 month-old mice and compare them to 16 month-old mice.

3.2.1 Markers for neuronal plasticity and integrity are similar

Next we tested whether the impaired learning, which is observed in 16 month-old mice, can be linked with structural changes in the hippocampus. Hippocampal levels of microtubule-associated protein 2 and synaptopodin (Fig 5A), as well as postsynaptic density-95, synaptophysin and glutamate receptor-1 (Fig 5B) were similar between 3- and 16 month-old mice. Thus, the memory impairment in the 16 month-old mice cannot be explained by major structural changes in the hippocampus.

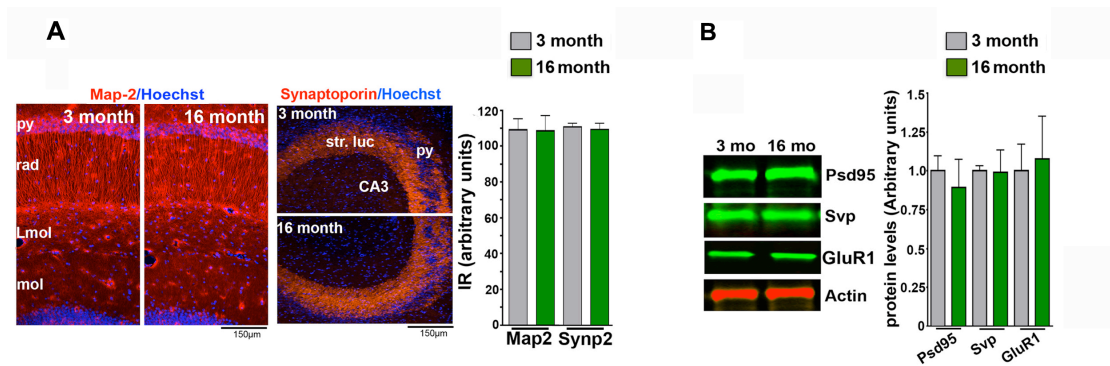


Figure 5. Morphological characterisation of naïve 3- and 16- month-old hippocampus.

(A) Hippocampal immunoreactivity of microtubule-associated protein 2 (MAP-2) and Synaptoporphin (Synp2). (B) Quantitative Immunoblot of postsynaptic density-95 (PSD-95), Synaptoporphin (SVP) and Glutamate receptor 1 (GluR1) in the hippocampus. Data normalized to actin, which served as loading control. Py, pyramidal cell layer of CA1 region; rad, stratum radiatum; str. Luc, stratum lucidum; Lmol, lower molecular layer; mol, molecular layer. Error bars indicate S.E.M.

3.2.2 Levels of hippocampal bulk histone-acetylation are similar among the naïve groups

Chromatin plasticity has been recently shown to be involved in memory formation (Levenson, 2004; Vecsey, 2007). We first investigated if hippocampal histone acetylation differs between 3- and 16 month-old naïve mice. Quantitative Immunoblot analysis reveals no difference between the groups of bulk levels of H3K9, K14 and H4K5, K8, K12 or K16 (Fig 6). These data suggest that prior to the learning experience the histone acetylation levels are similar between the groups and therefore, less likely to account for the memory impairment.

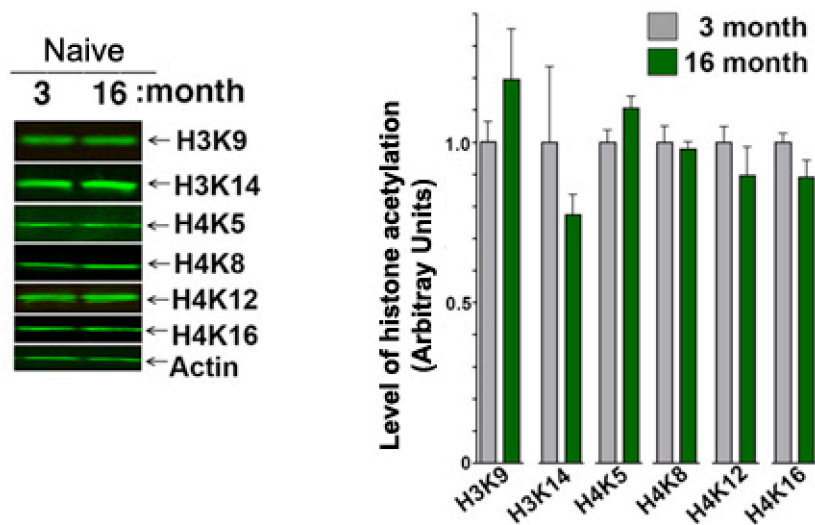


Figure 6. Levels of hippocampal bulk histone acetylation are similar among 3 and 16 month-old mice. Quantitative immunoblot analysis showed similar level of histone acetylation for H3K9, 14 and H4K5, 8, 12, 16 between 3 and 16 month-old mice. Data was normalized to Actin. N=4 per group. Error bars indicate S.E.M.

3.2.3 Similar HAT and HDAC levels and nuclear activity between the naïve groups

Next we wished to assess the profile of both expression and activity of various HATs and HDACs in the hippocampus of 3- and 16 month-old naïve mice. Quantitative PCR revealed no difference in the level of expression of neither HATs nor HDACs in naïve mice (Fig 7A). In addition, immunoblot analysis showed no difference in the hippocampal protein level of class I HDAC or Creb Binding Protein (Fig 7B). Finally, the nuclear activity levels of both total HDACs and HATs were similar between the groups (Fig 7C). These results, along with the previous figure, suggest similar epigenetic properties in naïve 3- and 16 month-old mice.

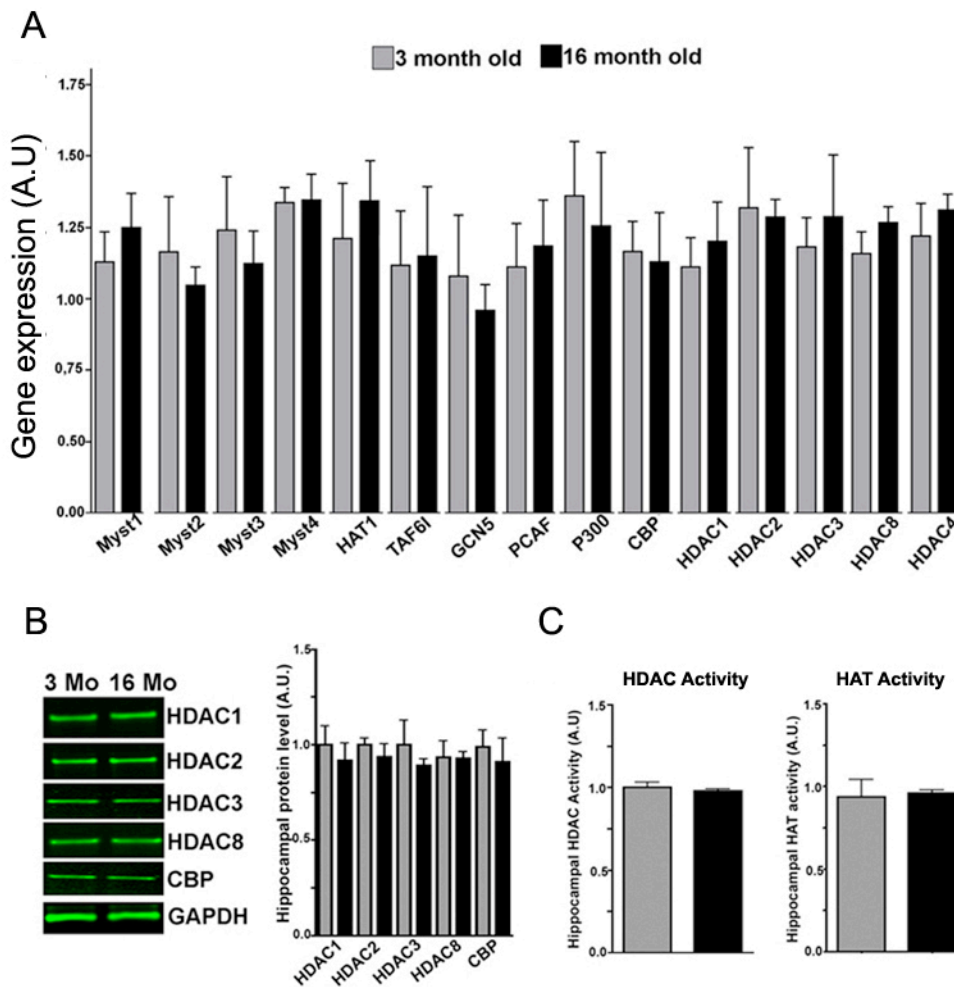


Figure 7. No differences in HAT and HDAC levels and activity in the hippocampus between naïve 3 and 16 month-old mice.

(A) Hippocampal tissue was isolated from naïve 3 and 16 month-old mice and levels of major HATs and HDACs were analyzed by qPCR. No significant differences were observed. (B) Quantitative immunoblot analysis of class I HDACs and Creb Binding Protein (CBP) supports (A). Data was normalized to GAPDH. (C) Nuclear lysates were tested for the activity of HAT and HDAC. The assays revealed no difference between the groups. N=4-6 per group. Error bars indicate S.E.M.

3.3 Impaired learning and memory in 16-month-old mice after fear conditioning correlates with H4K12 acetylation

A previous study suggested that histone acetylation might play a role in orchestrating the gene expression program, which is induced by memory consolidation (Levenson, 2004). Therefore we speculated that impaired histone acetylation might be linked to age related learning and memory impairment. We used a quantitative immunoblotting to analyze histone acetylation levels in 3- and 16 month-old mice at different time points after the beginning of the memory consolidation, induced by the electric shock (Fig 8A). Hippocampal tissue was isolated from control mice and mice which received foot. From fear-conditioned mice, the hippocampus was isolated at 10, 30, 60 minutes and 24 hours after the shock. When compared with naïve group, 3 month-old mice displayed a transient increase of H3K9, H3K14, H4K5, H4K8 and H4K12 acetylation 60 minutes after the shock (Fig 8B, C). A similar transient increase was observed in 16 month-old mice for H3K9, H3K14, H4K5 and H4K8 acetylation. In striking contrast, 16 moth- old mice failed to increase H4K12 acetylation after 60 minutes (Fig 3B, C). Notably, in both groups, acetylation levels returned to the basal level after 24 hours.

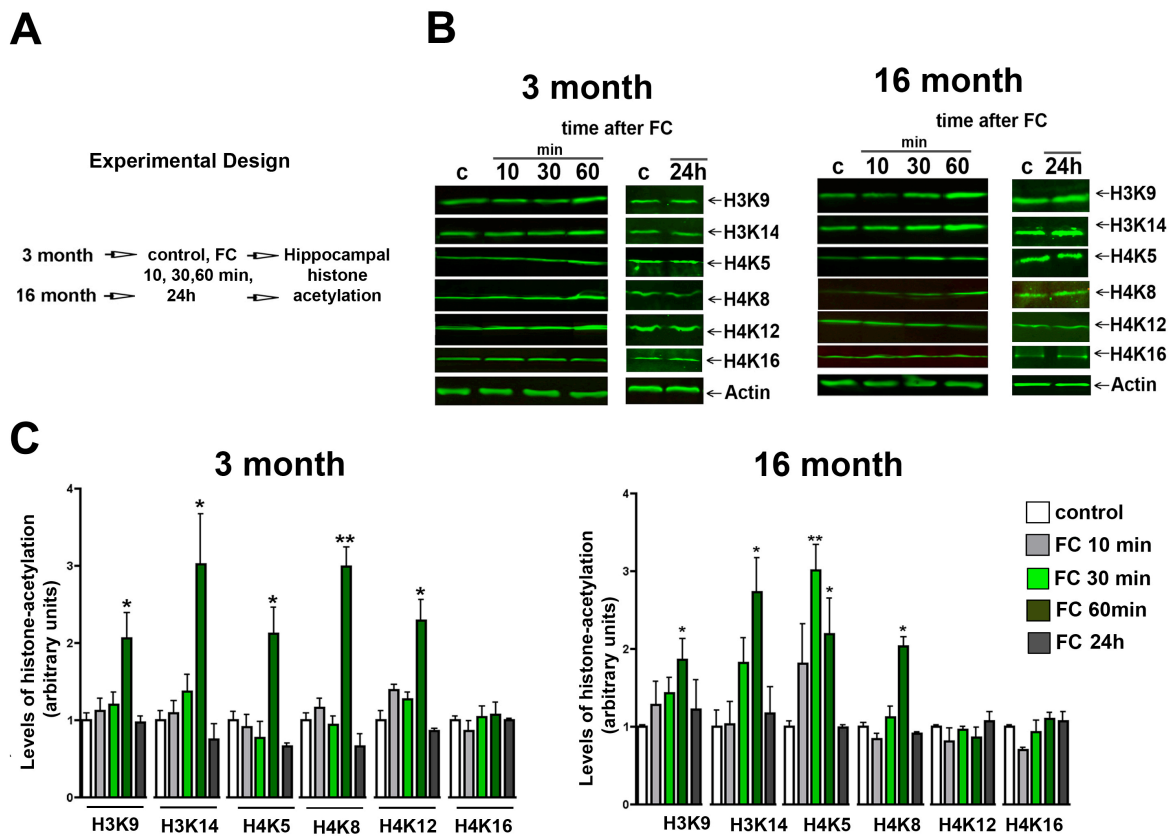


Figure 8. Impaired learning and memory in 16 month-old mice correlates with dysregulated H4K12 acetylation.

(A) Experimental design. (B) Representative immunoblot showing the hippocampal histone acetylation levels in 3- and 16 month-old mice in response to fear conditioning (FC). Control (c) groups did not receive any foot shock. (C) Quantification of (B). Data was normalized to actin levels (** $P < 0.01$, * $P < 0.05$). $N = 4-5$ per group. Error bars indicate SEM.

As a control for our previous experiment, total levels of Histone 4 were compared before and after fear conditioning. Total Histone 4 levels were not altered in fear conditioned 3 and 16 month-old mice (Fig 9). This suggests that an increase in histone acetylation is not likely to result from increase levels of total histones.

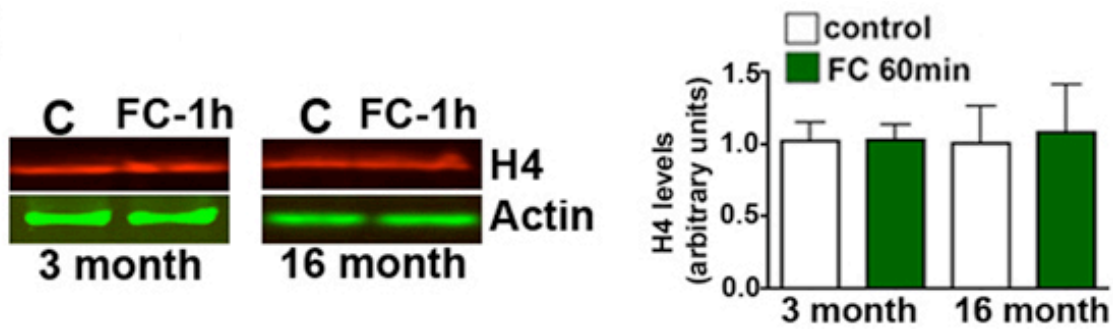


Figure 9. Histone 4 levels do not increase following fear conditioning.

Right panel: Representative Immunoblot of Histone 4. Left panel: Quantification. The levels of total H4 in 3 and 16-month old mice was not altered 1h after fear conditioning. Data was normalized to actin levels. Error bars indicate SEM.

3.4 Dysregulated H4K12 acetylation in 16-month-old mice after fear conditioning is observed in all hippocampal sub regions

In order to investigate whether H4K12 dysregulation in 16-month old mice is restricted to specific sub regions of the hippocampus, an Immunohistochemistry for H4K12 was performed on a hippocampus slice.

Confirming our immunoblot time line, 3 month-old mice up regulated H4K12 acetylation levels in response to fear conditioning, while 16 month-old mice failed to do so (Fig 10). The increase of histone acetylation in the 3 month-old mice was not restricted to specific sub regions or a specific cell type but rather generally regulated. Thus we continued with the experiments using the entire hippocampus (Microarray study, the ChIP, etc...). Interestingly, the immunoblot revealed an increase in H4K12 in naïve 16 month-old mice when compared to 3 month-old mice, which contradicts the immunoblot data showing no difference.

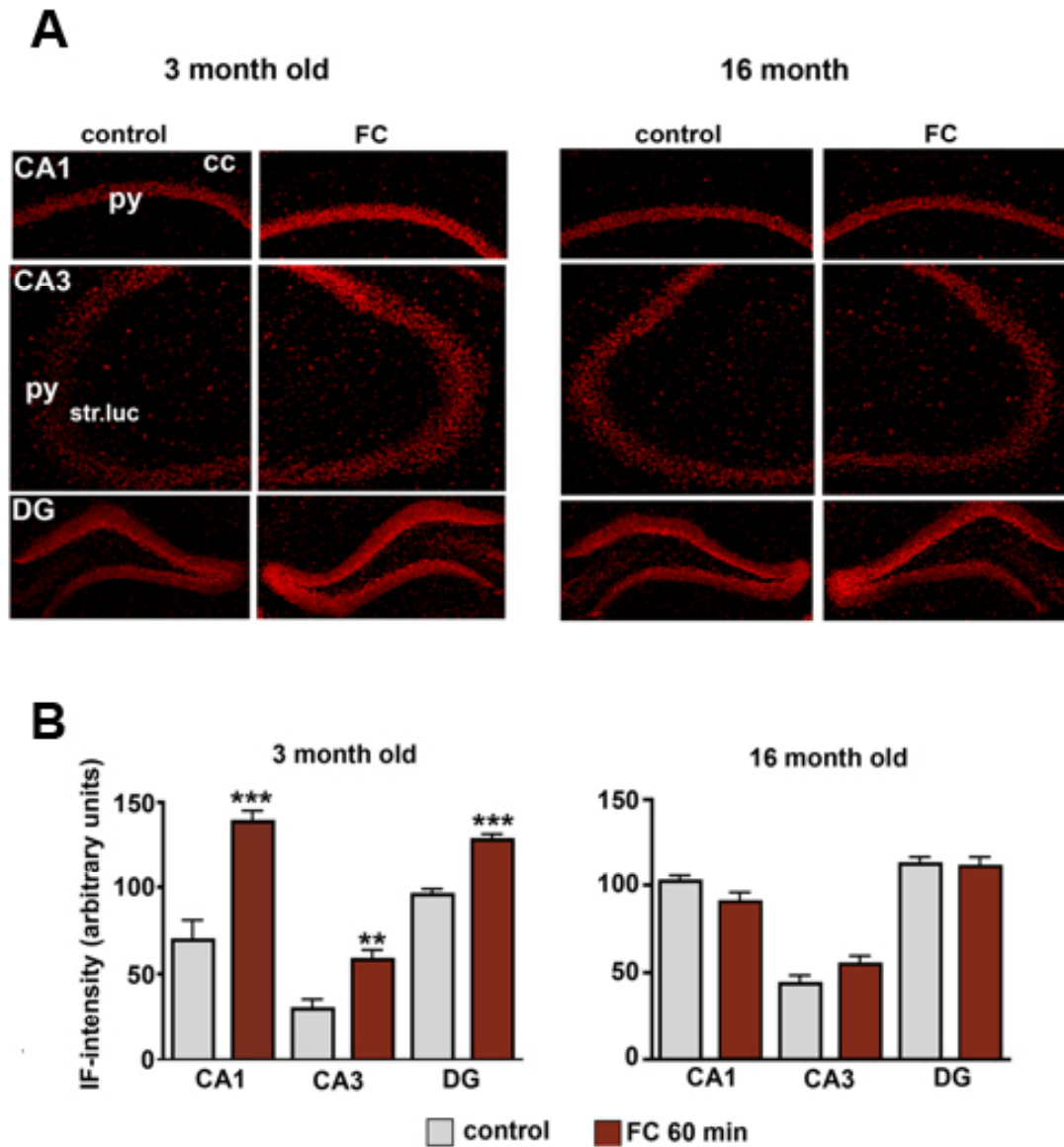


Figure 10. Impaired learning and memory in 16 month-old mice correlates with global hippocampal dysregulated H4K12 acetylation.

(A) Representative Immunohistochemistry picture showing the hippocampal H4K12 acetylation levels in 3- and 16 month-old mice in response to fear conditioning (FC). Control groups did not receive any foot shock. (B) Quantification of (A). (***) $P < 0.001$, (**) $P < 0.01$. $N = 4-5$ per group. cc, corpus callosum, DG, Dentate gyrus, Str. Luc, stratum lucidum Error bars indicates SEM.

3.5 Impaired transcriptome plasticity during memory consolidation in 16-month-old mice

In order to analyze if the impairment of learning and memory observed in 16 month-old mice correlates with dysregulation of gene expression, we performed a high-density oligonucleotide microarray. We compared the hippocampal tissue gene expression profile before and after memory consolidation, in both 3- and 16 month-old mice (Fig 11). Notably, the gene expression profile was similar among 3- and 16 month old naïve mice (Table 3). This is consistent with our previous findings (Figure 6) showing similar levels of histone acetylation between 3- and 16 month-old mice. In 3 month-old mice, 2229 genes (1977 up-regulated and 252 down-regulated) were differently expressed 60 minutes after fear conditioning compared with the age matched control group (Full microarray tables can be downloaded at <http://www.sciencemag.org/cgi/data/328/5979/753/DC1/1>). However, the hippocampal transcriptome of 16 month-old mice remained almost unchanged in response to fear conditioning. When compared with the age-matched control group, only six genes were differentially expressed among the fear-conditioned group (Table 4).

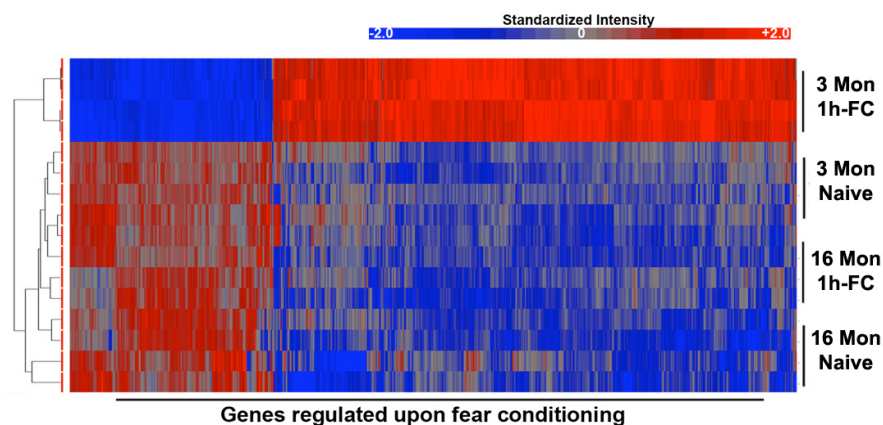


Figure 11. Impaired transcriptome plasticity in 16 month-old mice.

Heat map showing differentially expressed genes in 3 and 16 month-old mice after FC versus control.

N=4 mice per group.

Gene Name	16 month-old mice control vs. FC-1h. FDR<5%; Fold change (log2)≥1	Adjusted P value
Sult1c2	-1.9	0.00186
Erdr1	-1.7	0.00351
1700112E06Rik	-1.6	6.48e-06
C4b	-1.6	0.012
C3	-1.5	0.000141
Cox8b	-1.5	0.0287
Zic1	-1.1	0.000337
Col6a3	-1.1	0.0185
Plac9	-1.1	0.00172
Cd52	-1.1	0.0438
BC061194	-1.0	0.00482
BC038167	-1.0	0.0264
2810459M11Rik	1.3	0.0461
Wdfy1	1.6	1.64e-06

Table 3. Genes differentially expressed between 3 and 16-month-old naive mice.

By microarray analysis we identified only 14 genes that were differentially expressed between 3 and 16-month old mice that were not subjected to fear conditioning. This is consistent with our data, showing that no changes in hippocampal bulk histone-acetylation were detected between 3 and 16-month-old mice naïve mice (Figure 6). n=4/group.

Gene Name	16 month-old mice control vs. FC-1h. FDR<5%; Fold change (log2)≥1	Adjusted P value
Agxt211	1.14	0.0000766
Iandl	1.2	0.0014568
Unc13a	1.25	0.0125997
Slc17a6	1.3	0.0328686
Rab37	1.4	0.0004587
Fos	1.62	0.0456926

Table 4. Genes differentially expressed between 16-month-old 1hour after fear conditioning and age-matched control mice.

Analysis of the microarray data revealed that only 6 genes were differentially expressed between 16-month-old mice 1 hour after fear conditioning when compared to the age-matched control group. Four of those genes (Fos, Iandl, Rab37, Unc13c) are similarly regulated in 3-month old mice upon fear conditioning. Only two of those genes (Rab37 and Unc13-c) are specific to associative learning (After further data processing as described in figure 12). FDR, False Discovery Rate.

During fear conditioning, the mice were also exposed to novel environment, such as a novel cage and electric shock. We wished to isolate the genes specifically linked to associative memory, rather than to the exposure to the new environment and the shock itself. To this aim, we added additional microarray study to detect the genes that are specific to the memory consolidation. In addition to a fear conditioned (Context followed by shock, fig 12A) group, which shows increase freezing 24 hours when re-introduced to the context, we added two additional groups. The first group was exposed only to the novel context (Fig 12B) and therefore shows no freezing behaviour after 24 hours. The second mice group first received the shock and were then allowed to explore the cage (Fig 12C). These mice, as well, showed no freezing behaviour, as they did not learn to associate the shock with the cage. We first compared the gene expression of each of the groups with the control mice before further processed the results. The Venn diagram shows that out of the initial differentially regulated 2229 genes, 1539 (1362 up-regulated and 178 down-regulated) were specifically linked to associative learning (Fig 12D). These genes are hereafter called “learning induced genes”.

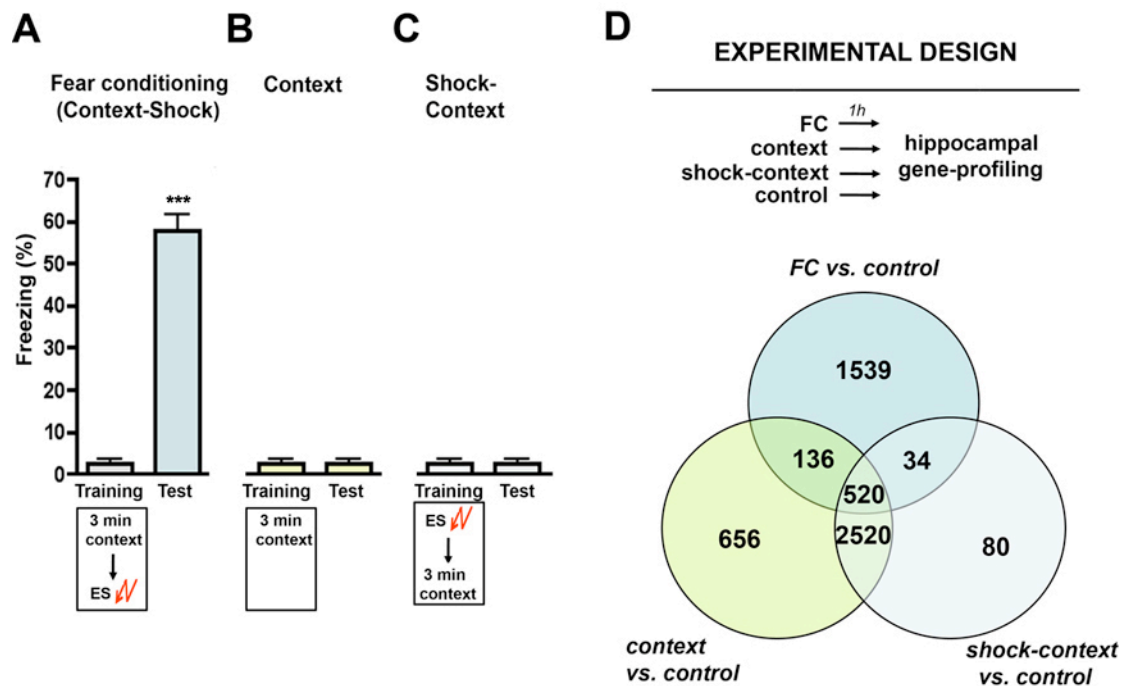


Figure 12. The majority of genes regulated upon fear conditioning are specific to associative learning.

(A) 3 month-old mice were subjected to a novel context for 3 minutes followed by a mild foot shock (2 seconds, 0.7MA). The mice displayed an increase in aversive freezing behaviour when re-exposed to the same context after 24 hours (B) When 3 month-old mice were subjected to novel context for 3 minutes without the shock, the mice did not show an increase in freezing when re-exposure to the context. (C) In addition, 3 month-old mice did not display an increase in freezing after re-exposure to the context, when during the training the mice received first the foot shock and only afterwards were allowed to explore the context. (D) A Venn diagram of gene expression comparison between FC vs. control, Context vs. control and Shock-context vs. control. Out of the 2229 genes, which were regulated in FC, 70% were specific to associative learning (1539 genes). All mice were 3 months old. (***) $P < 0.001$. $N = 4$ per group. Error bars indicate SEM.

Further data mining showed that the learning-induced genes were associated with biological processes such as transcription, protein modification or intracellular signalling (Fig 13).

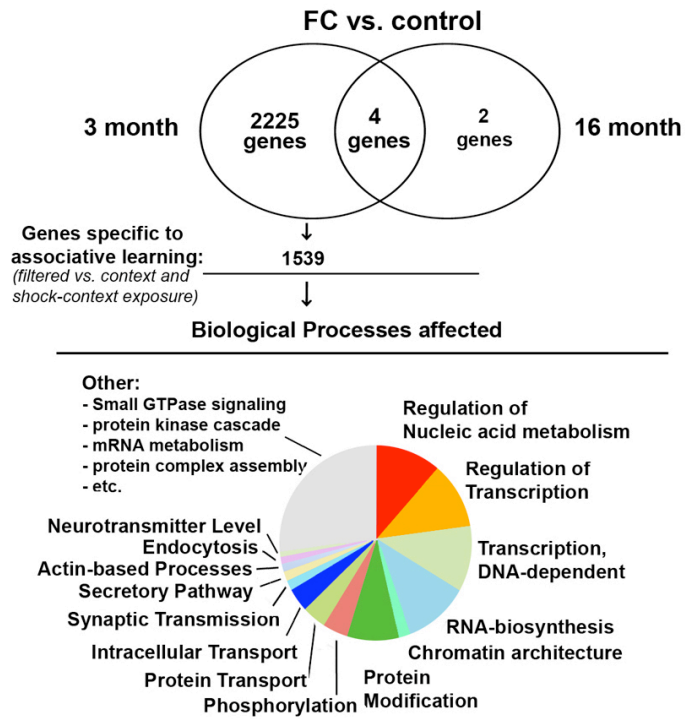


Figure 13. Biological processes analysis for the up regulated genes upon fear conditioning in 3 month-old mice.

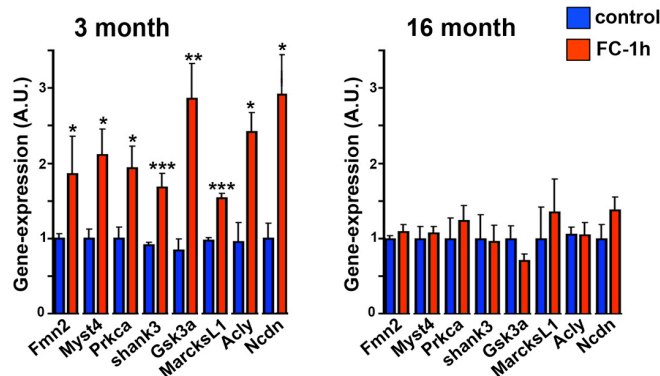
Upon fear conditioning, 3 month-old mice regulate 1539 genes, termed learning-regulated genes. The genes are associated with biological process such as transcription, chromatin architecture, protein modification nucleic acid metabolism and others.

Further analysis shows that 3 month-old mice regulate key signaling pathways implicated with memory formation and synaptic remodelling in response to fear conditioning (Table 5).

Significant KEGG pathways identified in the gene set of “learning-regulated genes”		
Term	P-Value	Benjamini
Phosphatidylinositol signaling system	0,010091396	0,109829511
ErbB signaling pathway	1,75E-04	0,008480029
MAPK signaling pathway	6,80E-04	0,021878567
Regulation of actin cytoskeleton	0,010905501	0,112007383
Long-term depression	9,99E-04	0,027453667
Long-term potentiation	0,013128751	0,120896837
Gap junction	0,002524448	0,043819107
Tight junction	5,09E-05	0,003299939

Table 5 . Molecular pathways regulated in 3-month-old mice during fear conditioning.

In order to confirm the microarray results, we chose eight representative learning-induced genes and performed qPCR. The results obtained confirmed the previous results (Fig 14).



Gene ID	Gene Name	Biological function
Fmn2	Formin 2	Regulation of Actin cytoskeleton
Myst4	MYST histone acetyltransferase monocytic leukaemia 4	Histone acetyltransferase
Prkca	Proteinkinase C alpha	Proteinkinase
MarcksL1	SH3/ankyrin domain gene 3	Regulation of synapse structure
Shank3	Myristoylated Alanine-Rich C Kinase Substrate-like 1	Cell differentiation; proteinkinase 3 signalling
Gsk3a	Glycogen Synthase Kinase 3 alpha	Proteinkinase
Acly	ATP-Citrate Lyase	Metabolism linked to histone-acetylation
Ncdn	Neurochondrin	Regulation of calcium signalling

Figure 14. Quantitative PCR confirms impaired transcriptome in 16 month-old mice for eight selected genes. Upper panel: RT-PCR showed an increase of eight selected genes in 3 month-old mice after 1 hour of FC, but not in 16 month-old mice. (* $P < 0.05$, ** $P < 0.01$, *** $P < 0.001$). $N = 4-5$ per group. Error bars indicate SEM. Lower Panel: The eight-selected genes represented signalling pathways identified by data mining in the previous figure and table.

3.6 16-month-old mice display reduced H4K12 acetylation levels along the coding regions of learning induced up regulated genes

Previously, we have observed that 16 month-old mice display impaired learning and memory behaviour in fear conditioning. We have also shown that, in contrast to 3 month-old mice, 16 month-old mice were unable to increase their H4K12 acetylation 60 minutes after fear conditioning. In addition, while 3 month-old mice were able to regulate their gene expression in response to fear conditioning, 16 month-old mice lacked the capacity to do so.

Therefore, we wished to investigate if and how, altered H4K12 acetylation contributes to the impaired transcriptome in 16 month-old mice. To this end, we used the Chromatin Immuno Precipitation followed by next-generation sequencing technology (ChIP-seq). Hippocampal tissue from 3- and 16- month-old fear conditioned mice was subjected to H4K12 and H3K9 ChIP-seq.

First we analysed the distribution of the ChIP-seq enriched region within the mouse genome. While the majority of the mouse genome consists of roughly 65% of non-coding regions, most of the ChIP-seq enriched regions are within coding regions (Fig 15A). These data partially validates the ChIP, as histone acetylation is mainly associated with gene transcription. For example, on part of chromosome 11, most of the TAG-counts are mainly distributed in gene-coding region (Fig 15B).

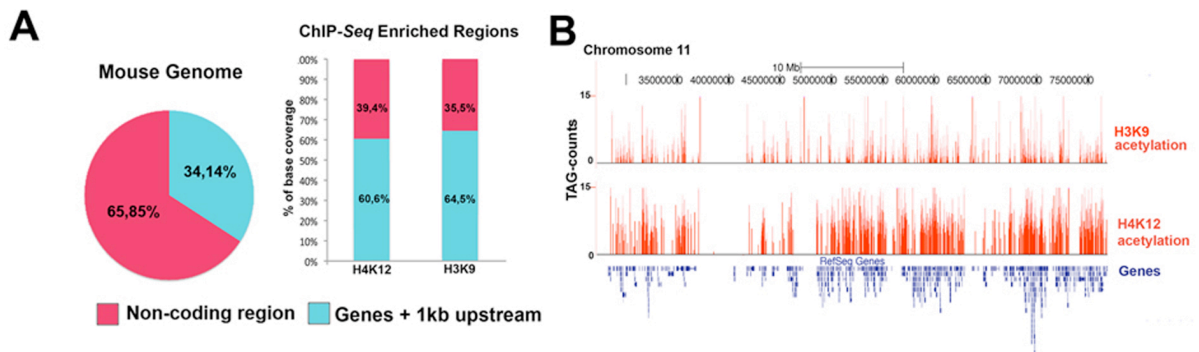


Figure 15. ChIP-seq enriched regions within the mouse genome.

(A) The diagram on the left shows that the mouse genome consists of 65.86% of non-coding regions, while 34.14% are associated with gene bodies (including 1kb upstream of the transcription start site). The bar diagram on the right shows the % base coverage of H4K12 and H3K9 ChIP-seq. (B) TAG counts of H4K12 and H3K9 along a randomly selected area of chromosome 11. Notably, H4K12 and H3K9 acetylation is mainly associated with genomic regions that encode for genes. N=6 for H4K12 ChIP, n=4 for H3K9 ChIP.

We first focused on the H4K12 ChIP-seq results (Fig 16A). We created three groups of genes based on our microarray study, (1) up-regulated genes, (2) randomly chosen genes which were non-regulated upon fear conditioning and (3) down-regulated genes. We compared the enrichment of H4K12 acetylation in 3- and 16 month-old mice at regions extending 1 KB upstream and 1 KB downstream of Transcription Start Site (Hereafter referred to as the TSS region). The TSS region is essential for transcriptional initiation. H4K12 acetylation of down- and non-regulated genes did not differ between the mice groups. However, H4K12 acetylation of up-regulated genes was altered in 16 month-old mice (Fig 16B).

Notably, the altered H4K12 acetylation of up-regulated genes was observed in the genomic region 1 KB downstream of the TSS, which marks the beginning of the gene-coding region. In contrast, the H4K12 acetylation is similar among the groups 1 KB upstream of the TSS, a region that marks the gene promoter. Therefore, we analyzed the distribution of H4K12 along the gene bodies of the three gene groups (Fig 16C). The level of H4K12 acetylation in up-regulated genes was lower in 16 month-old mice, compared with 3 month-old mice. No difference was observed for non- and down-regulated genes along the coding region. These data imply that the lack of gene expression up-regulation in 16 month-old mice is linked to dysregulated H4K12 acetylation along gene bodies.

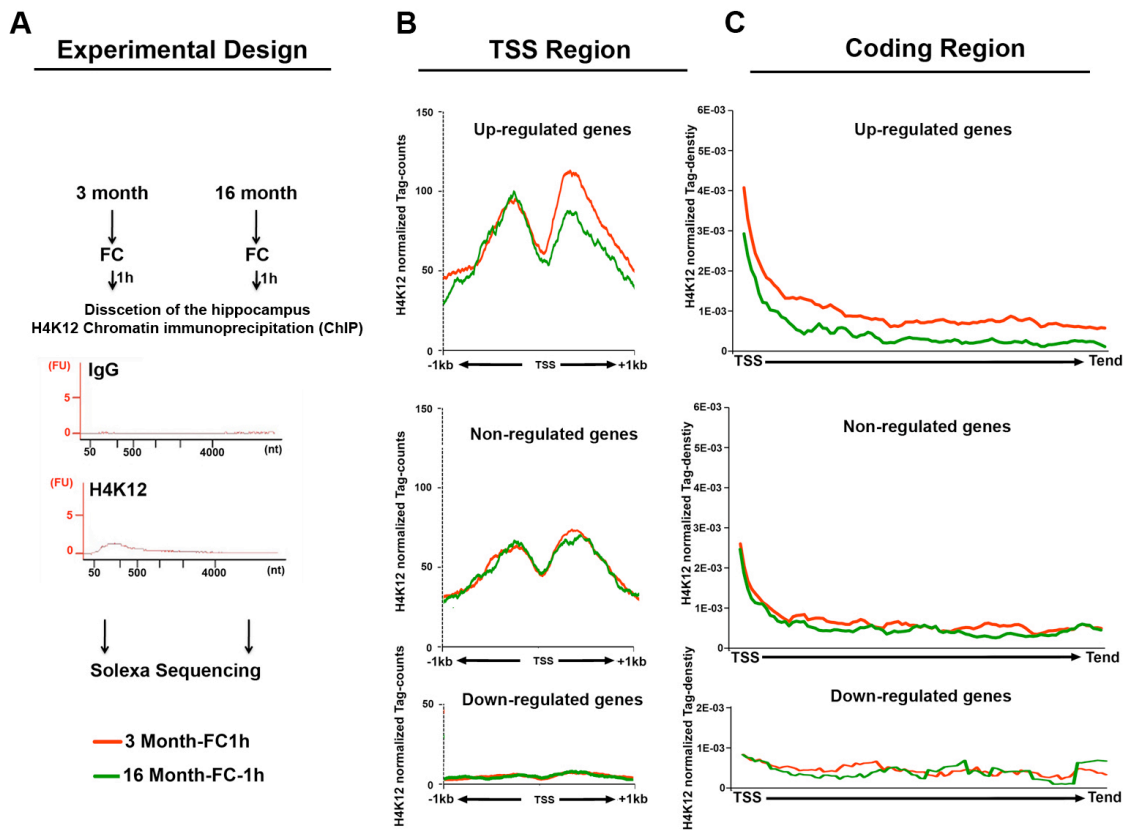


Figure 16. Impaired H4K12 acetylation level of learning-regulated during memory consolidation in 16 month-old mice.

(A) Experimental design for H4K12 ChIP-seq. Importantly, the negative control IgG antibody yields no DNA. (B) For non- and down-regulated, H4K12 acetylation levels in the TSS region is similar between 3 and 16 months old mice. However, 3 month-old mice display higher level of H4K12 acetylation around the TSS region for up-regulated genes. Notably, the difference is shown in the coding side of the TSS. (C) In line with (B), 3 month-old mice display higher H4K12 acetylation level in the coding regions of up-regulated genes. No such difference is observed for the non- and down- regulated genes. (TSS= Transcription Start Site). N=3 per group.

A similar trend was observed for the eight representative genes. For each of these genes, H4K12 acetylation was higher in 3 month-old mice compared with 16 month-old mice (Fig 17).

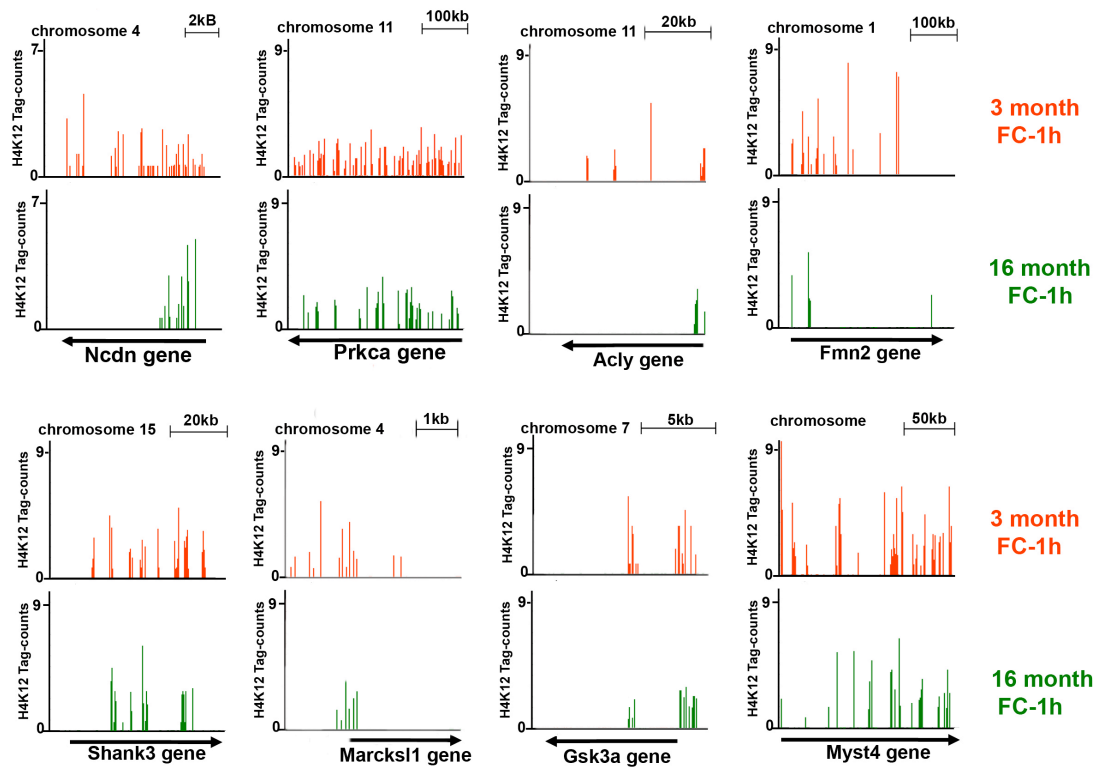


Figure 17. Reduced H4K12 acetylation in 16 month-old mice for the eight selected genes.

Representative images display the distribution of H4K12 TAG counts for enriched areas (E-value 10^4) within the TSS and coding regions for eight selected genes. Notably, 16 month-old mice display impaired level of H4K12 acetylation.

Next, we compared the enrichment of H3K9 acetylation (Fig 18A) in 3- and 16 month-old mice in the TSS region and the coding regions (Fig 18B). Similarly, we divided the genes into up-, non- and down-regulated. The TSS region was defined 5kb up-, and down-stream of the transcription start site. H3K9 acetylation was similar between the mice groups for all the gene groups, both in the TSS region and the coding regions (Fig 18C).

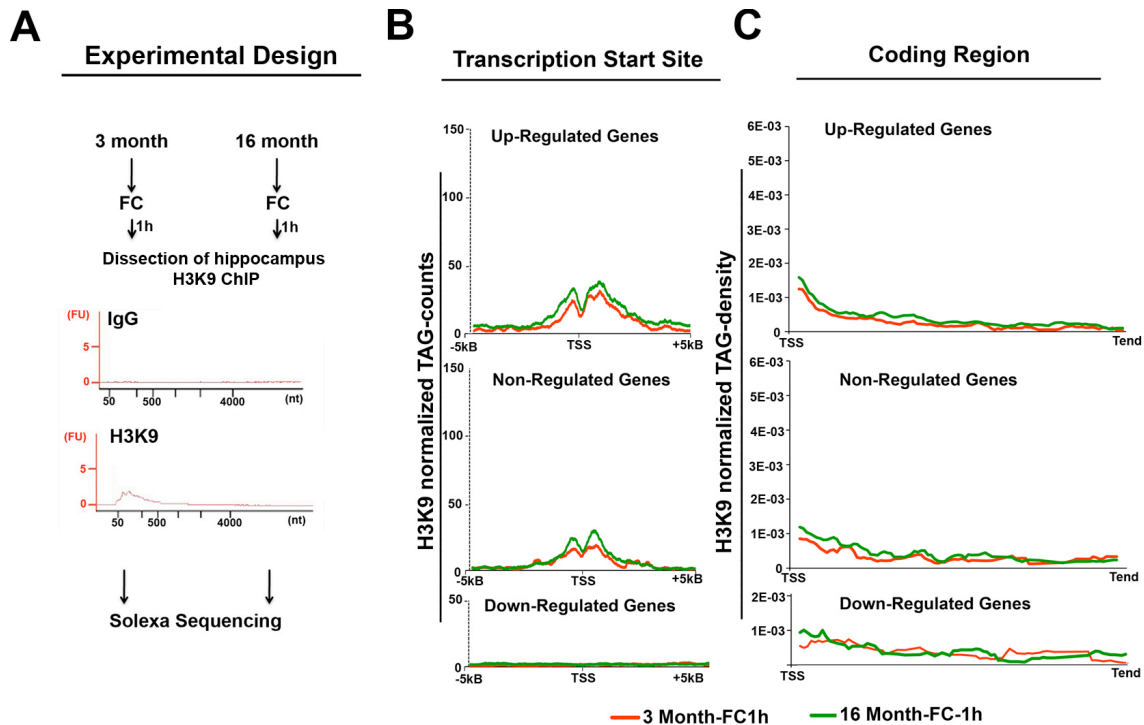


Figure 18. H3K9 acetylation level is similar between 3 and 16 month-old mice during memory consolidation. (A) Experimental design for H3K9 ChIP-seq. Importantly, the negative control IgG antibody yields no DNA. (B) H3K9 level of acetylation does not differ for up-, non- and down-regulated genes in both group around the TSS region, (C) nor in the coding regions. (TSS= Transcription Start Site). N=2 per group.

Because different antibodies are used for H4K12 and H3K9 ChIP-seq, a direct quantitative comparison of H4K12 and H3K9 levels in the coding regions of genes is difficult. However, it is possible to compare the pattern of their distribution. Based on the raw data of our gene array, we selected the 2000 genes that had the highest expression level in 3 month-old mice and the 2000 genes that displayed the lowest expression level. (Hence TOP 2000 versus BOTTOM 2000).

Notably, H4K12 acetylation throughout the entire coding regions was higher in the TOP 2000 genes when compared to the BOTTOM 2000 genes (Fig 19). In contrast, H3K9 acetylation was higher for the TOP 2000 genes only in the proximity of the promoter. In other words, high level of gene expression correlates with high H4K12

acetylation along the coding region but with H3K9 acetylation in the vicinity of the TSS.

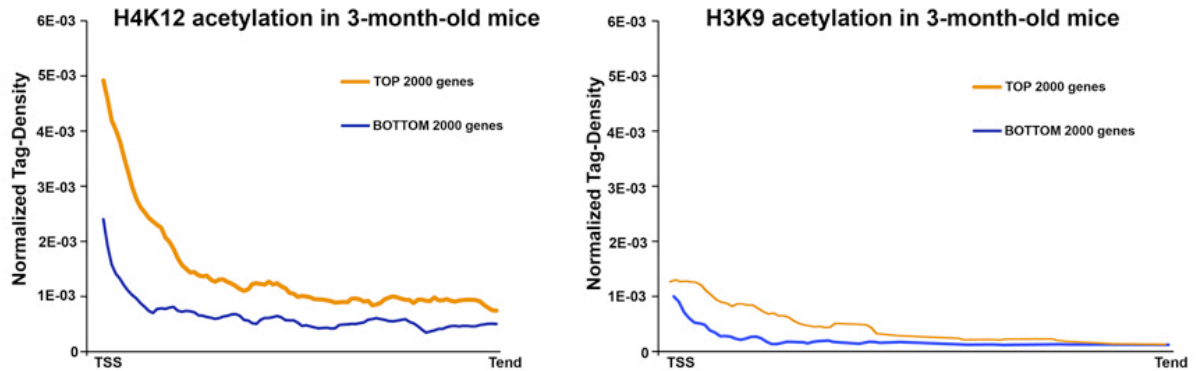


Figure 19. H4K12, but not H3K9 is enriched in the coding regions of active genes.

Left panel: H4K12 acetylation level is higher throughout the coding regions of active genes. Right panel: In contrast, H3K9 acetylation level is similar through most of the coding regions between active and silent genes. The active genes display higher level of acetylation only in the vicinity to the TSS. H4K14 acetylation; N=3 per group. H3K9 acetylation; N=2 per group.

4.7 Intrahippocampal injection of HDAC inhibitors, which increase H4K12 acetylation, restore gene expression and learning behaviour in 16-month-old mice

Based on our results so far, we hypothesized that elevating H4K12 acetylation in the hippocampus might be a suitable approach to restore learning abilities in 16 month-old mice. To test this hypothesis, we implanted microcannulae into the hippocampi of 16 month-old mice to enable us to inject directly HDAC inhibitor (Fig 20). We tested the effect of three different HDAC inhibitors, (1) suberoylanilide hydroxamic acid (SAHA) and (2) sodium butyrate (NaB), both inhibitors of Class I and II HDAC's, (3) MS-275 which is an inhibitor of HDAC 1 (100x more specific for HDAC1 than

HDAC2, Khan, 2008). Control mice were injected with either vehicle (Veh) or HDACi 2 hours prior to the isolation of hippocampus. In order to increase the histone acetylation during the memory consolidation, fear conditioned groups were injected one hour prior to fear conditioning.

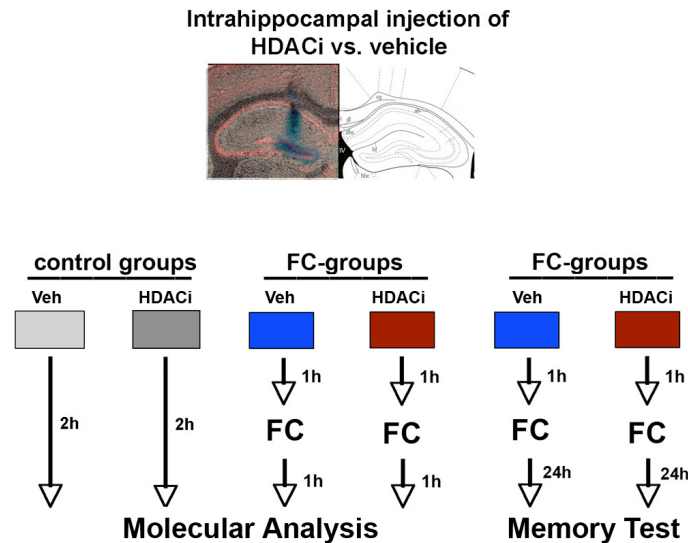


Figure 20. Experimental design of intrahippocampal injection of HDAC inhibitors.

Upper panel: Representative image showing the position of the intrahippocampal injection microcannulae made visible by methylene blue injection. Lower panel: Control groups were injected with HDAC inhibitor (HDACi) 2 hours before hippocampus isolation without being subjected to fear conditioning. FC group were injected one hour prior to the fear conditioning and were killed one hour after the training. N=4-6 mice per ‘molecular analysis’ group. N=8-9 mice per ‘memory test’ group.

3.7.1 SAHA

We first examined the affect of SAHA on bulk histone acetylation level in the hippocampus of 16 month-old mice. Two hours after injection, control mice did not display an increase in histone acetylation in both the Veh and the SAHA treated mice.

Fear conditioned SAHA-treated mice displayed a significant increase of H4K12 acetylation. Notably, there was a non-significant increase for the other acetylation sites in fear conditioned SAHA-treated mice (Fig 21).

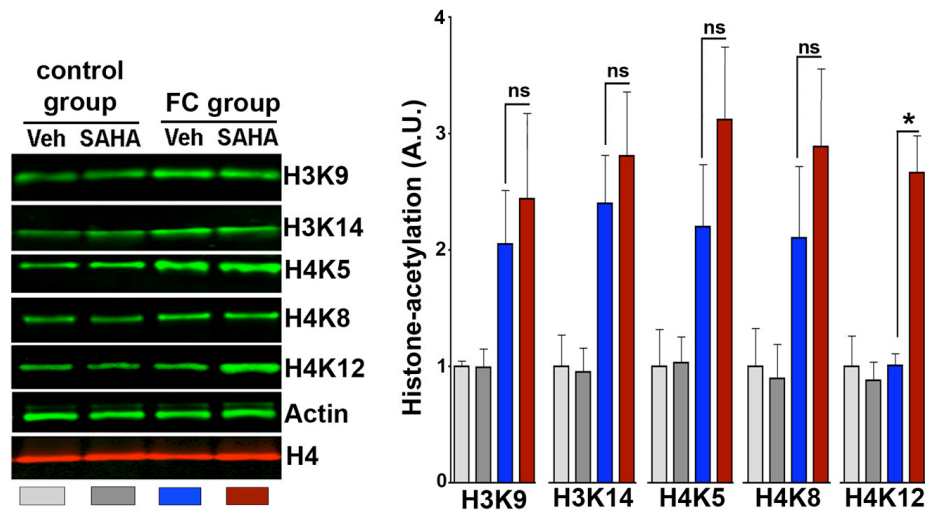


Figure 21. Intrahippocampal injection of SAHA restores H4K12 acetylation in 16 month-old mice. Left panel: Representative immunoblot showing the level of hippocampal acetylation in Veh (Vehicle) or SAHA 16 month-old mice after 1 hour FC. Right panel: Quantification of right panel. SAHA significantly increased H4K12 acetylation level after FC, while for the other acetylation sites; SAHA did not have a significant effect on the acetylation level. Data was normalized to actin. (* $P < 0.05$). $N = 4-5$ per group. Error bars indicate SEM.

Next we tested the affect of SAHA on the H4K12 acetylation level in the coding and the promoter regions. To this end, we performed H4K12 ChIP followed by qPCR. In agreement with the previous data, SAHA treatment was able to restore learning-induced H4K12 acetylation level in the coding regions of the learning-induced genes (Fig 22A). In addition, SAHA treatment elevates learning-induced H4K12 acetylation in the promoter region of FMN2 and Myst4 (Fig 22B).

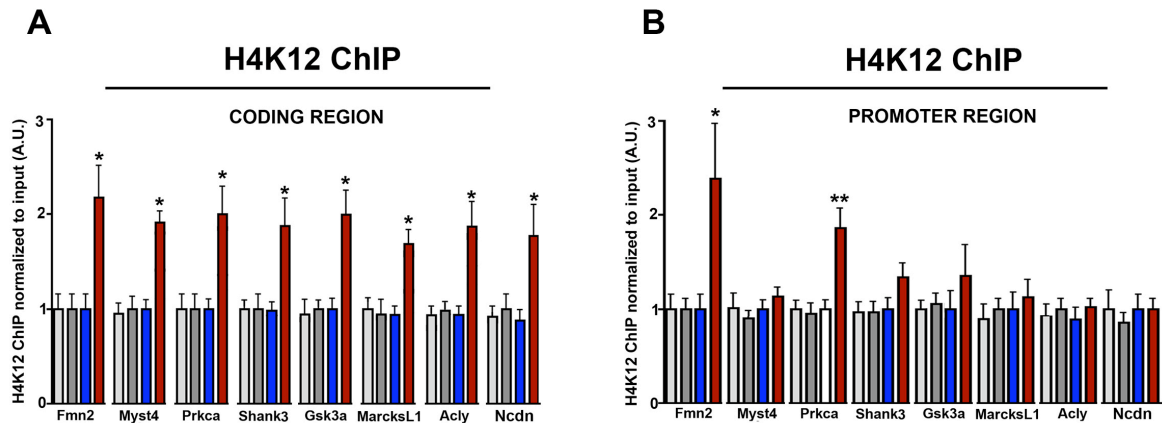


Figure 22. Intrahippocampal injection of SAHA restores H4K12 in the gene bodies of the eight selected genes.

H4K12 ChIP of coding and promoter regions of 16 month-old mice. SAHA treatment increased H4K12 acetylation level mainly in the gene bodies of the learning induced genes (eight representative genes). (*P<0.05, **P<0.01). N=4-5 per group. Error bars indicate SEM.

Since SAHA treatment was able to increase H4K12 acetylation, we wished to check whether SAHA would also increase the expression level of learning-induced genes. Quantitative PCR on chipped-DNA revealed that SAHA treatment significantly increased the expression of these genes in fear-conditioned mice (Fig 23). Therefore, increasing H4K12 acetylation restores learning-induced gene expression.

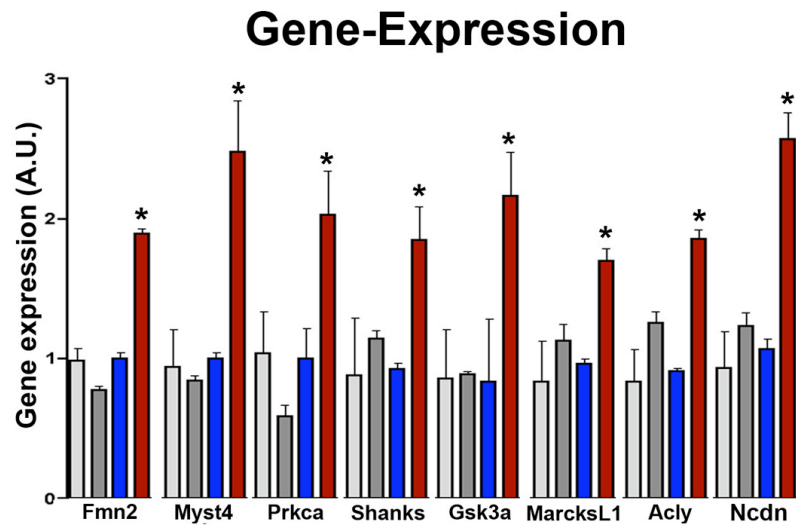


Figure 23. Intrahippocampal injection of SAHA restores gene expression of the eight selected genes.

SAHA treatment increased learning induced gene expression (eight representative genes) in 16 month-old mice. (* $P < 0.05$). $N = 4-5$ per group. Error bars indicate SEM.

Based on the positive effects of SAHA on H4K12 acetylation and the learning-induced gene expression, we reasoned that SAHA would improve the learning ability of 16 month-old mice. Indeed, 16 month-old mice treated with SAHA showed enhanced associative learning when compared with the Vehicle group (Fig 24B). Importantly, the explorative behaviour during the training and the response to the foot shock was not affected by SAHA (Fig 24A).

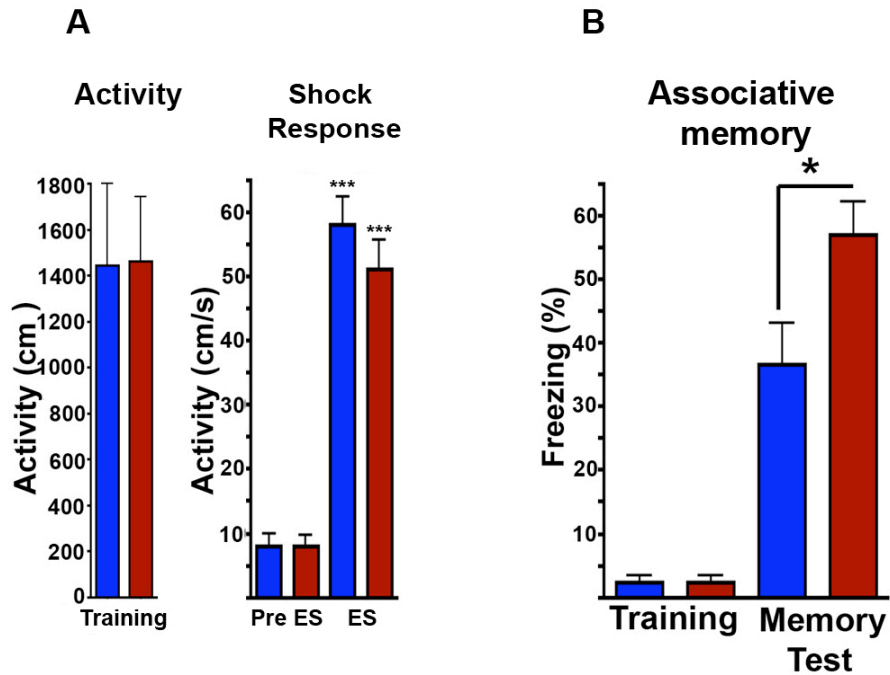


Figure 24. Intra-hippocampal injection of SAHA enhances associative learning and memory in 16 month-old mice.

(A) SAHA treatment did not alter the explorative behaviour during Fear Conditioning. (B) SAHA treated 16 month-old mice showed increased freezing behaviour 24 hours after training. (* $P < 0.05$, *** $P < 0.001$). $N = 8-10$ per group. Error bars indicate SEM. ES, electric stimulus.

3.7.2 Sodium-Butyrate

We have shown that SAHA treatment restores H4K12 acetylation, gene expression and learning behaviour in 16 month-old mice. Next we wished to replicate this essential result using a different HDAC inhibitor. As with SAHA, we carried out similar experiments to test the effects of another pan-HDAC inhibitor, Sodiumbutyrate (NaB). In line with our previous results, NaB significantly increased learning-induced H4K12 and non-significantly increases H3K9 (Fig 25A). Interestingly, NaB treatment increased the H4K12 acetylation level both in the coding and the promoter regions of the learning induced genes (Fig 25B).

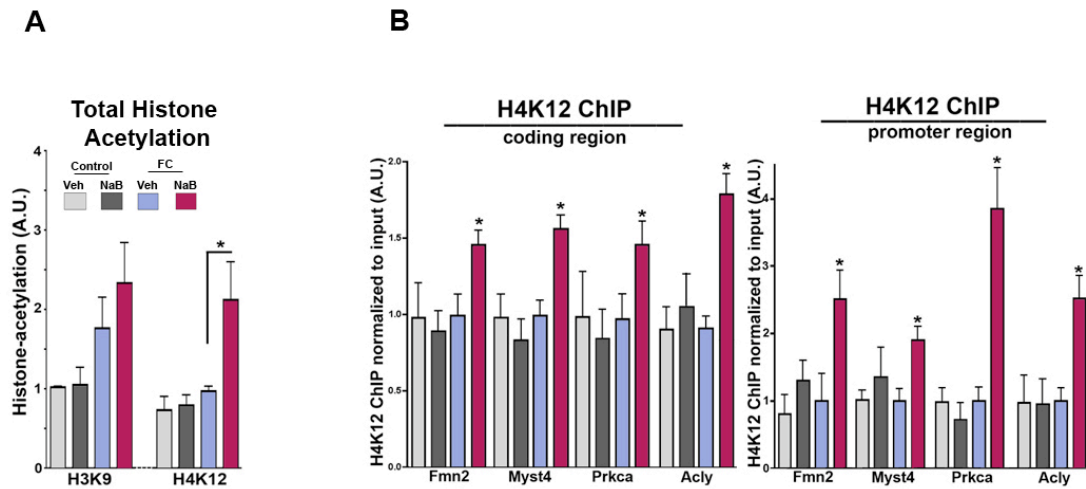


Figure 25. Intrahippocampal injection of Sodium butyrate (NaB) restores H4K12 acetylation level in 16 month-old mice.

(A) Similar to SAHA, learning induced H4K12 acetylation is rescued in NaB treated mice. N=4 (B) H4K12 ChIP of coding and promoter regions of 16 month-old mice. NaB treatment increased learning induced H4K12 acetylation level the learning induced genes (four representative genes). N=8 per group. (*P<0.05). Error bars indicate SEM.

Furthermore, NaB treatment was able to similarly restore learning-induced gene expression (Fig 26A). 16 month-old mice treated with NaB showed enhanced associative learning when compared with the Vehicle group (Fig 26C). Importantly, the explorative behaviour during the training and the response to the foot shock was not affected by NaB (Fig 26B).

The combined data from the SAHA and NaB experiments suggest that increasing the level of H4K12 acetylation by targeting and inhibiting HDAC's might serve as a suitable therapeutic avenue to treat age related memory impairment.

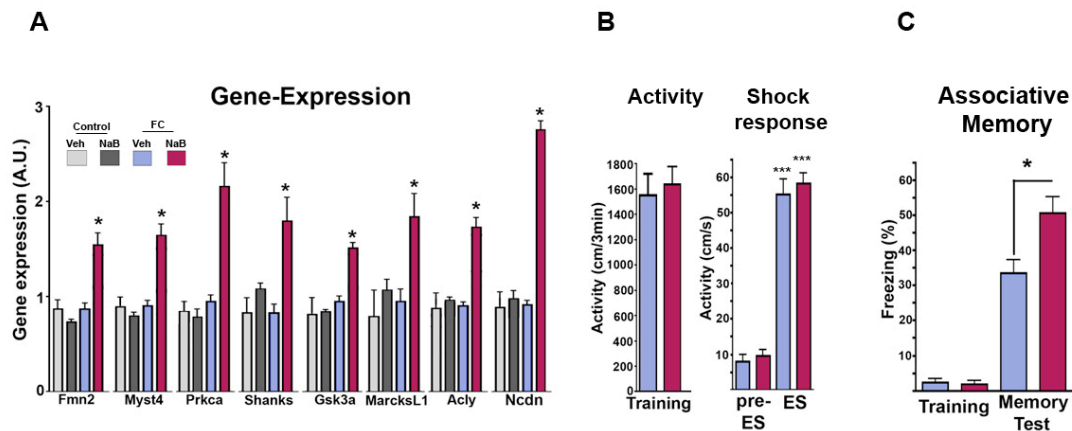


Figure 26. Intrahippocampal injection of Sodium butyrate (NaB) restores gene expression and learning behaviour in 16 month-old mice.

(A) Similar to SAHA, learning induced gene expression is rescued in NaB treated mice. N=5-6 (B) NaB treatment did not alter the explorative behaviour during Fear Conditioning (C) NaB treated 16 month-old mice show increased freezing behaviour 24 hours after training. N=8 per group. (* $P < 0.05$, *** $P < 0.001$). Error bars indicate SEM.

3.7.3 MS-275

A recent paper demonstrated that mice over expressing HDAC1 display normal hippocampal H4K12 acetylation (Guan, 2009). MS-275 is far more efficient in inhibiting HDAC1 than the rest of class I HDAC's (Khan, 2008). Moreover, administration of MS-275 was found to affect H3 but not H4 acetylation in brain tissue (Simonini, 2006). Therefore we were interested to test the effect of a more specific HDAC1 inhibitor on learning and memory formation in 16 month-old mice as a control experiment.

In line with those studies, MS-275 increase failed to increase H4K12 acetylation in 16 month-old fear conditioned mice (Fig 27A). Interestingly, MS-275 was able to increase H3K9 acetylation level. In addition, MS-275 treatment did not increase H4K12 acetylation both in the coding and promoter regions of the learning induced genes (Fig 27B).

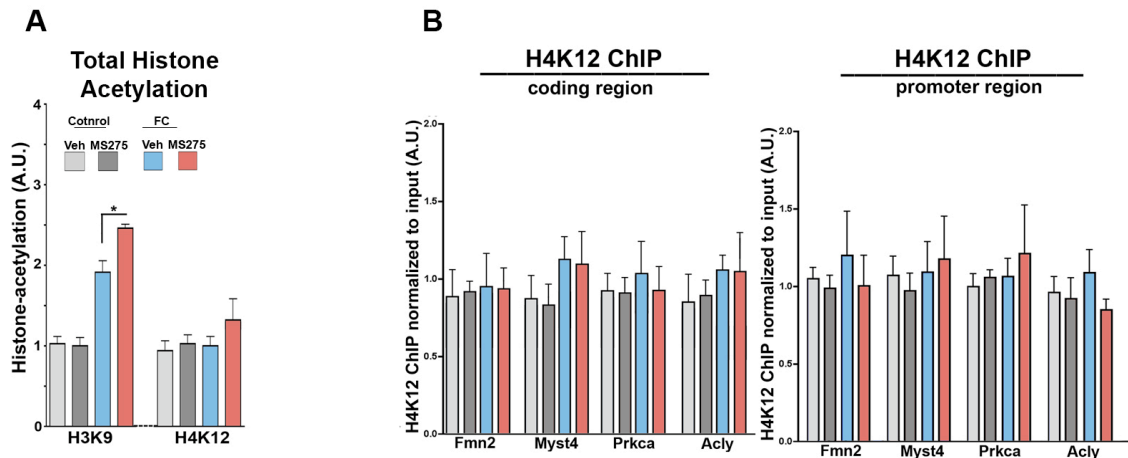


Figure 27. Intra-hippocampal injection of MS-275 fails to restore H4K12 acetylation level in 16 month-old mice.

(A) MS-275 was able to further elevate H3K9 acetylation upon fear conditioning. In contrast, learning induced H4K12 acetylation was not rescued in MS-275 treated mice. N=4 (B) H4K12 ChIP of coding and promoter regions of 16 month-old mice. In line with (A), H4K12 level of acetylation in coding/promoter regions of learning induced genes remained unchanged. N=4 per group. (*P<0.05). Error bars indicate SEM.

The MS-275 treatment did not increase the expression of learning-induced genes (Fig 28A). Consistently, MS-275 failed to facilitate associative learning when compared with the Vehicle group (Fig 28C). Importantly behaviour and the response to the foot shock during the fear conditioning were similar among groups (Fig 28B).

These data propose that HDAC inhibitors that fail to elevate H4K12 acetylation cannot reinstate learning behaviour in 16 month-old mice.

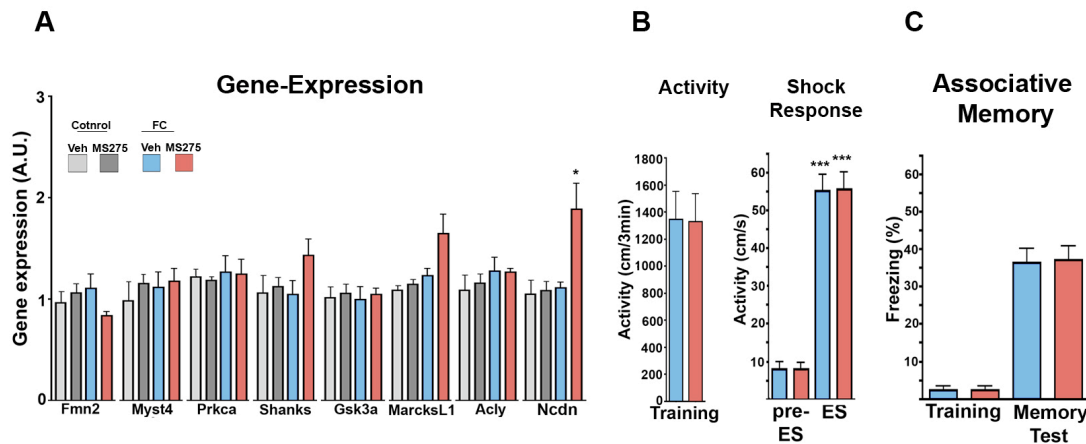


Figure 28. Intrahippocampal injection of MS-275 fails to restore gene expression and learning behaviour in 16 month-old mice.

(A) In line with the previous figure, learning induced gene expression was not elevated rescued in MS-275 treated mice. Notably, only NCDN level of expression is elevated. N=4 (B) MS-275 treatment did not alter the explorative behaviour during Fear Conditioning (C) MS-275 did not increase learning and memory in 16 month-old mice. N=9 per group. (* $P < 0.05$, *** $P < 0.001$). Error bars indicate SEM.

3.8 Mechanisms underlying H4K12 acetylation deficits in 16 month-old mice

Although we have demonstrated the importance of H4K12 acetylation in the formation of memory, and that dysregulated H4K12 may account for early onset of learning and memory impairment, the mechanisms underlying this dysregulation have not been investigated so far. First, it is likely that during aging, a combination of multiple factors contribute to H4K12 dysregulation. We decided to investigate two main options. Firstly, HAT and HDAC activity and secondly, the availability of the precursor for the process of acetylation itself.

3.8.1 HAT and HDAC activity

Although we could not detect significant differences between changes in the hippocampal HAT or HDAC activity in naïve mice, nor the level of expression and protein level of key HATs and HDACs we decided to repeat the experiments (Figure 7) and compare all the four groups together (Fig 29A).

Although there was a trend of elevated HAT activity in 3 month-old mice upon fear conditioning ($P=0.079$), no significant differences were observed among groups (Fig 29B). Similarly, no differences in HDAC activity were observed among the groups (Fig 29C). Finally, we confirmed the microarray study (Figure 7 c) and by showing that HDAC2, HDAC4, Myst 4 and Gcn5l2 expression was up regulated in fear conditioned 3 month-old mice (Fig 29D). The increase of Myst4 and Gcn5l2 (HATs) might account for the difference in H4K12 acetylation, which is observed after 1 hour of FC in the young and the old mice. However, it is more likely to be a secondary effect as the naïve groups show similar expression of Myst4 and Gcn5l2. It is more likely that an upstream mechanism is dysregulated and causing the lack of increase of these HATs in the old mice in response to fear conditioning.

The increase of HDAC2 and 4 might represent a negative feedback accounting for the transient nature of the histone acetylation increase.

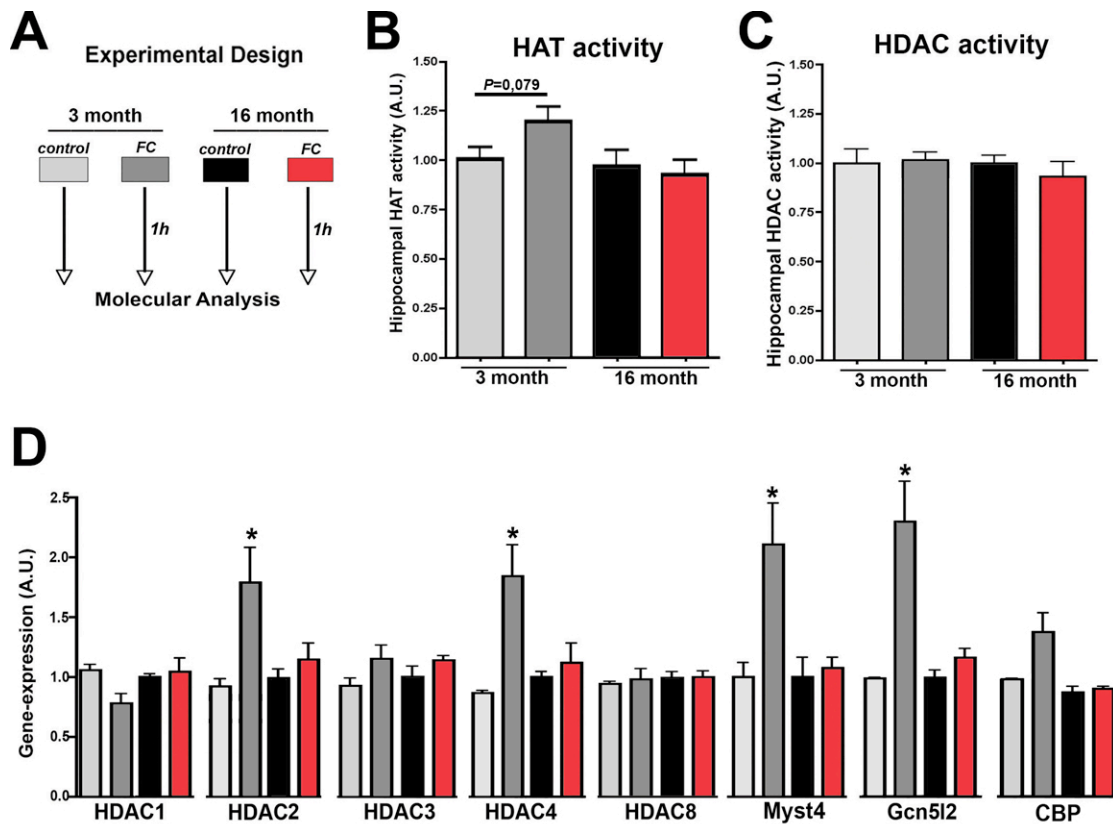


Figure 29. Hippocampal HAT and HDAC activity and gene expression in 3 and 16 month-old mice during fear conditioning.

(A) Experimental design. (B) Nuclear lysates were tested for HAT activity. No significant differences were observed among the groups. N=8 per group. (C) Similarly, HDAC activity level did not differ among the groups. N=8 per group. (D) In line with the gene array, qPCR analysis showed upregulation of HDAC2, HDAC4, Myst4 and Gcn5l2 in fear conditioned 3 month-old mice. (*P<0.05). Error bars indicate SEM.

3.8.2 16 month-old mice display a deficit in citrate up-regulation in response to fear conditioning

Histone acetylation is critically dependent on the availability of acetyl-CoA, which is the precursor for the process itself. A recent study demonstrated that histone acetylation depends on mitochondria-derived citrate levels (Wellen, 2009). Citrate itself can be converted by Acly (or Acl), one of the learning-induced genes, into acetyl-CoA. Therefore, we decided to investigate if citrate levels are altered in 16 month-old mice.

To this end, we measured the levels of hippocampal citrate at different time points after fear conditioning in 3- and 16 month-old mice (Fig 30A). The citrate levels significantly increase in 3 month old-mice 60 minutes after fear conditioning (Fig 30B). Importantly, already after only 20 minutes, 3 month-old mice showed increase in citrate levels. This trend however, was not significant. While the levels of citrate were similar among the control groups, there was no increase citrate level in 16 month-old mice upon fear conditioning. These data suggest that dysregulated histone acetylation might result from an indirect ability of the mitochondria to up regulate the level of citrate, resulting in lower amount of acetyl-CoA.

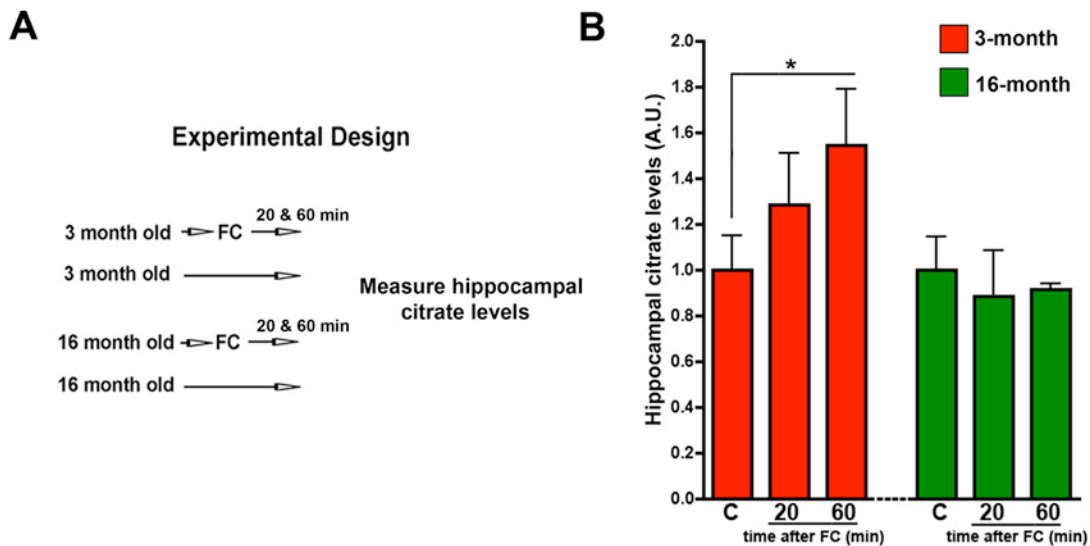


Figure 30. Hippocampal citrate levels increase in 3 but not in 16 month-old mice upon fear conditioning. (A) Experimental design. (B) Nuclear lysates were tested for citrate level. Citrate level gradually rose upon fear conditioning in 3 month-old mice, but not in 16 month-old mice. N=12 per group. (*P<0.05). Error bars indicate SEM.

IV Discussion

4.1 Histone acetylation and gene expression up-regulation are important for the formation of associative memory

In line with works of others (Verbitsky, 2004), we show that as early as 16 months of age, mice display impaired learning and memory. It is important to note that during the fear conditioning both young and old mice showed similar explorative behaviour and similar response for the shock, suggesting that the difference in freezing behaviour is not due altered explorative behaviour or pain sensation.

The memory impairment could have been explained by morphological changes in the hippocampus such as synaptic loss or microtubule instability, as observed in very old mice (Himeda, 2005). However, we did not observe structural changes in hippocampus in the old naïve mice. When taken into account that also the bulk histone acetylation level and various HATs/HDACs levels and activity were similar between the naïve young and old mice, we have to presume that the difference is manifested during the processing of the experience, rather than prior to the experience. We cannot exclude that although the bulk histone acetylation levels are similar between groups, that there might be a difference in the actual distribution of histone acetylation along the DNA. However, the microarray study shows that the gene expression profiles between the naïve groups were similar, supporting the similar histone acetylation levels and profile between the groups.

When comparing the fear-conditioned mice, we found that 1977 genes are up regulated and 252 down regulated. Before further processing the data, we wished to isolate the learning induced genes, as the mice are not only exposed to learning experience, but also to novel environment, and to the shock itself. We isolated 1539 differently regulated genes, specifically linked to associative learning, which most of them were up regulated. Notably, we did not explore the importance for the other

genes that were regulated by the novel environment and their relevance either to genome-environment interaction or aging.

The 1539 differentially expressed genes, hereafter referred to as the learning-induced genes, are associated with relevant processes such as protein modification, transcription and intracellular signalling. When sorted into signalling pathways, the genes are implicated with memory formation, synaptic remodelling, actin dynamics and others. We can see that the genes we found are relevant for a learning process. In addition, many of the genes were already implicated in other studies to be important for learning process/chromatin plasticity such as *Shanks3* (Baron, 2006), *Myst4* (Merson, 2006), *HDAC2* (Guan, 2009) *Acl1* (Wellen, 2009) and others. In addition, we now have many more candidate genes, which we can now investigate how they involved in memory formation in the hippocampus, such as the actin nucleator *FMN2*.

We have shown a very dramatic difference in gene expression in the hippocampus of young fear-conditioned mice when compared to the naïve young mice, while almost none in the older mice. The number of up regulated genes in young FC mice is very high. The tested mice were inbred mice. The laboratory mice are not as enriched by their laboratory environment, when compared with wild life mice in their natural habitat. This could explain for the extreme response in gene and histone up-regulation, observed in the young fear-conditioned inbred mice. It is plausible that such responses are more mild and subtle in enriched wild life mice. Nonetheless, by testing less enriched mice, we could detect learning induced hippocampal changes.

Previous studies have shown that during aging, a marked change in gene expression is observed in the human brain (Lu, 2004; Loerch, 2008). The shift in gene expression started at around 40-50 years old of age that is associated with the onset of cognitive decline. This perhaps correlates with 16 months old mice, which usually have mean life span of 26 to 28 months (Jucker, 1997). As previously

mentioned, we did not observe major transcriptome changes between the naïve 3- versus 16 month-old mice. However, in the human studies, it is impossible to compare “naïve” human, as human are constantly challenged. Comparing our fear conditioning results with the mentioned study (Lu, 2004) would also not be accurate for the opposite reason, as the mice have a single major event, and the result is extreme. It would be interesting to compare the transcriptome of constantly challenged and enriched young and older mice in order to detect the age related transcriptome shift. Nonetheless our data show that 16 month-old mice display altered gene expression in response to stimulus is supported by the observed gene expression alteration in middle age human brain (Lu, 2004).

It is worth noting that even though the older mice failed to show increase in the learning induced genes, they could still learn. There are several possible explanations. For example, other mechanisms are involved in the memory formation, and that they are enough to form new memories to some extent. Protein modifications such as phosphorylation and synaptic tagging can contribute to the memory consolidation (Segal, 1998). Another appealing explanation is that the basal levels of gene expression are enough for memory formation. It has been previously shown that when translation of proteins is blocked, an organism cannot acquire new long-term memory (Montarolo, 1986; Schacher, 1988). That places the translation and gene expression at the utter most importance in the formation of memory in the hippocampus.

In theory, the stimulus could have failed to cross a threshold and was not enough to initiate strong response. This is unlikely for several reasons. The foot shock did initiate a response in the hippocampus as both groups of mice reacted in similar way to the shock. One hour following the foot shock we observed that old mice hippocampus display histone acetylation increase for the other sites, excluding H4K12. This suggests that the electric shock elicited a response, which was processed and reached the hippocampus. Thus, the initiation of some process in the hippocampus seems to exist in old mice as well. Interestingly, levels of cFos, an

early intermediate gene, increase more in the old than the young mice, suggesting a possible compensatory mechanism.

The old mice do express the learning induced genes and they are not silent. Basically, the 16-month-old hippocampus is able to translate the basal mRNA to create the necessary proteins in various pathways. For example, the hippocampal cells of old mice can still use the basal level of FMN2 and actin in order to induce change in the actin cytoskeleton, a process intimately linked with formation of new memories (Fischer, 2004). The up regulation of such genes could serve as only an enhancement for stronger memory association in the young mice, rather than a complete prerequisite. In other words, the up regulation of certain genes increases the association of the memory, while the basal level of the same genes is enough to create weaker associative memory.

Furthermore, as we used a certain cut-off to define differentially regulated gene (Only genes at least twice up-, down- regulated), we could have missed many smaller differences in the older mice. It is likely that many of the learning induced gene were slightly up regulated, thus could still contribute to memory formation. Re-analyzing the micorarray with a lower cut-off might produce further insight. Finally, the mouse model is different than human model. It is difficult to fully understand the psyche of mice, in human terms. It is feasible that at 16 month old, mice simply have more life experience of a sort, that make them less interested in the test or less susceptible to fear-conditioning. It is tempting to assume that both age groups have similar life experience, since they were non-challenged throughout all their lives under the lab conditions. Still, we cannot rule out that somehow, older mice acquired some degree of subtle life experience and choose to react differently to the test. In any case, 16 month-old mice display altered interaction with the environment during fear conditioning.

4.2 The uniqueness of H4K12 acetylation

4.2.1 H4K12 acetylation in coding regions has a unique effect on level of gene expression

We found that both age groups were able to up regulate H3K9, H3K14, H4K5 and H4K8 one hour after fear conditioning. However, the young mice were able to up regulate H4K12 while old mice could not. Importantly, we did not observe change in the total number of Histone 4. The increase in H4K12 within the hippocampus is not restricted to a certain cell type nor a specific sub region. Therefore, we conducted our experiments with the entire hippocampal tissue, rather than isolate a specific region of the hippocampus.

At first glance, it might seem odd that compared with young mice, the older mice fail to up regulate only a single acetylation site. Interestingly, another group showed a unique trait of H4K12 in human T-cells (Wang, 2008). This study characterized histone acetylation distribution in the promoter and coding regions. This distribution pattern was analysed for silent, low, medium and highly expressed genes. Although H4K12 is not much discussed in the paper, a close examination revealed couple of unique traits for H4K12, which were essential for the interpretation of our results and to complement our data.

First unlike all the other acetylation sites, H4K12 is mainly distributed in the coding regions rather the promoter regions. In other words, when comparing silent genes to highly expressed genes, the difference is similar and constant from the promoter and coding regions until the very end of the gene. Almost all the other acetylation sites show a very large difference in the promoter site but much smaller or with no difference in the coding region. Some, like H4K5 and H4K8 (H4K16 is discussed separately) show also some difference in the coding region, although as stated, far smaller than the promoter sites.

However, when examining more closely how the histone acetylation levels differ between different levels of gene expression (silent, low, medium and high), we can point the second uniqueness of H4K12. H4K5 and K8, for example, show higher histone acetylation for expressed genes compared to silent. However between medium and high expressed genes, there is no difference in the beginning of the coding regions. In addition, there is not much difference between the low and higher expressed genes after 1000bp. That indicates that the initial increase of K5 and K8 in the coding area is enough to turn on a silent gene and initiate expression. However, once the K5/K8 acetylation crosses a certain threshold in the coding region, it has no effect on further up regulation. In striking contrast, H4K12 level of acetylation in the coding region is gradually increased with the increase of expression. Thus H4K12 tightly regulates different levels of expression. In other words the H4K12 level in the coding region is highly indicative for the exact level of the expression of a certain gene. It would be interesting if Wang et al (2008) showed a more detailed analysis for the entire gene bodies when comparing low-, medium- and high- gene expression.

Finally, based on the example of a representative gene (*ZMYND8*) in that study, we could speculate on another uniqueness of H4K12. Out of all the acetylation sites, H4K12 is the only one in the coding region to be both equally distributed along the gene and while at the same has almost no gaps. There are almost no stretches in which H4K12 is not represented on the gene. If true to the other gene's bodies, the shifting of nucleosomes aging could interrupt the transcription elongation, a topic I will discuss later when addressing H4K12 dysregulation in aging.

It is worth to note that H4K16 was not up regulated in both 3 and 16 month-old mice upon fear conditioning. H4K16 has been already shown to be the first acetylation site in H4 to be acetylated before the other sites are acetylated (Munks 1991; Zhang, 2002), before further progressive acetylation in other sites on H4 in the direction K16→K12→K8→K5 (“Zip” model). Therefore, it could be that the

relevant nucleosomes are already acetylated in the naïve mice in K16 and only the secondary acetylation site are up regulated during the memory formation. Also, H4K16 distribution (Wang, 2008) displays a combination of H4K5, K8 and K12 distribution features, as it is both presented in the coding regions and the promoters, thus averaging the other modifications. For example, the promoter site level of K16 is intermediate between the higher K5 and K8 to the lower of the K12.

This study shed new light on our previous finding. Since H4K12 is uniquely distributed on the coding region (Wang, 2008), it could hint why it is the first acetylation site to be deregulated with Aging during memory consolidation, as we shown. However, these data was true for human T-cells and the important question was whether this model would also be applicable in other organism, and as importantly, in aging process.

As we observed both unique H4K12 dysregulation and a major difference in the gene regulation following fear conditioning between young and old mice, we wished to correlate these two findings by using the ChIP-seq. The ChIP-seq analysis revealed a clear correlation between H4K12 up regulation and the learning induced genes. We showed that H4K12 level is higher specifically in the coding regions of young mice, when compared to the old mice, but this increase was restricted for up regulated genes (From the learning induced genes). No difference was observed for the other gene groups (non- and down- regulated genes) and for all the gene groups for H3K9 ChIP. It is very interesting that even for the up regulated genes, H4K12 was higher only on the coding side of the promoter but not for the non-coding side. As such, H4K12 acetylation seems to be of particular importance for transcriptional elongation and ultimately the regulation of gene expression. The striking correlation indicates that H4K12 dysregulation in old mice is responsible for the inability to induce the required gene expression programming, which is required for the enhancement of associative memory consolidation.

Moreover, when we compared the highly expressed genes versus silent genes in the

young mice, our data is in line with the results of Wang et al (2008), showing that H4K12 is mainly in the coding region, while H3K9 is mainly in the promoter or in the first portion of the coding region. Combining the results, it seems that H4K12 has unique properties in both *human* T-cells and *mice* hippocampus. In addition we show in our model that H4K12 seem to be uniquely deysregulated in aging.

4.2.2 Age-associated H4K12 acetylation deregulation in various models

As we set out to find a unified and basic aging process, could H4K12 dysregulation fit as candidate process?

Before addressing a plausible mechanism by which H4K12 is dysregulated during aging and thus is involved with AAMI in our model, it is important to see if H4K12 plays a role in other age related phenomena in other organisms. In other words, does H4K12 dysregulation is specific to learning impairment, or, and more excitingly, involved with various aspect of aging or stress. Indeed, in the last two years, H4K12 was uniquely shown to be de regulated in several different age-related or stress related models.

In yeast, H4K12 was shown to have a critical role in growth under stressful conditions (Chang, 2009). The yeast could not grow normally in 35 degrees when *Esal*, a HAT, was mutated. However, deletions of Rpd or SDS3 (both part of the Histone deactylase complex RPD3L) suppressed the growth defect in the *esal* mutants. Next, *esal* mutants were constructed with a histone specific lysine (K) replacement with another amino acid (A), which cannot be acetylated. Interestingly, Rpd3 and Sds3 suppressed the growth deficits in *Esal* mutants when combined with H4K5A, 8 and 16. However, when H4K12 was replaced with H4K12A, *esal* mutants displayed a dramatic growth reduction even when Rpd3 and SDS3 were deleted. It is important to point out that other studies demonstrated already that *rpd3* yeast mutant display longer life span that wild type yeast (Kim, 1999). Hence,

H4K12 has a unique and possibly conserved role in the ability of the organism to respond to stress even in a primitive eukaryote and quite possibly, also in aging.

H4K12 dysregulation was also observed in mice aged-oocytes (Manosalva, 2009). Age related infertility is linked with the reproductive potential of the oocytes. It was previously shown that aging alters the gene expression and protein function in metaphase II stage (MII) oocytes, a stage when the oocyte is mature. The study revealed dual abnormal levels of H4K12, one during MII and the second in the earlier germinal vesicle (GV) stage. During GV, H4K12 acetylation levels gradually decreased with aging, while in MII, H4K12 acetylation levels uniquely gradually increased in aged oocytes. Transient HDAC inhibitor (TSA) treatment during GV stage increased H4K12 acetylation levels at this stage. Interestingly, this transient treatment results later in lower, and therefore normal, H4K12 acetylation levels during MII. The study suggests a unique role of H4K12 in age-related oocytes infertility. The fact that aging decreases H4K12 in one stage while increases it in another, points to a specific and precise pattern of H4K12 acetylation levels during different stages in the life of a cell. In other words, it is possible that some cells could present age-related dysregulation of gene expression both by an abnormal increase or a decrease of healthy H4K12 acetylation levels.

Aging is a major risk factor for cancer. In colon cancer, H4K12 acetylation level is altered in cancer cells (Ashktorab, 2009), as was shown in human cell culture. H4K12 level is gradually increasing from normal cells to adenoma (benign tumor) and to cancer. This gradual increase pattern is similar to the one observed in aged MII.

It is worthy of note that H4K12 seems to be linked with various aspect of Aging, from oocyte infertility, stress response, cancer and early memory impairment. Moreover, H4K12 seems to be uniquely dysregulated both in the yeast, mice and human. One major drawback in many of these papers is that not all histone acetylation were tested as possible controls. Moreover, all these papers showed that

levels of H4K12 are simply dysregulated but offered no mechanism explaining the phenomena.

However, by incorporating our data with Wang's data (Wang, 2008), one can provide such a mechanistic explanation, as will be discussed in length in the next section. By its unique and its possible conserved distribution pattern in different tissue and organisms, H4K12 is likely to be first site, which is affected in different age related phenomena.

For instance, although not yet tested, one exciting hypothesis might suggest that T-Cells could require an increase of H4K12 in order to elevate specific gene expression when they need to activate immune defense. In a similar fashion, the process of modulating H4K12 acetylation level could be altered in aged T-cells, thus decreasing the efficiency of T-Cells to help fend off pathogens.

It would be very exciting to investigate in detail, and see if H4K12 is deregulated in more aged tissues and more variety of organisms.

In addition, our Immunohistochemistry data reveal a difference in the hippocampal H4K12 between naïve mice. 16 month-old naïve mice levels of H4K12 acetylation are higher when compared with the younger mice. This method though, is less accurate than immunoblot and represents only several hippocampal sections rather than the entire hippocampus. Nonetheless, we recently found that 24 month-old naïve mice display higher levels of H4K12, when compared with 3 month-old naïve mice. In line with this finding, we also observe higher levels of H4K12 acetylation in aged human brain tissue, when compared to young tissue. It could be postulated that the onset of this increase is around 16 months of age in mice. This change is perhaps restricted to specific sub parts of the hippocampus (Anterior, posterior, etc...), and is not detected when the whole hippocampus, which was analysed in the immunoblot. Current work in 24 month-old mice and aged human brain tissue is underway to investigate the importance of this phenomenon.

4.3 The involvement of acygenetics in aging

It would be straightforward to assume, that H4K12 dysregulation in aging occurs due to changes in the levels of specific HATs or HDACs. However, once more, since no such unanimous age deregulated genes were found across different tissues, organisms and sexes, it seems to be unlikely.

Interestingly, a recent study (Wellen, 2009) demonstrated that histone acetylation is critically depended on the activity of ATP-citrate lyase (Acl), an enzyme metabolizing acetyl-CoA. The HATs require acetyl-CoA as a precursor for the acetylation process. This study showed that the availability of acetyl-CoA is specifically catalyzed from mitochondrial-derived citrate. Importantly, some acetyl-CoA syntheses had more impact on histone acetylation than other, a curious finding, as the end product of all this class of enzymes is the same acetyl-CoA. It could well be postulated, that the exact location in which acetyl-CoA is synthesized is of the utter most importance for achieving specific reactions such as histone acetylation compared with acetylation of other proteins.

In acygenetics there is an important connection between mitochondria function and epigenetic. Therefore there must be a connection between aging and histone acetylation. It has been shown extensively that during aging, the mitochondria function is declining (Linnane, 1989; Bishop, 2010). Thus, during aging, the availability of the metabolites can decline with aging. In other words, in the aged cells there is less available acetyl-CoA/citrate for histone acetylation, during a signal, which induces gene-expression change. One study demonstrated that in the aged brain of SAMP8 mice (Jiang, 2008), a model of premature aging, citrate levels are decreasing, among other metabolites.

In CB57B6/j mice, we found that the levels of citrate are similar between the naïve 3 and 16 month-old mice. However, young mice were able to increase their Citrate

levels during the memory consolidation, while the older mice could not. It is plausible that as early as 16-month-old mice, the mitochondria could not as readily (or as fast) produce the necessary citrate for the increase of histone acetylation.

In order to achieve increase in gene expression of a certain gene, the cell needs to acetylate, for most the histone acetylation sites, a rather short DNA fragment around the promoter. In other words, the metabolic demand to acetylate such histone sites, such as H3K9 and the others, is low. In contrast, H4K12 affects a gradual increase in gene expression in the long coding regions. Thus the metabolic demand is much higher. This can partly explain, mechanistically, why H4K12 is the first histone acetylation site to be affected in the aged mice brain. Its unique distribution makes it perhaps the one histone acetylation site that demands the most energy to maintain or up regulate in response to relevant stimulus. With the decline in the function of mitochondria in aging, it is the first to be affected. Connecting the mitochondria with H4K12 regulation also explains the conserved age dependant dysregulation of H4K12 along various tissues and organisms. The mitochondria dysfunction with aging is indeed observed in Eukaryotes (Bishop, 2010).

There are also other possible and complementary mechanisms. For instance, since the distribution-effect of H4K12 is significantly different, the acetylating complex might be unique as well. Such complex could be composed of various proteins, including HATs, which might be part of the elongation machinery. The complex integrity could be disrupted with aging or inhibited for various reasons. For instance, the pH alteration of the aged cell alters and as such, disturbs the proteins integration for this specific complex. For example, one key protein might be part of the complex, still metabolizing acetyl-CoA, but not in close proximity to allow an efficient acetylation.

Another plausible explanation for H4K12 unique dysregulation lies within the possible uniqueness of the structural formed by the acetylation of the K12 site. It was shown by X-ray crystal structure of HAT1 enzyme (Zoroddu, 2010), that its

active site, along with acetyl-CoA complex interact with the peptide of H4 in such a way, which brings K12 residue the closest to the active site. In addition, it has been proposed that K12 may serve as a memory mark (Smith, 2002); when unacetylated the chromatin region will be silent, and when acetylated the chromatin region will be active. This demonstrates a possible unique acetylation mechanism for H4K12 based on the structure of the histone tail in respect with the HAT. Therefore, during aging, some alterations might occur, which makes it more difficult to increase H4K12 acetylation when needed. Once more it points to the possibility that the availability of acetyl-CoA is critical for H4K12 acetylation. The structure suggests that acetyl-CoA possibly has to present in an extreme proximity for the K12 when compared to the other lysine residues, thus indicating indirectly the relative higher energy investment to acetylate this residue. Hence, when acetyl-CoA/citrate is not increase in old mice in response to fear conditioning, the level of H4K12 does not increase, while the others are less affected.

An interesting underlying possible mechanism can be explained by the possibility of “Nucleosomes shifting”. With aging, a cell undergoes many DNA repair events. In some cases, mutations occur on the genomic DNA. Either way, many of these repair events involve the excision of whole fragments of DNA. Once the damage is repaired, the DNA fragment is re-synthesized. Afterwards, new histones need to be incorporated into the DNA. In one line of thought, the histone nucleosomes could be placed in a slightly altered position. When such alterations accumulate, nucleosomes could cluster at some DNA regions, while creating gaps in other regions. This might interrupt first the elongation process rather than the promoter, as clustered histones would disrupt the speed of the elongation, which could be also linked with altered H4K12 acetylation. Testing the distribution of the nucleosomes along aging could prove or disprove such theory.

It is likely that during aging a combination of multiple factors contributes to deregulated histone acetylation and the exact mechanism remained to be described. Furthermore, one cannot exclude the involvement of other histone acetylation

sites, histone methylation, other less studied histone modifications or DNA methylation, in aging. Nonetheless, we presented here that H4K12 could be an attractive therapeutic target for various age related maladies. It would be extremely exciting to collect more results in the near future concerning H4K12 and its unique mechanism.

4.4 HDAC inhibitors as therapeutic avenue for AAMI

Previous studies have shown that increasing histone-acetylation via administration of HDAC inhibitors could facilitate synaptic function and learning behaviour in rodents (Vecsey, 2007; Fischer, 2007; Kligore, 2010). A recent study shown that knocking out HDAC2 (Guan, 2009), but not HDAC1, in young mice had a beneficial effect on memory consolidation. In these mice, H4K12 was observed to be higher in the knockout mice. Interestingly, over expressing HDAC2 resulted in decrease in freezing behaviour and at the same time, lower H4K12 levels.

In our study, HDAC2 increase in young mice after one hour of fear conditioning. At first glance this seems odd, as we observe increase of histone acetylation 1 hour upon fear conditioning. However, the increase of HDAC2 levels could account for the transient nature of the histone acetylation increase, which if followed by the decrease of histone acetylation later. We can postulate that HDAC2 is responsible for the decrease in histone acetylation observed during 1 hour and 24 hours after the fear conditioning. By inhibiting HDAC2 or knocking it out, we might extend the window of histone acetylation increase, thus enhancing the memory consolidation via prolonged gene expression increase.

We observed, that young mice show enhanced memory consolidation when administrated with HDAC inhibitors, SAHA and TSA straight to the hippocampus (Data not shown). However, the more interesting question was whether HDAC inhibitor will increase memory consolidation in our old mice, and through which mechanism.

When the old fear conditioned mice were injected with SAHA, H4K12 was the only site to show a significant increase. It is unlikely though, that SAHA can selectively increase this single site, as SAHA is a general inhibitor for Class I HDACs. However, as H4K12 was the only one to be down regulated to begin with, it had the most room to improve. Moreover, as the drug was able to increase H4K12, we can speculate that the relevant HATs and HDACs are still present in 16 months-old hippocampus.

We were further able to show that SAHA mainly increases H4K12 in the coding genes of the learning induced genes, rather than the promoters. This increase was sufficient, in turn, to increase the gene expression of these genes. This is in line with our previous findings that H4K12 is mainly in the coding regions and is responsible to changes in the genes level of expression. Similar results were shown with another HDAC inhibitor Sodium Butyrate (NaB). One interesting difference was that NaB treatment also increases the level of H4K12 in the promoter site of the learning induced genes. This indicates that the spectrum of effect of these two drugs could be different.

Old mice, which were treated with both SAHA and NaB, showed increase in freezing. We cannot rule out that these drugs might be involved with hyper acetylation of other relevant proteins in the cytoplasm of nucleus that might contribute to the formation of memory. However, when we used another HDAC inhibitor, MS275, that is more specific to HDAC1 (Khan, 2008), we did not observe H4K12 increase, gene expression increase nor increase in freezing. We did notice an increase in H3K9 level. This result is in line with previous study demonstrating that MS275 has greater effect on H3 acetylation than H4 (Simonini, 2006). Taken together, our data indicate that H4K12 is an attractive target for therapeutic intervention for AAMI. It would be very exciting to find the specific mechanism that is responsible for H4K12 acetylation. When characterised, we

could isolate it, thus excluding other factors such as other protein acetylation, and test in greater detail the exact impact of H4K12 on memory formation.

Notably non- fear conditioned mice did not display any increase in histone acetylation even when injected with HDAC inhibitor. This can be explained by the fact that we used a rather small amount of the drugs and that two hours passed from the injection until the hippocampal removal. Had we used a more potent drug like TSA, or higher dosages, we might have observed increase in these mice as well. In addition, the increase in histone acetylation is also due to a possible increase in the HAT activity, such as the one observed in young fear conditioned mice (Although not significant, $p=0.079$, but the trend is visible). It is plausible that inhibiting the HDAC's in the old mice primes secondary events, such as increase in the relevant HATs (Gcn5l2 and Myst4 up regulated in fear conditioned mice), which contribute to the global increase in histone acetylation. Recently GCN5 was shown (Ciurciu, 2006 Ciurciu, 2008) to be part of a complex critical for the acetylation level of H4K5 and K12.

In conclusion, we showed that administration of HDAC inhibitors that increase H4K12 are able to reinstate learning induced gene expression and memory function in 16 month old mice. In the future, more potent and specific drug, targeting H4K12 levels could help us to enhance our memory capabilities in middle age.

V Summary

The remarkable capability of the nervous system of animals to adapt their behavioral responses to an ever-changing environmental conditions is thought to rely on the plasticity of neuronal circuits and synaptic connections. This capability reaches its highest form in the human brain. During aging, a marked decline is frequently observed in the performance of cognitive and memory tasks that require such plasticity. Age-associated memory loss and memory impairment during neurodegenerative diseases such as Alzheimer's disease (AD) affect millions of people worldwide. No treatment to this day has been successful in restoring these memory deficits. This lack of therapy is primarily due to the fact that little is known about the underlying molecular mechanisms that lead to memory formation. A number of recent studies suggest that epigenetic factors may play a central role in memory formation and age related pathologies. In addition to the role of transcription factors, the availability of genes for transcription is controlled by a series of proteins that regulate epigenetic chromatin remodeling, especially histone-acetyltransferases (HATs) and histone-deacetylases (HDACs). The goal of this research was to further elucidate the molecular and cellular terms of how the aging process modifies the capability of the hippocampus to generate plastic responses and the consequences that epigenetic alterations have in learning and memory in elderly mice.

We showed that already at 16 month-old, mice show impaired freezing behaviour in the fear conditioning test. We demonstrate that during the memory consolidation H4K12 acetylation site is uniquely dysregulated in 16 month-old mice when compared with 3 month-old mice. This deficit is linked with failure to up-regulate learning induced gene expression, required for consolidation of associative memory. The deficit in H4K12 acetylation observed in 16 month-old mice is uniquely observed in the gene bodies of the up regulated genes. As such, H4K12 acetylation seems to be of particular importance for transcriptional elongation.

We found that the administration of HDAC inhibitors that shift the balance of H4K12 acetylation is able to reinstate learning-induced gene expression and memory function in 16-month-old mice. Our data also suggest that H4K12 acetylation–dependent changes in gene expression may serve as an early biomarker for an impaired genome–environment interaction in the aging brain.

Finally our novel findings, along with other recent publications, suggest that H4K12 dysregulation may be linked with other age related phenomena due to the special dependence of histone acetylation on metabolism. Thus H4K12 may serve as a general therapeutic target for age related diseases. Future studies will be able to determine the H4K12 acetylation mechanism more in detail and reveal further novel targets to treat age related maladies.

References

Abel T, Zukin RS. (2008). Epigenetic targets of HDAC inhibition in neurodegenerative and psychiatric disorders. *Curr Opin Pharmacol* 8(1): 57-64.

Alarcón JM, Malleret G, Touzani K, Vronskaya S, Ishii S, Kandel ER, Barco A. (2004). Chromatin acetylation, memory, and LTP are impaired in CBP^{+/-} mice: a model for the cognitive deficit in Rubinstein-Taybi syndrome and its amelioration. *Neuron* 42(6): 947-59.

Alexa A, Rahnenfuhrer J, Lengauer T. (2006). *Bioinformatics* 22, 1600.

Alfrey VG, Faulkner R and Mirsky AE. (1964). Acetylation and methylation of histones and their possible role in the regulation of RNA synthesis. *Proc Natl Acad Sci USA* 51(5): 786–794.

Ashktorab H, Belgrave K, Hosseinkhah F, Brim H, Nourai M, Takkikto M, Hewitt S, Lee EL, Dashwood RH, Smoot D. (2009). Global histone H4 acetylation and HDAC2 expression in colon adenoma and carcinoma. *Dig Dis Sci* 54(10): 2109-17.

Awe S, Renkawitz-Pohl R. (2010). Histone H4 acetylation is essential to proceed from a histone- to a protamine-based chromatin structure in spermatid nuclei of *Drosophila melanogaster*. *Syst Biol Reprod Med* 56(1): 44-61.

Baron MK, Boeckers TM, Vaida B, Faham S, Gingery M, Sawaya MR, Salyer D, Gundelfinger ED, Bowie JU. (2006). An architectural framework that may lie at the core of the postsynaptic density. *Science* 311(5760): 531-5.

Bednarik DP, Duckett C, Kim SU, Perez VL, Griffis K, Guenther PC, Folks TM. (1991). DNA CpG methylation inhibits binding of NF-kappa B proteins to the HIV-1 long terminal repeat cognate DNA motifs. *New Biol* 3(10): 969-76.

- Benjamini Y, Hochberg Y.** (1995). Controlling the false discovery rate: a practical and powerful approach to multiple testing. *J Roy Statist Soc Ser B* 57 289-300.
- Berchtold NC, Cribbs DH, Coleman PD, Rogers J, Head E, Kim R, Beach T, Miller C, Troncoso J, Trojanowski JQ, Zielke HR, Cotman CW.** (2008). Gene expression changes in the course of normal brain aging are sexually dimorphic. *Proc Natl Acad Sci U S A* 105(40): 15605–15610.
- Best PJ, White AM.** (1999). Placing hippocampal single-unit studies in a historical context. *Hippocampus* 9(4):346-51.
- Bishop NA, Lu T, Yankner BA.** (2010). Neural mechanisms of ageing and cognitive decline. *Nature* 464(7288): 529-35.
- Blankenberg D, Taylor J, Schenck I, He J, Zhang Y, Ghent M, Veeraraghavan N, Albert N, Miller W, Makova KD, Hardison RC, Nekrutenko A.** (2007). A framework for collaborative analysis of ENCODE data: making large-scale analyses biologist-friendly. *Genome Res* 17(6): 960-4.
- Bradford MM.** (1976). A rapid and sensitive method for the quantitation of microgram quantities of protein utilizing the principle of protein-dye binding. *Anal Biochem* 72, 248-254.
- Brandl A, Heinzl T, Krämer OH.** (2009). Histone deacetylases: salesmen and customers in the post-translational modification market. *Biol Cell* 101(4): 193-205.
- Burgess RJ, Zhang Z.** (2010). Roles for Gcn5 in promoting nucleosome assembly and maintaining genome integrity. *Cell Cycle* 9(15): 2979-85.
- Carew JS, Giles FJ, Nawrocki ST.** (2008). Histone deacetylase inhibitors: mechanisms of cell death and promise in combination cancer therapy. *Cancer Lett* 269(1): 7-17.
- Cedar H, Bergman Y.** (2009). Linking DNA methylation and histone modification: patterns and paradigms. *Nat Rev Genet* 10(5): 295-304.
- Chang CS, Pillus L.** (2009). Collaboration between the essential Esa1

acetyltransferase and the Rpd3 deacetylase is mediated by H4K12 histone acetylation in *Saccharomyces cerevisiae*. *Genetics* 183(1): 149-60.

Chen CC, Carson JJ, Feser J, Tamburini B, Zabaronick S, Linger J and Tyler JK. (2008). Acetylated Lysine 56 on Histone H3 Drives Chromatin Assembly after Repair and Signals for the Completion of Repair. *Cell* 134(2): 231-43.

Ciurciu A, Komonyi O, Pankotai T, Boros IM. (2006). The *Drosophila* histone acetyltransferase Gcn5 and transcriptional adaptor Ada2a are involved in nucleosomal histone H4 acetylation. *Mol Cell Biol* 26(24): 9413-23.

Ciurciu A, Komonyi O, Boros IM. (2008). Loss of ATAC-specific acetylation of histone H4 at Lys12 reduces binding of JIL-1 to chromatin and phosphorylation of histone H3 at Ser10. *J Cell Sci* 121(Pt 20): 3366-72.

Clayton AL, Hazzalin CA, Mahadevan LC. (2006). Enhanced Histone Acetylation and Transcription: A Dynamic Perspective. *Molecular Cell* 23(3): 289-96.

Colman RJ, Anderson RM, Johnson SC, Kastman EK, Kosmatka KJ, Beasley TM, Allison DB, Cruzen C, Simmons HA, Kemnitz JW, Weindruch R. (2009). Caloric restriction delays disease onset and mortality in rhesus monkeys. *Science* 325(5937): 201-4.

Coons AH, Creech HJ, Jones RN, Berliner E. (1942). The demonstration of pneumococcal antigen in tissues by the use of fluorescent antibody. *J Immunol* 45:159-70.

Crews L, Masliah E. (2010). Molecular mechanisms of neurodegeneration in Alzheimer's disease. *Hum Mol Genet* 19(R1):R12-20.

Crook T, Bartus RT, Ferris SH, Whitehouse P, Cohen GD, Gershon S. (1986). Age-associated memory impairment: Proposed diagnostic criteria and measures of clinical change - report of a national institute of mental health work group. *Developmental Neuropsychology* 2(4): 261-276.

Dang W, Steffen KK, Perry R, Dorsey JA, Johnson FB, Shilatifard A, Kaeberlein MM, Kennedy BK, Berger SL. (2009). Histone H4 lysine 16 acetylation regulates cellular lifespan. *Nature* 459(7248): 802-7.

De Ruijter AJ, van Gennip AH, Caron HN, Kemp S, van Kuilenburg AB. (2003). Histone deacetylases (HDACs): characterization of the classical HDAC family. *Biochem J* 370(Pt 3): 737-49.

Dennis GJ, Sherman BT, Hosack DA, Yang J, Gao W, Lane HC, Lempicki RA. (2003). DAVID: Database for Annotation, Visualization, and Integrated Discovery. *Genome Biol* 4(5): P3.

Drummond DC, Noble CO, Kirpotin DB, Guo Z, Scott GK, Benz CC. (2005). Clinical development of histone deacetylase inhibitors as anticancer agents. *Annu Rev Pharmacol Toxicol* 45:495-528.

Eberharter A, Becker PB. (2002). Histone acetylation: a switch between repressive and permissive chromatin. Second in review series on chromatin dynamics. *EMBO Rep* 3(3): 224-9.

Ferrante RJ, Kubilus JK, Lee J, Ryu H, Beesen A, Zucker B, Smith K, Kowall NW, Ratan RR, Luthi-Carter R, Hersch SM. (2003). Histone deacetylase inhibition by sodium butyrate chemotherapy ameliorates the neurodegenerative phenotype in Huntington's disease mice. *J Neurosci* 23(28): 9418-27.

Fischer A, Sananbenesi F, Schrick C, Spiess J, Radulovic J. (2002). Cyclin-dependent kinase 5 is required for associative learning. *J Neurosci* 22(9): 3700-7.

Fischer A, Sananbenesi F, Schrick C, Spiess J, Radulovic J. (2004). Distinct roles of hippocampal de novo protein synthesis and actin rearrangement in extinction of contextual fear. *J Neurosci* 24(8): 1962-6.

Fischer A, Sananbenesi F, Wang X, Dobbin M, Tsai LH. (2007). Recovery of learning and memory is associated with chromatin remodelling. *Nature* 447(7141): 178-82.

Gao J, Wang WY, Mao YW, Gräff J, Guan JS, Pan L, Mak G, Kim D, Su SC, Tsai LH. (2010). A novel pathway regulates memory and plasticity via SIRT1 and miR-134. *Nature* 466(7310): 1105-9.

Gao L, Cueto MA, Asselbergs F, Atadja P. (2002). Cloning and functional characterization of HDAC11, a novel member of the human histone deacetylase family. *J Biol Chem* 277(28): 25748-55.

Gentleman RC, Carey VJ, Bates DM, Bolstad B, Dettling M, Dudoit S, Ellis B, Gautier L, Ge Y, Gentry J. (2004). Bioconductor: open software development for computational biology and bioinformatics. *Genome Biol* 5(10): R80.

Görisch SM, Wachsmuth M, Tóth KF, Lichter P, Rippe K. (2005). Histone acetylation increases chromatin accessibility. *J Cell Sci* 118(Pt 24): 5825-34.

Gregoretta IV, Lee YM, Goodson HV. (2004). Molecular evolution of the histone deacetylase family: functional implications of phylogenetic analysis. *J Mol Biol* 338(1): 17-31.

Grozinger CM, Schreiber SL. (2000). Regulation of histone deacetylase 4 and 5 and transcriptional activity by 14-3-3-dependent cellular localization. *Proc Natl Acad Sci U S A* 97(14): 7835-40.

Guan JS, Haggarty SJ, Giacometti E, Dannenberg JH, Joseph N, Gao J, Nieland TJ, Zhou Y, Wang X, Mazitschek R, Bradner JE, DePinho RA, Jaenisch R, Tsai LH. (2009). HDAC2 negatively regulates memory formation and synaptic plasticity. *Nature* 459(7243): 55-60.

Guarente L. (2006). Sirtuins as potential targets for metabolic syndrome. *Nature* 444(7121): 868-74.

Gupta S, Kim SY, Artis S, Molfese DL, Schumacher A, Sweatt JD, Paylor RE, Lubin FD. (2010). Histone methylation regulates memory formation. *J Neurosci* 30(10): 3589-99.

Haass C, Selkoe DJ. (2007). Soluble protein oligomers in neurodegeneration:

lessons from the Alzheimer's amyloid beta-peptide. *Nat Rev Mol Cell Biol* 8(2): 101-12.

Hayflick L. (2000). The future of ageing. *Nature* 408(6809): 267-9.

Himeda T, Mizuno K, Kato H, Araki T. (2005). Effects of age on immunohistochemical changes in the mouse hippocampus. *Mech Ageing Dev* 126(6-7): 673-7. * This paper describes hippocampal changes between young mice and 59 weeks (roughly 12 months) old mice. The mice strain in this paper have average life span of only 16 months, compared with 26-28 months in the mice that we conducted our experiments.

Hockly E, Richon VM, Woodman B, Smith DL, Zhou X, Rosa E, Sathasivam K, Ghazi-Noori S, Mahal A, Lowden PA, Steffan JS, Marsh JL, Thompson LM, Lewis CM, Marks PA, Bates GP. (2003). Suberoylanilide hydroxamic acid, a histone deacetylase inhibitor, ameliorates motor deficits in a mouse model of Huntington's disease. *Proc Natl Acad Sci U S A* 100(4): 2041-6.

Huang DW, Sherman BT, Lempicki RA. (2009). Systematic and integrative analysis of large gene lists using DAVID Bioinformatics Resources. *Nature Protoc* 4(1): 44-57.

Huber W, von Heydebreck A, Sueltmann H, Poustka A, Vingron M. (2002). Variance stabilization applied to microarray data calibration and to the quantification of differential expression. *ISMB* 1:S96-104.

Jackson V. (1978). Studies on histone organization in the nucleosome using Formaldehyde as a reversible cross-linking agent. *Cell* 15(3): 945-54.

Jiang N, Yan X, Zhou W, Zhang Q, Chen H, Zhang Y, Zhang X. (2008). NMR-Based Metabonomic Investigations into the Metabolic Profile of the Senescence-Accelerated Mouse. *Journal of Proteome Research* 7(9): 3678-3686.

Jucker M, Ingram DK. (1997). Murine models of brain aging and age-related neurodegenerative diseases. *Behav Brain Res* 85(1): 1-26.

- Kandel ER.** (2001). The molecular biology of memory storage: a dialogue between genes and synapses. *Science* 294(5544): 1030-8.
- Kanehisa M, Goto S.** (2000). KEGG: kyoto encyclopedia of genes and genomes. *Nucleic Acids Res* 28(1): 27–30.
- Kenyon C, Chang J, Gensch E, Rudner A, Tabtiang R.** (1993). A *C. elegans* mutant that lives twice as long as wild type. *Nature* 1993 366(6454): 461-4.
- Khan N, Jeffers M, Kumar S, Hackett C, Boldog F, Khramtsov N, Qian X, Mills E, Berghs SC, Carey N, Finn PW, Collins LS, Tumber A, Ritchie JW, Jensen PB, Lichenstein HS, Sehested M.** (2008). Determination of the class and isoform selectivity of small-molecule histone deacetylase inhibitors. *Biochem J* 409(2): 581-9.
- Kilgore M, Miller CA, Fass DM, Hennig KM, Haggarty SJ, Sweatt JD, Rumbaugh G.** (2010). Inhibitors of class 1 histone deacetylases reverse contextual memory deficits in a mouse model of Alzheimer's disease. *Neuropsychopharmacology* 35(4): 870-80.
- Kim S, Benguria A, Lai CY, Jazwinski SM.** (1999). Modulation of life-span by histone deacetylase genes in *Saccharomyces cerevisiae*. *Mol Biol Cell* 10(10): 3125-36.
- Korzus E, Rosenfeld MG, Mayford M.** (2004). CBP histone acetyltransferase activity is a critical component of memory consolidation. *Neuron* 42(6): 961-72.
- Kral VA.** (1962). Senescent forgetfulness: benign and malignant. *Can Med Assoc J* 86: 257-60.
- Kucharski R, Maleszka J, Foret S, Maleszka R.** (2008). Nutritional control of reproductive status in honeybees via DNA methylation. *Science* 319(5871):1827-30.
- Laemmli UK.** (1970). Cleavage of structural proteins during the assembly of the head of bacteriophage T4. *Nature* Bd. 227, S. 680–685.

- Lande-Diner L, Zhang J, Ben-Porath I, Amariglio N, Keshet I, Hecht M, Azuara V, Fisher AG, Rechavi G, Cedar H.** (2007). Role of DNA methylation in stable gene repression. *J Biol Chem* 282(16): 12194-200.
- Levenson JM, O'Riordan KJ, Brown KD, Trinh MA, Molfese DL, Sweatt JD.** (2004a). Regulation of histone acetylation during memory formation in the hippocampus. *J Biol Chem* 279(39): 40545-59.
- Lin YY, Lu JY, Zhang J, Walter W, Dang W, Wan J, Tao SC, Qian J, Zhao Y, Boeke JD, Berger SL, Zhu H.** (2009). Protein acetylation microarray reveals that NuA4 controls key metabolic target regulating gluconeogenesis. *Cell* 136(6): 1073-84.
- Linnane AW, Marzuki S, Ozawa T, Tanaka M.** (1989). Mitochondrial DNA mutations as an important contributor to ageing and degenerative diseases. *Lancet* 1(8639): 642-5.
- Loerch PM, Lu T, Dakin KA, Vann JM, Isaacs A, Geula C, Wang J, Pan Y, Gabuzda DH, Li C, Prolla TA, Yankner BA.** (2008). Evolution of the aging brain transcriptome and synaptic regulation. *PLoS One* 3(10):e3329.
- Lu T, Pan Y, Kao SY, Li C, Kohane I, Chan J, Yankner BA.** (2004). Gene regulation and DNA damage in the ageing human brain. *Nature* 429(6994): 883-91.
- Manosalva I, González A.** (2009). Aging alters histone H4 acetylation and CDC2A in mouse germinal vesicle stage oocytes. *Biol Reprod* 81(6): 1164-71.
- Merson TD, Dixon MP, Collin C, Rietze RL, Bartlett PF, Thomas T, Voss AK.** (2006). The transcriptional coactivator Querkopf controls adult neurogenesis. *J Neurosci* 26(44): 11359-70.
- Michan S, Sinclair D.** (2007). Sirtuins in mammals: insights into their biological function. *Biochem J* 404(1): 1-13.
- Miller DM, Williams R, McCarty KS.** (1973). Localization and in vitro specificity of histone acetylation. *Biochim Biophys Acta* 317(2):437-46.

- Montarolo PG, Goelet P, Castellucci VF, Morgan J, Kandel ER, Schacher S.** (1986). A Critical period for macromolecular synthesis in long-term heterosynaptic facilitation in *Aplysia*. *Science* 234(4781): 1249-54.
- Morris RGM.** (1981). Spatial Localization Does Not Require the Presence of Local Cues. *Learning and Motivation* 12(2): 239-260.
- Munks RJ, Moore J, O'Neill LP, Turner BM.** (1991). Histone H4 acetylation in *Drosophila*. *FEBS Lett* 284(2): 245-8.
- Nishida H, Suzuki T, Kondo S, Miura H, Fujimura Y, Hayashizaki Y.** (2006). Histone H3 acetylated at lysine 9 in promoter is associated with low nucleosome density in the vicinity of transcription start site in human cell. *Chromosome Res* 14(2): 203-11.
- Norton VG, Imai BS, Yau P, Bradbury EM.** (1989). Histone acetylation reduces nucleosome core particle linking number change. *Cell* 57(3): 449-57.
- O'Keefe J, Dostrovsky J.** (1971). The hippocampus as a spatial map. Preliminary evidence from unit activity in the freely-moving rat. *Brain Res* 34(1): 171-5.
- Oeppen J, Vaupel JW.** (2002). Demography, Broken limits to life expectancy. *Science* 296(5570): 1029-31.
- Qiu J.** (2006). Epigenetics: unfinished symphony. *Nature* 441(7090): 143-5.
- Renthal W, Maze I, Krishnan V, Covington HE 3rd, Xiao G, Kumar A, Russo SJ, Graham A, Tsankova N, Kippin TE, Kerstetter KA, Neve RL, Haggarty SJ, McKinsey TA, Bassel-Duby R, Olson EN, Nestler EJ.** (2007). Histone deacetylase 5 epigenetically controls behavioral adaptations to chronic emotional stimuli. *Neuron* 56(3): 517-29.
- Rice JC, Allis CD.** (2001). Histone methylation versus histone acetylation: new insights into epigenetic regulation. *Curr Opin Cell Biol* 13(3): 263-73.
- Rosenzweig ES, Barnes CA.** (2003). Impact of aging on hippocampal function: plasticity, network dynamics, and cognition. *Prog Neurobiol* 69(3):1 43-79.

Schacher S, Castellucci VF, Kandel ER. (1988). cAMP evokes long-term facilitation in Aplysia sensory neurons that requires new protein synthesis. *Science* 240(4859): 1667-9.

Scoville WB, Milner B. (1957). Loss of recent memory after bilateral hippocampal lesions. *J Neurol Neurosurg Psychiatry* 1957 20(1):11-21.

Segal M, Murphy DD. (1998). CREB activation mediates plasticity in cultured hippocampal neurons. *Neural Plast* 6(3):1-7.

Shimohata T, Nakajima T, Yamada M, Uchida C, Onodera O, Naruse S, Kimura T, Koide R, Nozaki K, Sano Y. (2000). Expanded polyglutamine stretches interact with TAFII130, interfering with CREB-dependent transcription. *Nat Genet* 26(1): 29-36.

Simonini MV, Camargo LM, Dong E, Maloku E, Veldic M, Costa E, Guidotti A. (2006). The benzamide MS-275 is a potent, long-lasting brain region-selective inhibitor of histone deacetylases. *Proc Natl Acad Sci U S A* 103(5): 1587-92.

Smith CM, Haimberger ZW, Johnson CO, Wolf AJ, Gafken PR, Zhang Z, Parthun MR, Gottschling DE. (2002). Heritable chromatin structure: mapping "memory" in histones H3 and H4. *Proc Natl Acad Sci U S A* 99 Suppl 4:16454-61.

Smyth GK. (2004). *Stat Appl Genet Mol Biol* 3, article 3.

Solomon MJ, Larsen PL, Varshavsky A. (1988). Mapping protein-DNA interactions in vivo with formaldehyde: evidence that histone H4 is retained on a highly transcribed gene. *Cell* 53(6): 937-47.

Steffan JS, Bodai L, Pallos J, Poelman M, McCampbell A, Apostol BL, Kazantsev A, Schmidt E, Zhu YZ, Greenwald M, Kurokawa R, Housman DE, Jackson GR, Marsh JL, Thompson LM. (2001). Histone deacetylase inhibitors arrest polyglutamine-dependent neurodegeneration in *Drosophila*. *Nature* 413(6857): 739-43.

Strahl BD, Allis CD. (2000). The language of covalent histone modifications.

Nature 403(6765): 41-5.

Taipale M, Rea S, Richter K, Vilar A, Lichter P, Imhof A, Akhtar A. (2005). hMOF histone acetyltransferase is required for histone H4 lysine 16 acetylation in mammalian cells. *Mol Cell Biol* 25(15): 6798-810.

Taylor J, Schenck I, Blankenberg D, Nekrutenko A. (2007). Using galaxy to perform large-scale interactive data analyses. *Curr Protoc Bioinformatics*. Chapter 10:Unit 10.5

Vecsey CG, Hawk JD, Lattal KM, Stein JM, Fabian SA, Attner MA, Cabrera SM, McDonough CB, Brindle PK, Abel T, Wood MA. (2007). Histone deacetylase inhibitors enhance memory and synaptic plasticity via CREB:CBP-dependent transcriptional activation. *J Neurosci* 27(23): 6128-40.

Verbitsky M, Yonan AL, Malleret G, Kandel ER, Gilliam TC, Pavlidis P. (2004). Altered hippocampal transcript profile accompanies an age-related spatial memory deficit in mice. *Learn Mem* 11(3): 253-60.

Waddington CH. (1942). The epigenotype. *Endeavour* 1:18–20.

Wang Z, Zang C, Rosenfeld JA, Schones DE, Barski A, Cuddapah S, Cui K, Roh TY, Peng W, Zhang MQ and Zhao K. (2008). Combinatorial patterns of histone acetylations and methylations in the human genome. *Nat Genet* 27(23): 6128-40.

Wang Z, Zang C, Cui K, Schones DE, Barski A, Peng W, Zhao K. (2009). Genome-wide mapping of HATs and HDACs reveals distinct functions in active and inactive genes. *Cell* 138(5): 1019-31.

Weindruch R, Walford RL, Fligiel S, Guthrie D. (1986). The retardation of aging in mice by dietary restriction: longevity, cancer, immunity and lifetime energy intake. *J Nutr* 116(4): 641-54.

Wellen KE, Hatzivassiliou G, Sachdeva UM, Bui TV, Cross JR, Thompson CB. (2009). ATP-citrate lyase links cellular metabolism to histone acetylation.

Science 324(5930): 1076-80.

Zang C, Schones DE , Zeng C, Cui K, Zhao K, and Peng W. (2009). A clustering approach for identification of enriched domains from histone modification ChIP-Seq data. *Bioinformatics* 25(15): 1952-8.

Zhang K, Williams KE, Huang L, Yau P, Siino JS, Bradbury EM, Jones PR, Minch MJ, Burlingame AL. (2002). Histone acetylation and deacetylation: identification of acetylation and methylation sites of HeLa histone H4 by mass spectrometry. *Mol Cell Proteomics* 1(7): 500-8.

Zoroddu MA, Peana M, Medici S, Casella L, Monzani E, Costa M. (2010). Nickel binding to histone H4. *Dalton Trans* 239(3): 787-93.

Curriculum vitae

Personal data

Name: Shahaf Peleg
Current Address: Robert Koch str. 38/111
 Goettingen 37075
 Germany
Date of Birth and place: 28.11.1980, Beer-Sheva, Israel
Country: Germany
E-mail: Shahafpeleg3@googlemail.com

Education

<i>Institution and Location</i>	<i>Degree</i>	<i>Years</i>	<i>Field of Study</i>
European Neuroscience Institute (ENI), Goettingen Germany.	Ph.D.	2006-10	Epigenetic and Aging
Ben Gurion University, Beer-Sheva, Israel	B.Sc.	2003-06	Biology

Prizes and Awards:

2010 Top best three student talks, Horizons International Symposium
 2010 Best poster prize, Spetses Summer School
 2010 Spetses Summer School stipend
 2009-2010 Minerva stiftung
 2006-2008 Stipend from International Max Planck Research School (IMPRS)
 2005 The Amos De-Shalit Summer program for selected students in Life Science, Weizmann Institute of Science, Israel

List of Publications

Shahaf Peleg, Farahnaz Sananbenesi, Athanasios Zovoilis, Susanne Burkhardt, Sanaz Bahari-Javan, Roberto Carlos Agis-Balboa, Perla Cota, Jessica Lee Wittnam, Andreas Gogol-Doering, Lennart Opitz, Gabriella Salinas-Riester, Markus Dettenhofer, Hui Kang, Laurent Farinelli, Wei Chen & Andre Fischer. (2010) Altered histone acetylation is associated with age-dependent memory impairment. *Science* 28(5979): 753-6. (Research Highlight in *Nature, Cell, F1000*)

Appendix

Shearing, one day ChIP protocol and SYBR Green RT-PCR

Shearing

Prepare:

10ml DPBS + 1 tablet of complete

10ml 1M Glycine in DPBS

Sonication epis

Bucket of ice

Icy water

In General:

- To mix always invert and/or vortex briefly
 - Always work on ice
1. Add 500µl DPBS (or sterile PBS) to tissue and homogenize well
 2. Add 500µl DPBS and transfer to Bioruptor e-cups
 3. Add 27µl (or 54µl for whole Hippocampus) of 37% Formaldehyde and incubate 15min on Rotation Mixer (@RT, speed 14)
 4. Add 300µl 1M Glycin (in PBS), incubate 5min on RotationMixer (@RT)
 5. Centrifugation: 3000 rpm, 5 minuets, 4°C Remove Supernatant
 6. Wash with 1000µl DPBS + Protease inhibitor, pipet up and down gently
 7. Centrifugation: 3000 rpm, 5 minuets, 4°C
 8. Remove supernatant and resuspend pellet with 600µl (1ml whole hippocampus) of Buffer A + 6µl DTT (12µl whole hippocampus)
 9. Incubate 15min on ice, then 15 minuets @30°C, 800 rpm on shaker
 10. Vortex briefly, Centrifugation: 5500 rpm, 5 minuets, 4°C
 11. Resuspend pellet gently with 600µl (1000µl whole hippocampus) Buffer B (also take out Buffer D to warm up)

12. Centrifugation: 5500 rpm, 5 minutes, 4°C
13. Resuspend gently with 600µl (100µl whole hippocampus) of Buffer C
14. Centrifugation: 5500 rpm, 5 minutes, 4°C. Remove supernatant and resuspend pellet in 240µl (480µl whole hippocampus) Buffer D + 9.6µl (19.2µl whole hippocampus) Protease Inhibitor (which is dissolved in H₂O)
15. Shear chromatin:
 - a. Power setting on high, ice cold
 - b. 10 minutes (30 seconds on / 30 seconds off [0.5minutes])
 - c. Change ice
 - d. 5 minutes (30 seconds on / 30 seconds off)
 - e. Change ice
 - f. Repeat until a total time of 25 minutes (10 minutes+ 3x5 minutes)
16. Centrifuge at 10,000g for 5 minutes
17. Keep supernatant and discard the pellet
18. For checking sheared DNA, there is a need to reverse the cross-linking with proteinase K etc
19. Store @ -80°C

One day ChIP protocol

Prepare:

- Dilute chip-buffer 1:5 on 4°C (33ml per sample)
- Falcons:
 - o Chip-PI (protease inhibitor 1:200) 242µl x sample + 1
 - o 2 per sample with 12ml ChIP buffer (label 1,2) in cold room
- Sheared chromatin thawed
- Epis: 3 per sample: 1x input, 1x output, 1x beads (each for AB)
- Ice in a long cubic ice box or bucket
- Glass or pot of water for boiling

In general:

- Work on ice
 - Cut pipet-tip when handling beads
 - Centrifuge everything with table centrifuge (TC) before use
 - Look one to two steps ahead
1. Add 242µl of chip-PI to **output** epi (or **input** epi) and add 66µl of sheared chromatin (=308µl), pipet up and down
 2. Take approx. 10% (e.g. 35µl) to **input** epi (or 90% to **output** epi)
 3. Spin down input with TC, place input on -20°C
 4. **Add 3-4µl of IgG Antibody (negative control) to corresponding output**
 5. **Add Xµl of AB (1:90, depending on the AB, for ChIP-seq usually 4µl or more) to corresponding output**
 6. **Vortex for 5 seconds on medium power**
 7. **Put outputs in ultrasonic bath for 60 minutes (use epi-swimmer and icy water)**
 8. During this 60 minutes prepare beads (*alternatively start here and go on with step 1 afterwards*):
 - a. Washing: Add 42µl beads per sample to 500µl (+ extra) per sample of chip buffer in a falcon, pipet up and down, centrifuge 1500 rpm, 3 minutes, 4°C
 - b. Blocking: Remove supernatant with Pasteur pipette, add 500µl per sample (+extra) of chip buffer + 1:100 of BSA (thaw in advance), place on rotating wheel for 20 minutes, speed 11 in 4°C room, centrifuge 1500rpm, 3 minutes, 4°C
 - c. Resuspend pellet in 500µl per sample (+extra) and take 500µl of homogeneous bead-solution to beads-epis, centrifuge 2500 rpm, 2 minutes, 4°C. Do not disturb the pellet. Check by eye that pellets are equal.
 9. **Centrifuge Antibody solution 12.000 rpm, 10 minutes, 4°C, thaw input from -20°C**
 10. **From the supernatant take 240µl and mix with beads (No pipetting up and down), take to rotating wheel 60 minutes, speed 11, 4°C**
 11. Label new epis for each ChIP, put on ice

12. Take all μl of the input and add $30\mu\text{l}$ 100%EtOH, incubate 10 minutes on ice
13. Centrifuge 10,000g, 10 minutes, discard the supernatant (take $50\mu\text{l}$ off with pipet)
14. Add $50\mu\text{l}$ 70%EtOH, centrifuge 10,000g, 10min, discard supernatant (take $50\mu\text{l}$ off again), let pellet dry at RT
15. To the AB-chromatin-beads mix add $500\mu\text{l}$ ChIP buffer
16. Invert tubes twice, put water to boil
17. Centrifuge 2 minutes, 500g (2500 rpm), 4°C
18. Take off the supernatant, add 1ml ChIP buffer (from now on, no ChIP buffer needed anymore)
19. Take 15ml tubes with 12ml ChIP Buffer
20. Transfer 1ml including beads to the very top of the falcon tube on the wall gently (beads should sink down in the 15ml tube), take first $500\mu\text{l}$, then $500\mu\text{l}$ including beads and some foam, pipet up and down several times, check for leftover beads
21. Incubate 5 minutes on ice
22. Centrifuge 1500 rpm, 3 minutes, 4°C , check for pellet, discard supernatant till 1ml is left
23. Repeat this with 2nd 15ml tube
24. After centrifugation transfer the last 1ml to labeled epi (step 11)
25. Centrifuge 2 minutes, 2500 rpm, 4°C
26. Discard supernatant as good as you can, now stop working on ice
27. Incubate with open caps at RT for 10 minutes
28. Add $100\mu\text{l}$ PCR-grade water to input DNA, resuspend the pellet, incubate at RT
29. Take slurry, open half, vortex shortly, immediately pipet up and down once and add $100\mu\text{l}$ to beads mix and input sample
30. Invert tubes, add blue locking caps to epis
31. Incubate for 10min in boiling water, set thermomixer to 55°C , thaw Proteinase K, label final epis

32. Take out from boiling and wait ca. 2 minutes to cool down, add 1 μ l of ProtK to each sample, vortex for 2 seconds and medium power
33. Incubate on thermomixer for 50min at 55°C to reverse crosslinking
34. Incubate again 10 minutes in boiling water, wait to cool down again
35. Centrifuge 1 minute, 12,000 rpm, 4°C
36. Transfer 70 μ l of supernatant to labeled epis
37. Add 130 μ l of PCR grade water to pellet
38. Vortex for 10 seconds at medium power
39. Centrifuge 1 minute, 12,000 rpm, 4°C
40. Take 130 μ l from supernatant to the 70 μ l from step 36 (total volume: 200 μ l)
41. Go on with PCR or store at -20°C

Real Time PCR for ChIP with Sybr Green

RT-PCR with SYBR green

The making of the mix is like it is stated in the protocol. But somehow, it proved to be a bit trickier than the UPL's.

So here are some tips (some of them might not prove to really make a difference, but that is how we made it work):

- Pipetting work under no hood light
- First check by normal PCR that your primers work and which temperature. More importantly, check if you have double band. If you have more than one, you can't use it in SYBR green
- Take few samples to check if it works in RT-PCR first, before running the whole experiment. Sybr green is expensive

-
- The standard curve should be 1:1, 1:2, 1:4, 1:8 and 1:16. The positive calibration is the same as 1:1. So since you have only 200 μ l of ChIP-DNA, think clearly how you distribute it all before you start the experiments. Use fresh eppies (new, not autoclaved)
 - No need to dilute the samples 1:10, since there is not so much DNA. I use 3 μ l per well of un-diluted sample
 - Once the sample/std. curve are thawed, spin down, but do not spin them again. Instead, before pipetting, just tap the eppi several times with your finger
 - As a reference, you use your input, not house keeping gene
 - To save time, you can pipet the master mix on the wells wall und not at the bottom. The mix is "heavy" and falls down
 - If the results of your samples were worse than 33 cycles (the variation then becomes very large), I would not trust the results. Try to put more of the DNA sample